**TECHNISCHE
UNIVERSITÄT
WIEN**

Dissertation

Advanced Polymer Characterization using LA-ICP-MS and LIBS

ausgeführt zum Zwecke der Erlangung des akademische Grades des Doktors der technischen Wissenschaften unter der Anleitung von

Univ.Prof. Dipl.-Ing. Dr.techn. Andreas LIMBECK

am Institut für Chemische Technologien und Analytik (E164)
eingereicht an der
Fakultät für Technische Chemie, TU Wien
von

Dipl.-Ing. Lukas BRUNNBAUER

e01126054
Meiselstraße 14/1/5
1150 Wien

Wien, am 21.03.2021 _____

Abstract

Since their invention in the early 20th century, the properties of synthetic polymers have been steadily improved and therefore, polymers became one of the most widely used materials in our modern world. To open up new application fields for polymers, constant improvement of the materials' properties is still necessary. Nowadays, a common approach to fine-tune the required properties is the employment of (in)organic additives, making industrial polymers a very complex material. As further development of material properties goes hand-in-hand with thorough characterization and analysis of the material, analytical tools which enable characterization of polymers also need constant improvement.

There are several well-established analytical tools such as FT-IR- and Raman-spectroscopy, Py-GC-MS, DTA/TGA or MALDI-TOF-MS which are conventionally used for polymer characterization, all coming with unique advantages and limitations. Nevertheless, there are still several characteristics such as spatially resolved classification and degradation studies, or quantitative assessment of trace metals' content which are beneficial for polymer characterization but are not accessible with conventional techniques. To overcome these limitations, the benefits of the two analytical techniques Laser Ablation-Inductively Coupled Plasma-Mass Spectrometry (LA-ICP-MS) and Laser Induced Breakdown Spectroscopy (LIBS) for polymer analysis are evaluated. Providing elemental and also molecular information, high sensitivity for trace metal analysis and the possibility of laterally resolved analysis and depth profiling, these two techniques offer favorable figures of merit for polymer analysis. Although frequently applied in fields such as geochemistry, biomedical applications, or materials science LA-ICP-MS and LIBS are only scarcely reported in the literature for the analysis of synthetic polymers. There is some work reporting the use of LIBS for the classification of bulk polymer samples, and LA-ICP-MS has been used for quantitative metal analysis when required reference materials are available. Therefore, there is still a lot of room for improvements of LA-ICP-MS and LIBS to establish them as useful techniques for polymer characterization.

In this work, LA-ICP-MS and LIBS are employed to tackle three different applications of polymer characterization which are not easily accessible with conventional techniques:

- **Spatially Resolved Polymer Classification**: With further developments, composite materials consisting of multiple polymer types have emerged. To fully characterize these materials, spatially resolved polymer classification is necessary to ensure the desired distribution of the polymer within the material. With some conventional techniques such as FT-IR or MALDI-TOF-MS, investigation of the lateral distribution of different polymer types is already possible. Nevertheless, analysis of polymeric multilayer systems is not accessible, since these techniques allow only the investigation of the sample surface. Using different sample types and various data evaluation strategies, the possibility of using LIBS for 2D as well as 3D imaging of polymer distributions within a sample was investigated.

iv

- **Investigation of Polymer Degradation**: In many different fields where polymers are used, the material is exposed to harsh (environmental) conditions, such as UV-radiation, humidity, elevated temperatures and sometimes corrosive species. To ensure a safe application, characterization of polymers' degradation behavior as well as uptake of different species from the surrounding environment is important. LA-ICP-MS and LIBS provide unique features that could be used for comprehensive characterization of polymer degradation. The detection of polymer specific emission signals may be used to assess degradation of the polymeric network and detection of oxygen may allow to investigate oxidation of the sample. Additionally, a high sensitivity for inorganic species can be used to determine uptake of these species. Both degradation and uptake of inorganic species can be performed not only on the sample surface but also in depth profile analysis. Using these benefits, the degradation behavior of a wide range of different polymeric samples under different aging conditions was investigated.

- **Quantitative Metal Analysis in Polymers**: Analysis of polymers' metal content is of great interest in many different fields ranging from the assessment of toxic metals in polymers used in the food packaging industry to the necessity of high purity polymers used in the semiconductor industry. Even though reliable, conventional approaches for the quantitative determination of polymers' metal content such as microwave-assisted digestion or combustion followed by liquid ICP-MS or ICP-OES analysis are time-consuming, laborious and have a high usage of harsh and hazardous chemicals. Additionally, only information about the bulk concentration within the polymer is accessible. All these reasons make conventional approaches both economical and ecological unfavorable. Using direct-solid sampling techniques, all of the aforementioned disadvantages can be overcome. Nevertheless, for quantitative analysis usually matrix-matched standards are necessary which are scarcely available. In this work, the application of LIBS combined with multivariate statistics for quantitative metal analysis in polymers without matrix-matched standards is evaluated. Results indicate adequate performance of the developed approach.

v

Kurzfassung

Seit der Erfindung und Einführung von synthetischen Polymeren zu Beginn des 20. Jahrhunderts wurden deren Eigenschaften stetig verbessert und haben sich daher über die letzten Jahrzehnte zu einem weitverbreiteten Material entwickelt. Um auch in Zukunft immer neue Anwendungsgebiete zu eröffnen, ist eine weitere Verbesserung der Materialeigenschaften nötig. In modernen Polymeren wird häufig eine Vielzahl von (an)organischen Additiven eingesetzt, um die Eigenschaften für spezielle Anwendungen zu optimieren, wodurch sich sehr komplexe Materialzusammensetzungen ergeben. Weiterentwicklung von Materialien ist immer eng verbunden mit deren umfassenden Charakterisierung, wodurch sich auch die Notwendigkeit der Verbesserung von analytischen Methoden für Polymercharakterisierung ergibt.

Häufig eingesetzte analytische Techniken zur Charakterisierung von Polymeren sind FT-IR- und Raman Spektroskopie, Py-GC-MS, TGA/DTA oder auch MALDI-TOF-MS. Jede dieser Techniken ermöglicht die Untersuchung von speziellen Eigenschaften von Polymeren. Obwohl mit diesen Techniken bereits ein Großteil von charakterisierbaren Merkmalen abgedeckt ist, gibt es immer noch einige Eigenschafte, die mit konventionellen Messmethoden nur schwer zugänglich sind. Dazu zählen etwa Bereiche der Polymerklassifizierung, Untersuchung von Polymerdegradation, oder die quantitative Bestimmung des Metallgehalts von Polymeren. Um die Analyse dieser wichtigen Bereiche zu ermöglichen, wird in dieser Arbeit die Anwendung von Laser Ablation-Inductively Coupled Plasma-Mass Spectrometry (LA-ICP-MS) und Laser Induced Breakdown Spectroscopy (LIBS)) untersucht. Diese beiden Techniken ermöglichen nicht nur eine hohe Empfindlichkeit für die Detektion des Metallgehalts sondern auch die direkte Detektion der Hauptbestandteile von Polymeren sowie molekularer Fragmente der Probe. Zusätzlich ist eine ortsaufgelöste Analyse in Form von Images und Tiefenprofilen möglich. LA-ICP-MS und LIBS sind etablierte analytische Techniken, die in den Bereichen der Geowissenschaften, Materialwissenschaften oder auch in medizinischen Fragestellungen bereits routinemäßig eingesetzt werden. Im Bereich der Polymeranalyse gibt es jedoch kaum Literatur, die sich mit der Anwendung von LA-ICP-MS und LIBS auseinandersetzt. In den wenigen publizierten Arbeiten wird lediglich die Anwendung von LIBS für die Klassifizierung von Bulk-Polymerproben gezeigt. Mit Hilfe von zertifizierten Referenzmaterialen wurde LA-ICP-MS bereits für die quantitative Bestimmung des Metallgehalts verwendet. Daher werden in dieser Arbeit weitere Anwendungen von LA-ICP-MS und LIBS im Bereich der Polymeranalytik untersucht:

- **Ortsaufgelöste Polymerklassifizierung**: Mit der Weiterentwicklung von Polymeren wurden in den letzten Jahren Kompositmaterialien entwickelt, welche aus mehreren unterschiedlichen Polymertypen zusammengesetzt sind. Um eine vollständige Charakterisierung dieser Kompositmaterialien zu gewährleisten, ist es notwendig die räumliche Verteilung der unterschiedlichen Polymertypen im Material zu bestimmen. Mit manchen konventionell verwendeten Techniken (FTIR oder MALDI-TOF-MS) ist bereits

die zweidimensionale Klassifizierung von Polymertypen an Probenoberflächen möglich. Allerdings gibt es keine Möglichkeit Schichtsysteme aus verschiedenen Polymeren zu charakterisieren. An Hand von verschiedenen Proben wurde die Anwendung von LIBS für zwei- und dreidimensionale Klassifizierung von Polymertypen untersucht.

- **Untersuchung von Polymerdegradation:** Durch die Anwendung von Polymeren in den unterschiedlichsten Gebieten wird dieses Material häufig verschiedensten Umwelteinflüssen wie zum Beispiel UV-Strahlung, korrosiven Spezies, Feuchtigkeit, und erhöhte Temperaturen ausgesetzt, wodurch es zu Degradation kommen kann. Um eine sichere Anwendung zu gewährleisten, ist daher die Untersuchung des Degradationsverhaltens und dem Aufnahmevermögen von unterschiedlichen Spezies aus der Umwelt notwendig. Für diese Untersuchungen bieten LA-ICP-MS und LIBS herausragende Eigenschaften. Durch die Detektion von polymerspezifischen LIBS-Signalen kann die Degradation des Polymernetzwerks untersucht werden. Zusätzlich bietet LIBS die Möglichkeit durch die Detektion von Sauerstoff, die Oxidation der Probe zu bestimmen. Die hohe Empfindlichkeit von LA-ICP-MS kann zur Bestimmung der Aufnahme von anorganischen Bestandteilen genutzt werden. Zusätzlich ist mit beiden Techniken die Messung von Tiefenprofilen möglich, was ebenfalls einen Mehrwert liefert. Diese Vorteile wurden genutzt, um das Degradationsverhalten von unterschiedlichen Polymeren in verschiedenen Umweltbedingungen zu charakterisieren.

- **Quantitative Bestimmung des Metallgehalts in Polymeren:** In vielen Anwendungsgebieten ist die Bestimmung von Metallgehalten in Polymeren von großer Relevanz. So muss zum Beispiel in der Lebensmittelverpackungsindustrie der Gehalt von toxischen Schwermetallen überprüft werden. Auch bei Polymeren, die in der Halbleiterindustrie eingesetzt werden, ist eine hohe Reinheit der Materialien zu gewährleisten. Für die quantitative Bestimmung des Metallgehalts in Polymeren gibt es etablierte Ansätze, welche auf der Überführung des Polymers in eine Lösung und anschließender flüssig ICP-MS oder ICP-OES Messung beruhen. Da Polymere meist chemisch inert sind, ist für die Überführung in Lösung oft ein Mikrowellenaufschluss oder auch eine Veraschung notwendig. Diese Ansätze sind zeit- und arbeitsintensiv und benötigen eine Vielzahl an gesundheits- und umweltgefährdenden Reagenzien, welche sowohl aus ökologischer als auch ökonomischer Sicht zu vermeiden sind. Zusätzlich bietet ein Aufschlusses mit anschließender Flüssigmessung nur Information über den Gesamtgehalt der Probe. Ortsaufgelöste Information geht dabei verloren. Durch die Verwendung von direkten Feststoffanalyse-Techniken können sämtliche oben erwähnte Nachteile vermieden werden. Allerdings werden für quantitative Messungen mit direkten Feststoffanalyse-Techniken matrix-angepasste Standards benötigt, die nur selten verfügbar sind. Daher werden in dieser Arbeit Ansätze untersucht, wie mit LIBS durch Kombination mit multivariater Statistik auch ohne matrix-angepasster Standards quantitative Bestimmungen in Polymeren möglich sind.

Acknowledgements

First of all, I would like to thank Andreas Limbeck, who supervised this thesis. I highly appreciate, that the door to his office was always open and he always found the time to discuss new results and different approaches when experiments got stuck. Besides providing outstanding scientific supervision, our discussion on all kinds of different sports were always a pleasant break from work. Maybe at some point in the future we will see a Champions League final where Red Bull Salzburg beats Bayern München. I also like to express my gratitude that he gave me the opportunity to attend and present my work at ten international conferences in Europe and the USA and enabling me to spent three months in California working as a guest researcher at Applied Spectra, Inc.

I am grateful to Infineon Austria AG and KAI GmbH for the opportunity to carry this work out in close cooperation with an industrial partner. From the company I want to thank Michael Nelhiebel, Carsten Schäffer, Holger Döpke, Steffen Jordan, Stefan Schwab, Thomas Augustin and Stefan Miethaner who took part in my monthly telefon conferences and who provided not only constant feedback and critical questions on my work but also helped with providing a wide range of different samples.

Special thanks go to Silvia Larisegger who was the main link between TU Wien and Infineon during my work. Her deep insight and understanding of the Infineon network was an important factor to assure the fruitful cooperation. Additionally, she offered seemingly endless input of ideas on which scientific questions to pursue and therefore is highly responsible for the scientific success of this work. Besides providing academic guidance, she always was there with advice for all kinds of life situations. No matter what, her support was always something I could count on.

I would also like to thank Jhanis Gonzalez and Jong Yoo who offered to welcome me as a guest researcher at Applied Spectra, Inc. in Sacramento, California. Even though being interrupted by a global pandemic, this visit helped me a lot to improve my scientific skills and allowed me to get different perspectives not only in the scientific field.

Hans Lohninger I want to thank for his immense input on statistics and data evaluation which highly contributed to this work. Whenever I got stuck or was unsure on how to proceed, I could always count on him finding the time to discuss my results and approaches.

I would like to thank my fellow PhD colleagues from our research group: Christopher Herzig, Stefan Smetaczek, Maximilian Weiss, Felix Horak, and Jakob Willner. It was a pleasure working with you. I think we had a great work environment with outstanding mutual support in all situations. Many thanks also go to all bachelor and master students who contributed to this work:

viii

Maximilian Mayr, Lisa Laa, Stefan Jäger, Tobias Schöberl and Zuzana Gajarská, I highly appreciate your effort, commitment, and contribution to this work.

With finishing my PhD, my journey at TU Wien now lasts almost ten years. During this time I met a lot of different people and made new friends which were one of the main reasons for having a great and successful time at university. Special thanks go to Christopher Herzig. I think it is safe to assume that since our Bachelor program, we studied (very successfully) together for more than 90 % of all our exams. I would also like to thank Christopher Herzig and Stefan Smetaczek for all the entertaining lunch breaks combined with heated discussions we had on all kinds of different topics. Due to our lunch breaks I now have a solid knowledge on how to restore old brickwork and what types of paints to avoid when painting a wall. Katharina Mairhofer and Lars Varain I want to thank for the good times we had at the numerous company meetings and workshops we attended together. A special thank also goes to Dorian Bader for the fun times we had hiking and biking together and overall being a good friend.

Of course I also want to thank all other friends outside from university who all were an important part providing the necessary work-life balance: Thank you to the "Salzburger"-group who made the last ten years in Vienna an amazing chapter of my life. I really appreciate the friendship, great memories and activities we all share and that even after more than ten years, we are all still in contact and all supporting each other. A special thanks also goes to the DnD-group for all the fun evenings we had. I would also like to thank my brother for being a great companion for all the outdoor activities we did together in the last few years. Riding a bike for 14 hours is an outstanding way to clear the head.

My gratitude also goes to my parents who always supported me and my decisions in every possible way. I especially want thank them for their financial support during the first few years in Vienna which allowed me to solely focus on my studies. Last but not least I want to thank my partner Sandra. Thank you for walking this path together for the last ten years and helping and supporting me in every imaginable way. Also thank you for your understanding for the occasional long evenings or weekends I had to spend in the lab.

List of Abbreviations

ABS	**A**rylonitrile **B**utadiene **S**tyrene
ANN	**A**rtificial **N**eural **N**etworks
DTA	**D**ifferential **T**hermal **A**nalysis
DRC	**D**ynamic **R**eaction **C**ell
EPMA	**E**lectron **P**robe **M**icro **A**nalysis
FT-IR	**F**ourier **T**ransform-**I**nfrared spectroscopy
KED	**K**inetic **E**nergy **D**iscrimination
LA-ICP-MS	**L**aser **A**blation - **I**nductively **C**oupled **P**lasma - **M**ass **S**pectrometry
LIBS	**L**aser **I**nduced **B**reakdown **S**pectroscopy
LOD	**L**imit **O**f **D**etection
MALDI-TOF-MS	**M**atrix **A**ssisted **L**aser **D**esorption/**I**onization - **T**ime **o**f **F**light - **M**ass **S**pectrometry
M/Z	**M**ass-to-**C**harge **R**atio
PAK	**P**oly**a**crylate
PAN	**P**oly**a**crylo**n**itrile
PCA	**P**rincipal **C**omponent **A**nalysis
PCR	**P**rincipal **C**omponent **R**egression
PE	**P**oly**e**thylene
PI	**P**oly**i**mide
PLA	**P**oly**l**actic **A**cid
PLS	**P**artial **L**east **S**quares
PMMA	**P**oly**m**ethyl**m**eth**a**crylate
PS	**P**oly**s**tyrene
PSU	**P**oly**su**lfone
PVA	**P**oly**vinyl**a**cetate
PVC	**P**oly**vinyl**c**hloride
PVP	**P**oly**vinyl**p**yrrolidone
Py-GC-MS	**Py**rolysis - **G**as **C**hromatography - **M**ass **S**pectrometry
RDF	**R**andom **D**ecision **F**orest
SIMS	**S**econdary **I**on **M**ass **S**pectrometry
SNR	**S**ignal-to-**N**oise **R**atio
SRM	**S**tandard **R**eference **M**aterial
TGA	**T**hermo **G**ravimetric **A**nalysis
XRF	**X**-**R**ay **F**luorescence analysis
XPS	**X**-ray **P**hotoelectron **S**pectroscopy

Contents

1. Introduction

In the last decades, synthetic polymers have become omnipresent in most parts of our daily lives. In the year 2019, 359 million tonnes of plastics have been produced worldwide [1]. As polymers are a material class which comes with a wide range of different physical and chemical properties, they are applied in many different industries. Polymers are mainly employed as packaging material for consumer goods in the form of boxes and bottles but are also commonly used as a construction material [2]. With their wide-spread use as one-way packaging material great effort is taken to adapt adequate recycling and waste management systems [3]. Nevertheless, at the end of their life-cycle, polymers often end up in the form of microplastics causing a threat to the environment [4]. More demanding applications for polymers include e.g. the semiconductor industry, where polymers are often used as a packaging and encapsulation material for electronic devices [5, 6]. In this case, the main function of the polymer is to protect the underlying electronic device from environmental influences such as humidity, UV-radiation, and contaminations. Additionally, the polymeric encapsulation material provides electronic insulation and mechanical stability. Employed materials usually consist of a polymer with a wide range of (in)organic additives allowing to tune the necessary characteristics [7]. Inadequate protection of the packaging material may lead to corrosion phenomena which can lead to failure of the electronic device. With the wide spread use of electronic devices not only in the consumer-goods field but also in more critical applications such as medical appliances, cars, and aviation where device failure may lead to severe consequences, reliable application is of utmost importance [8]. Figure 1.1 shows a schematic drawing of an encapsulated microchip. With increasing miniaturization in the semiconductor industry, the demand for polymers employed in this field is constantly increasing. This demand of novel high-performance polymers goes hand-in-hand with the need for novel analytical tools for a more comprehensive characterization of employed polymers as e.g. bulk analysis is not sufficient anymore. These tools will not only be able to help to improve and characterize polymers employed in the semiconductor industry but are applicable to all fields where polymers are used.

Polymers usually consist of a carbon-based back-chain with various lengths and different functional groups influencing the properties of the material. Besides the basis material, often additives (e.g. plasticizers, antioxidants, antistatic agents, lubricants, flame retardants or inorganic pigments) are used to fine-tune the material properties for individual, high-demanding applications [9]. As improvements of material properties can only be achieved with analytical
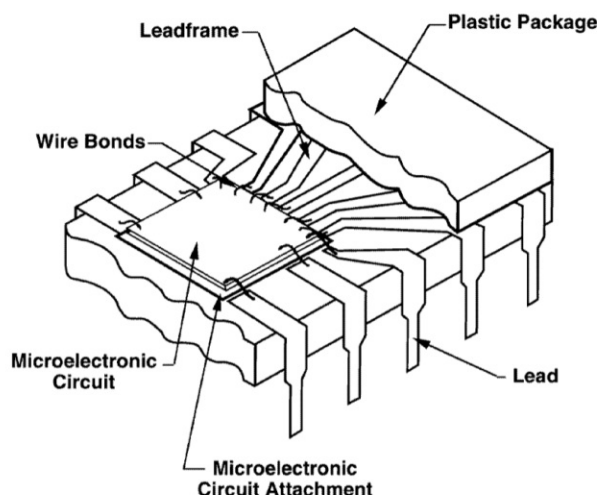
FIGURE 1.1: Schematic drawing of an encapsulated microchip
using a polymeric packaging material [8].

techniques which enable a thorough material characterization, there are several
well-established methods which are used for this purpose.

Conventionally, techniques such as Fourier Transform-Infrared spectroscopy
(FT-IR) and Raman-spectroscopy are used for the characterization of poly-
mers [10]. Besides being able to classify different polymer types by providing
molecular specific information [11, 12, 13], these techniques are also used to
investigate the degradation behavior of polymers [14, 15]. Other techniques
which are used for the characterization of polymers include Matrix Assisted
Laser Desorption/Ionization - Time of Flight - Mass Spectrometry (MALDI-
TOF-MS), which is an established technique for the determination of a polymers'
structure, composition and molecular mass [16]. Pyrolysis-Gas-Chromatography
(Py-GC-MS) [17] and Thermo Gravimetric Analysis/Differential Thermo Anal-
ysis (TGA/DTA) [18, 19] are techniques which are capable of characterizing
the degradation behavior of polymeric materials when exposed to elevated tem-
perature by either detecting the degradation products or measuring the mass
loss. X-ray based techniques, such as X-ray Photoelectron Spectroscopy (XPS)
have been employed to study the polymer-air interface and to characterize the
surface morphology of polymers [20, 21]. Even though, the aforementioned
techniques provide great insight into the chemical and physical characteristics of
polymers, there are still some properties which can not be analyzed with these
methods. In the last few decades, detecting bulk properties was sufficient for
material characterization but in recent years, with the development of more
sophisticated analytical techniques, spatially resolved analysis has become the
state-of-the-art for material characterization which in many cases is not yet
possible for polymer analysis. Additionally, the quantitative determination of
trace metal content with a high sensitivity is gaining more and more interest,
not only because of material properties but also due to environmental regulations.

In this work analytical approaches are developed using the two laser-based analytical techniques LA-ICP-MS and LIBS for a more comprehensive polymer characterization. LA-ICP-MS and LIBS are both analytical techniques which use the process of laser ablation for the analysis. In general, a high-energy pulsed laser-beam is focused on the samples surface. When the laser beam interacts with the sample, material is ablated and a localized plasma is formed on the ablation spot. In this plasma, the ablated material is partly atomized, ionized and excited. When performing LIBS experiments, light emitted from the laser-induced plasma is collected and detected [22, 23]. After a certain time particles begin to condense from the ablated material. When performing LA-ICP-MS, these particles are transported to an ICP-MS usually using a helium gas flow [24]. Depending on the pulse duration of the employed laser system different properties of the laser-induced plasma as well as the generated particles are obtained [25, 26]. In the LA-ICP-MS and LIBS community usually laser pulses in the nanosecond (ns) or femtosecond (fs) time regime are used. Figure 1.2 illustrates the time-depending processes happening after laser irradiation interacting with a sample surface.
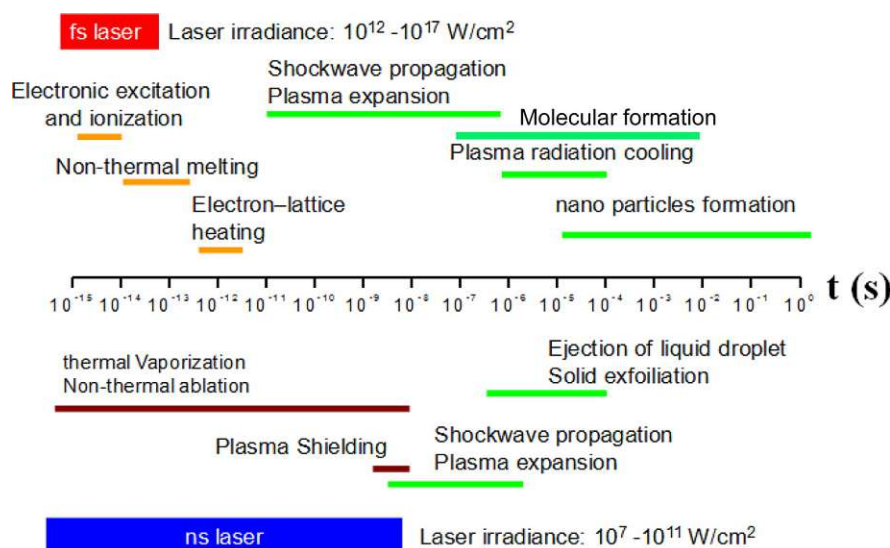

FIGURE 1.2: Physical mechanisms occurring after pulsed laser (ns and fs) radiation interacting with a solid sample over a time frame of 15 orders of magnitude [24]

As LIBS and LA-ICP-MS both operate on the same principle of analyzing a solid sample with a pulsed laser, instrumentation for a combined use in a so-called tandem LA-ICP-MS/LIBS-setup was recently proposed and developed. By combining the two techniques, several complementary advantages can be exploited. With LIBS enabling the detection of H, O, C, F, and N, important elements which are not accessible with ICP-MS can be detected in a tandem setup [27]. Elements such as Mg and Ca which are difficult to analyze with ICP-MS due to interferences show a high sensitivity in LIBS measurements. Additionally, as especially in imaging and single-shot depth profiling experiments, a conventional quadrupole ICP-MS system is restrained to a limited number

of detected elements due to the nature of its sequential measurement, a tandem LA-ICP-MS/LIBS setup can be beneficial for multi element analysis [28, 29].

LA-ICP-MS and LIBS being mainly considered analytical techniques for the characterization of the elemental composition in materials science, geo-science or biological samples [30, 31]. Besides conventional bulk analysis, LA-ICP-MS and LIBS both offer lateral resolved analysis with resolutions in the low single-digit µm up to several hundred µm range. Additionally, depth profiles can be recorded with depth resolutions ranging from hundreds of nm up to several µm. A very promising feature for polymer characterization is the possibility to use LIBS for the detection of elements such as H, O, C, and N, which are usually the major constituents of synthetic polymers.

In the literature, there is already work published where these two laser-based methods are used for the characterization of organic polymers. Especially LIBS has proofed to be an innovative analytical tool in the field of discrimination and classification of synthetic polymers [32, 33]. Nevertheless, LA-ICP-MS and LIBS have not been used to their full potential in the field of polymer analysis yet. Therefore, the main goal of this work was to investigate novel applications of LA-ICP-MS and LIBS in the field of polymer characterization.

2. Analytical Challenges

In this chapter, the analytical challenges and main research topics of this work are introduced and presented. The analytical challenges can be divided in three different sections:

- Spatially resolved analysis

- Investigation of polymer degradation

- Quantitative metal analysis in polymers

2.1 Spatially Resolved Analysis

In the last few decades, the field of analytical chemistry was mainly focused on the determination of bulk properties (e.g. measuring the total content of major, minor, or trace constituents) for material characterization. With current improvements and development of novel techniques and with increasing requirements for a more comprehensive characterization of materials, spatially resolved analysis has become the state-of-the-art in many fields. Spatially resolved analysis is usually based on either measuring the lateral distribution on the sample surface or on recording depth profiles of a materials' properties. In other cases even three dimensional analysis is possible. When it comes to spatially resolved (elemental) analysis, besides sensitivity and selectivity, the lateral as well as the depth resolution arises as an important figure of merit for an analytical technique. When performing spatially resolved analysis, different properties of interest of a material, such as the elemental distribution in regions of interest (e.g. on the interface between two materials, or concentration gradients within a material) can be investigated [34]. Besides recording so-called elemental maps, various analytical techniques additionally offer the possibility to perform spatially resolved classification of materials by using e.g. elemental finger-printing (the distribution of a marker element is correlated with a certain material type) or using another material specific signal [35].

Nowadays, there are many different analytical techniques, such as X-Ray Fluorescence Analysis (XRF), Electron Probe Micro Analysis (EPMA), Auger Electron Spectroscopy (AES), X-ray Photoelectron Spectroscopy (XPS) or Secondary Ion Mass Spectroscopy (SIMS), that can provide either laterally resolved elemental analysis, depth profiling or even spatially resolved analysis. Each of these techniques comes with certain advantages and limitations: EPMA, AES,

XPS and SIMS require complex instrumentation for the analysis. AES, XPS and SIMS offer excellent depth resolution in the nm range which is beneficial for the characterization of thin films in the nm range. Nevertheless, when characterization of samples in the µm range is required, these techniques can not be employed. Besides providing elemental analysis, XPS and AES can also be used to gain additional information about the chemical bonds of the analyte [36]. Figure 2.1 gives an overview of commonly used analytical techniques for elemental imaging and their respective lateral resolution and detection range. LA-ICP-MS and LIBS both offer an excellent sensitivity covering a detection range of the sub-ppm range up to the detection of major constituents while still providing adequate lateral resolution enabling the analysis of sample areas up to cm^2 [37].
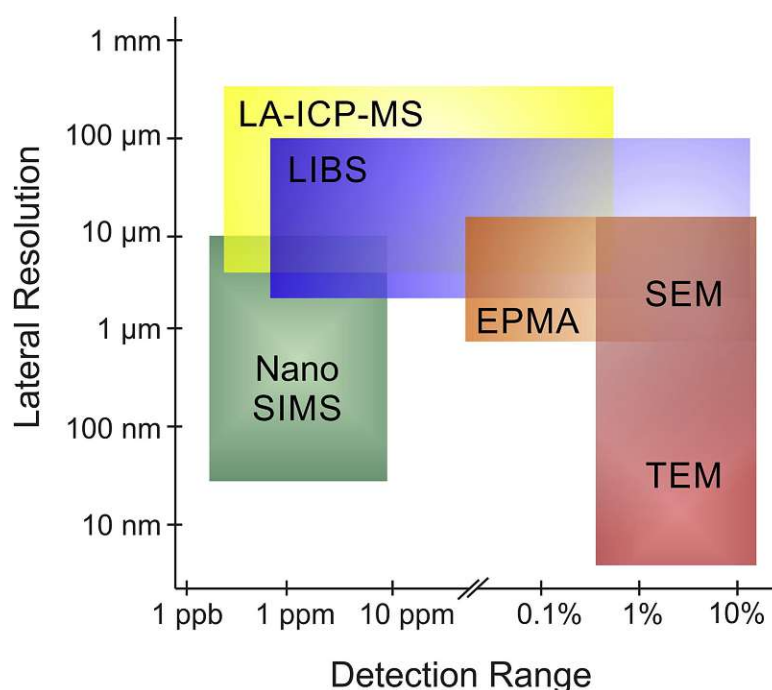

FIGURE 2.1: Figures of merit (lateral resolution and detection range of common analytical techniques used for elemental imaging [37].

When it comes to polymer analysis, often the determination of the elemental distribution within a polymeric sample is not sufficient for characterization. As several materials have been developed consisting of multiple different polymer types [38, 39], spatially resolved classification of different polymer types becomes important for the characterization of such materials. Besides spatially resolved classification of composite materials, the possibility to differentiate polymer types with minimal instrumental requirements and short measurement times is also important for the recycling industry [40]. Spatially resolved identification of different polymer types is not only important in the field of materials' science and the recycling industry but also can find applications in the field of cultural heritage science where polymers are often used in combination with pigments as paints [41]. In this case, identification of materials used in artworks

is crucial for choosing proper restoration techniques and to identifying art forgery.

Using LIBS for spatially resolved polymer classification provides significant advantages over established analytical techniques such as FT-IR or Raman spectroscopy. As LIBS ablates material with each laser shot, analysis of distributions of different polymer types in depth becomes accessible. Additionally, simultaneous to polymer classification, LIBS provides elemental information from the sample under investigation enabling a more comprehensive characterization of a material with only one measurement. Nevertheless, as polymers usually consist of the same elemental components (C, H, O, and N) differentiating between different polymer types using LIBS data is not always an easy task as small differences in the obtained LIBS spectra have to be used. Often sophisticated multivariate data evaluation strategies are required to obtain reliable results. For this reason, until now polymer classification from LIBS data was usually carried out by accumulating multiple measurements on a sample improving the signal-to-noise ratio (SNR) and therefore facilitating the classification task. This approach though prohibits spatially resolved classification of polymers with a high resolution from LIBS data.

In this work, the applicability of LIBS for spatially resolved polymer classification (2D and 3D mappings) combined with multivariate statistics using single-shot spectra is evaluated for the first time.

2.2 Investigation of Polymer Degradation

For reliable application, for every material expected changes in the physical and chemical properties over application time caused by exposure to environmental conditions have to be estimated. This is also the case for polymers which are often exposed to different conditions such as UV-radiation, corrosive conditions, humidity and temperature changes due to their wide application range. It is important to evaluate not only degradation of polymer properties but also to develop models for specific degradation mechanisms resulting in a deeper understanding of the material. This allows to design novel polymers with high-performance properties withstanding harsh conditions opening up new application fields. Besides developing new materials, often the stability of existing materials can be enhanced using different additives. Material degradation is often assessed by performing accelerated stress tests in time-dependent studies where samples are exposed to harsh conditions for various times to determine material failure [42].

When it comes to polymer degradation, several different mechanisms causing degradation have been reported in the literature [43, 44]. As polymers consist of a carbon-based backbone chain with different functional groups, these molecules are usually prone to oxidation [45]. In many cases, degradation is caused by the presence of UV-radiation [46, 47] or elevated temperatures combined with oxygen [48]. An overview of different forms of polymer degradation is shown in Figure 2.2. Besides the degradation of the polymeric network, also the uptake

of (in)organic species may affect the material properties and therefore its applicability. Polymers are often used as protective coatings for materials such as steel, metallic alloys but also electronic devices [49, 50, 51]. In this case, the main function of the polymer is to prevent diffusion of mobile, corrosive species to the underlying material.
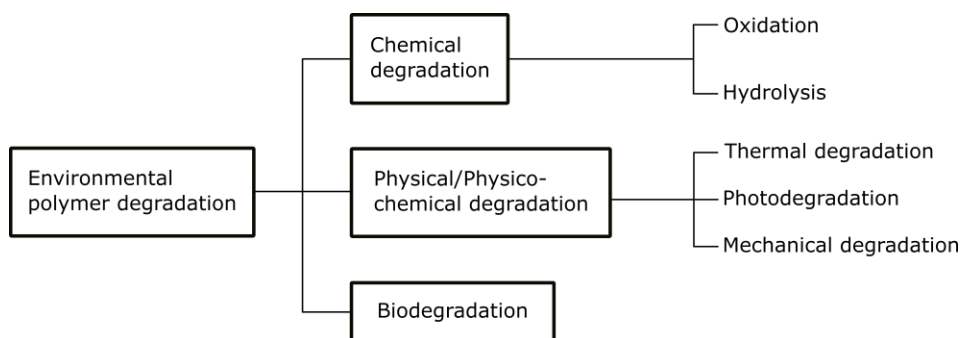

FIGURE 2.2: Overview of different forms of polymer degradation adapted from Abioye et al. [52].

There are several analytical techniques commonly used to study the degradation behavior of polymers which all come with unique advantages and disadvantages. FT-IR and Raman spectroscopy provide polymer specific signals that change if the the investigated sample degrades. For investigations of changes in functional- or side groups of the polymer structure, FT-IR spectroscopy proofs to be useful, whereas Raman-spectroscopy is used to study the chain conformation of a polymer [53, 54]. With these two techniques, not only bulk characterization but also laterally resolved analysis of the sample surface is accessible [15, 55]. With TGA and DTA mainly the thermal stability as well as the decomposition products of polymers can be investigated. This is useful to assess degradation mechanisms [19, 18]. However, these techniques only provide bulk information of the sample. Information about degradation of polymers with regard to the sample depth, which is of interest when investigating polymer used as protective layers, is not accessible with any of the aforementioned techniques.

As LIBS provides polymer specific signals, the assessment of polymer degradation using LIBS spectra should be investigated. If LIBS signals can be identified that correlate with polymer degradation, this would bring many benefits and new opportunities for characterizing polymer degradation. First of all, LIBS allows the analysis of depth profiles. Therefore, investigations of polymer degradation would not be limited to surface near regions or the bulk, as it is with current techniques. As polymer films are often used to protect the underlying material from corrosive inorganic species (such as SO_2, H_2S or Cl^-), information about the migration of these species is available from LIBS analysis as it allows simultaneous multi-element analysis. If the concentrations of the inorganic species under investigation is below the limit of detection (LOD) for LIBS, a combined use of LA-ICP-MS and LIBS in a tandem setup is possible improving the sensitivity significantly. Therefore, the combined use of LA-ICP-MS and LIBS is a

promising tool for a more comprehensive characterization of polymer degradation.

One element of interest, when investigating the migration behavior of inorganic species in polymer is sulfur. Sulfur is an element that is very challenging to detect with either optical methods like LIBS or mass-spectrometry like ICP-MS due to various reasons. The most intense emission line of sulfur is in the UV-range at 180.73 nm. Since the oxygen present in the air absorbs UV-radiation, special instrumentation, in which the optical path and detection unit are flushed with an inert gas such as argon, are necessary to allow the detection of radiation with a wavelength < 200 nm. With conventional instrumentation, other, less intense emission lines of sulfur in the IR-region are used limiting the sensitivity. There are also challenges that have to be taken into account using ICP-MS for the detection of sulfur. First of all, ionization efficiency within an argon-based ICP is limited due to the high first ionization energy of 10.4 eV [56]. Sulfur has 4 stable isotopes, namely ^{32}S, ^{33}S, ^{34}S, and ^{36}S with ^{32}S showing the highest abundance with 95%. As ^{32}S has an isobaric interference with ^{16}O^{16}O, which can not be resolved using a conventional quadrupole ICP-MS, the less abundant isotope ^{34}S is used for detection. This sulfur isotope is also interfered by the (less abundant) species ^{16}O^{18}O. To resolve this interference, special measurement modes such an kinetic energy discrimination (KED) or a dynamic reaction cell (DRC) can be employed [57, 58].

In this work, the ability of LIBS to detect degradation and oxidation of polymers exposed to harsh environmental conditions is investigated. Additionally, the advantages of a tandem LA-ICP-MS/LIBS setup is used to allow a combined detection of polymer degradation using LIBS with a simultaneous highly sensitive detection of the uptake of inorganic species.

2.3 Quantitative Metal Analysis in Polymers

In the polymer industry often (in)organic additives are used for the fine-tuning of material properties. The concentration levels of these additives and also inorganic contaminations, which may originate from the manufacturing process, have a huge influence on the applicability of the product. For example, in the food packaging industry where polymers are often used as a packaging material, concentrations of heavy metals have to be monitored to assure their safe application [59]. Due to these reasons, an accurate analysis and characterization of metal contents in polymers is of great interest. As mentioned in Chapter 2.1, conventional bulk analysis is still the most-widely accepted approach for this type of analysis in the industry.

The procedure of conventional bulk analysis of metal content of a material usually includes dissolving the material under investigation and performing either a liquid ICP-MS or liquid ICP-OES measurement. Quantitative results are usually easily obtained by a subsequent analysis of liquid standard reference material (SRM). With this procedure being developed and validated for many different material types, it still poses many challenges when it comes to polymer

analysis.

One of the biggest challenges for conventional bulk analysis of polymers is that polymers are usually difficult to dissolve because they are often chemically inert. To achieve quantitative digestion, depending on the polymer type harsh and hazardous chemicals have to be used. Additional procedures such as a microwave-assisted digestion or combustion protocols are often necessary to transform the sample into a solution [60, 61]. Besides requiring large amounts of chemicals, which is neither ecological nor economical favourable, these procedures are prone to contaminations causing an overestimation of the investigated elements. Additionally, underestimation of the analyte of interest may be caused by the formation of volatile components during the digestion procedure. Due to the application of harsh chemicals for the digestion, dilution steps are usually obligatory to ensure a compatibility of the obtained solution with the analytical instrumentation. These dilution steps, which are also required to achieve a matrix-adjustment to the liquid standards used for quantification, limit the sensitivity of this approach.

The aforementioned reasons led to an increasing interest in the development of quantitative direct-solid sampling techniques such as LA-ICP-MS and LIBS which are capable of overcoming the above-mentioned drawbacks by eliminating the need of sample preparation. Nevertheless, these methods come with one significant drawback: due to matrix-effects obtaining reliable quantitative results is a challenging task [62, 24, 63].

In general, matrix-effects, occur when the signal response obtained from a measurement is dependent on physical or chemical properties of the sample under investigation. During LA-ICP-MS and LIBS measurements matrix-effects mainly originate from the laser-matter interaction which is highly dependent on the physical properties of the sample. In the case of LIBS, depending on the material different amounts of the provided energy of a laser pulse are used for sample ablation, resulting in different amounts of energy being available for subsequent excitation in the laser-induced plasma. This results in different plasma conditions and therefore matrix-dependent excitation efficiencies of the analytes [63].

For LA-ICP-MS, the size distribution of the generated particles after the laser ablation process is one of the main reasons for different signal responses. Different materials ablated with the same laser conditions show different ablation rates and size distributions of the generated particles. The size distributions of the generated particles is not only crucial for the transport efficiency from the laser system to the ICP-MS but also for the evaporation, atomization and ionization efficiency within the ICP [25]. Besides particle size influencing the signal response in LA-ICP-MS, elemental fractionation may occur during laser ablation which is caused by different physical properties (e.g melting and boiling point) of different elements [64]. Even though, it was reported in the literature that the use of laser pulses in the range of femtoseconds can significantly reduce

matrix-effects in LA-ICP-MS [65], they are rarely available in analytical laboratories due to there high cost.

Therefore, the application of matrix-matched standards for quantitative measurements for LA-ICP-MS and LIBS analysis is necessary [66, 67]. Before the application of standards for instrument calibration, a comprehensive characterization of the standard has to be carried out where the nominal concentration of the analytes present in the standard is determined and also a homogeneous distribution is assured. For a selected number of commonly-used materials, SRMs are available from accredited institutions like the National Institute of Standards and Technology (NIST) or the Institute for Reference Materials and Measurements (IRMM). Even for a limited number of polymer types, SRMs are available. Nevertheless, SRMs usually contain only a limited number of certified elements and do not cover the wide range of different polymeric materials used nowadays. Additionally, usually only the bulk properties of these materials are certified as it is difficult to assure adequate homogeneity on the µm scale. Therefore, often in-house prepared standards or other approaches (e.g. multivariate data evaluation strategies or identification of a proper internal standard) have to be developed to obtain reliable quantitative results from direct solid-sampling techniques.

In this work, a library of in-house prepared standards of different polymer type is prepared. Using LIBS data from this library combined with multivariate statistics, different data evaluation strategies are investigated which can overcome the limitations of matrix-matched standards for quantitative measurements in polymers.

3. Proposed Approaches for Polymer Characterization

3.1 LA-ICP-MS/LIBS Imaging and Depth Profiling

LIBS and LA-ICP-MS are analytical techniques which use a pulsed laser do probe the sample under investigation. When a high energy pulsed laser interacts with a solid sample, material is ablated and a laser induced plasma is formed on the sample surface. In the laser induced plasma, the ablated material is partly atomized, ionized and excited. When the excited states of the atoms, ions, and molecule fragments present decay, radiation is emitted. In the case of LIBS, the emitted radiation of the laser induced plasma is collected using a collection optics. The collected light is transported to a monochromator using optical fibers. In the monochromator the collected light is separated by the wavelength using either a prism or a grating. The separated light is detected using a CCD chip and a spectrum is recorded. Broadband LIBS spectra cover a wavelength range from UV-radiation to IR-radiation enabling simultaneous multi-element analysis of all elements of the periodic table. Additionally, to some extend also molecular information originating from incomplete atomization or recombination within the laser induced plasma is accessible [68]. Figure 3.1 shows a schematic overview of the principle and required instrumentation for LIBS analysis.

When the laser induced plasma cools down, the atomized sample material condensates and particles are formed. In the case of LA-ICP-MS, the formed particles are purged from the ablation chamber using a helium gas flow and transported to an ICP-MS. In the ICP, the particles are atomized and ionized. The formed ions are transferred to a high vacuum where they are separated by their mass-to-charge (M/Z) ratio and detected. Conventionally, a quadrupole mass analyzer is used for the ion separation. Due to the sequential operation mode of a quadrupole, limitations in the number of elements detected in LA-ICP-MS experiments arises. LA-ICP-MS offers a highly sensitive detection of the elemental composition of the sample [69]. A schematic overview of LA-ICP-MS is shown in Figure 3.2.

Both LA-ICP-MS and LIBS can correlate the obtained signal with the spatial coordinates on the sample enabling imaging and depth profiling. By combining
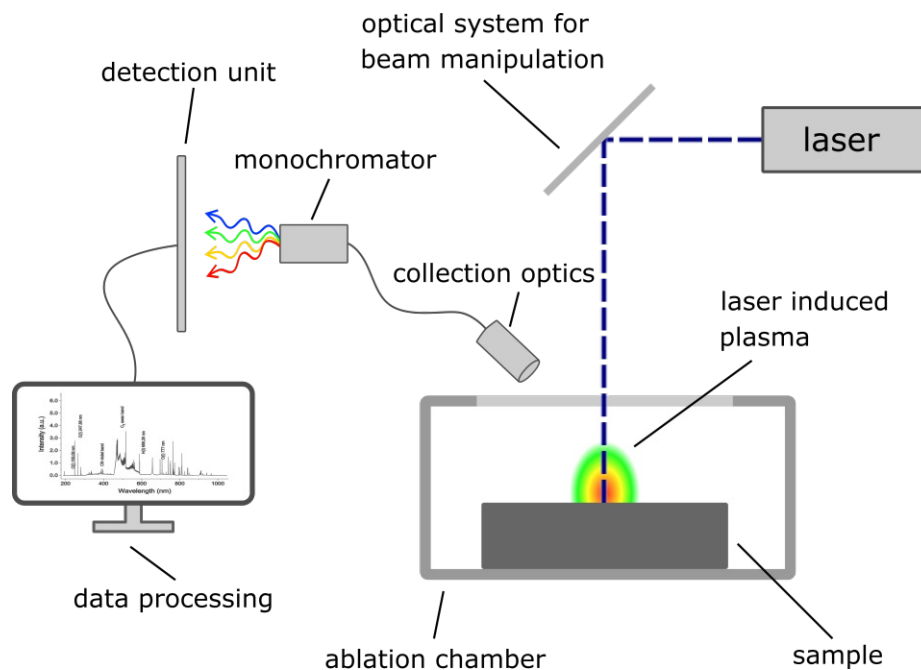
FIGURE 3.1: Schematic drawing of the principle and required instrumentation for LIBS analysis.

imaging and depth profiling also 3D analysis is possible. There are different approaches on how to obtain spatially resolved information using LA-ICP-MS and LIBS. Both measurement modes come with distinct advantages and disadvantages and usually the measurement parameters have to be optimized individually to guarantee a high quality analysis. As both LA-ICP-MS and LIBS operate on the same principle of probing the sample with a pulsed laser, the concept of spatially resolved analysis is similar for both techniques [68, 70].

For LA-ICP-MS imaging experiments, the sample is scanned with the laser either using line-scans or spot-scans. Regarding line-scans, the individual laser shots can usually not be resolved due to a limited washout efficiency of the ablation chamber and a transient signal is obtained on the ICP-MS. Images can be calculated from the transient signal using the information of the spot-size of the laser and the scan-speed of the stage. In the case of spot-scans, adjacent laser shots are performed on the sample and the signal produced from each individual shot is evaluated. This approach offers an improved image quality but requires longer measurement times. With the emerging of ultra-fast washout cells for LA-ICP-MS, spot-scans for imaging have become more popular in the last few years as with these cells washout times in the ms-range are possible. This enables measurement with much higher laser repetition rates resulting in faster analysis and therefore either the investigated area or the lateral resolution can be increased. Nevertheless, with smaller spot-sizes, the amount of material ablated is reduced and therefore limited by the SNR of the obtained signal. Therefore, parameters have to be optimized carefully in preliminary experiments for a successful measurement. As LIBS is independent from the washout speed of the ablation chamber, LIBS imaging experiments are usually carried out using
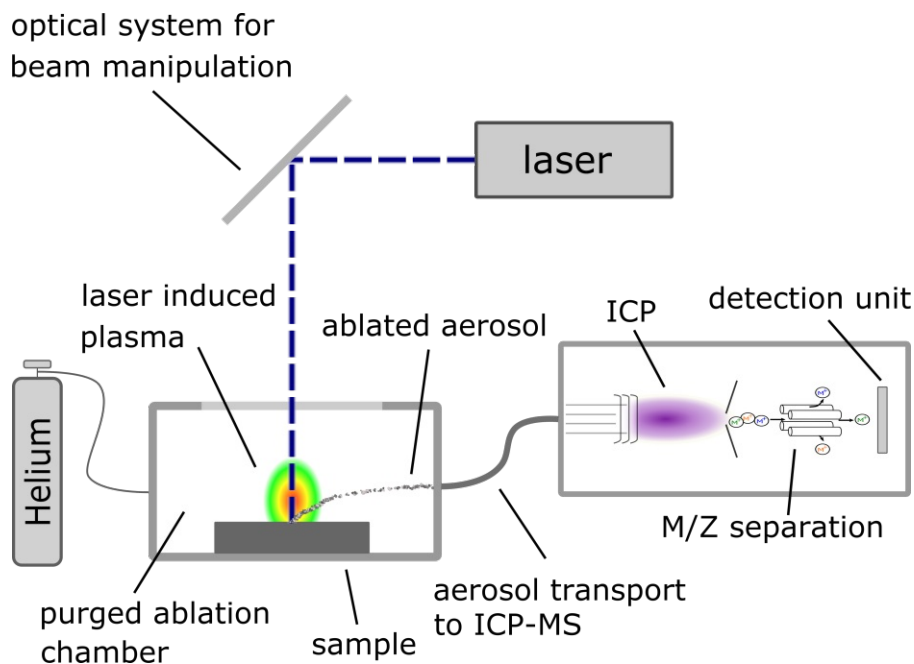
FIGURE 3.2: Schematic drawing of the principle and required instrumentation for LA-ICP-MS analysis.

spot-scans. [34, 69].

When depth profiles are performed using LA-ICP-MS and LIBS many different influences have to be considered to accomplish optimal results. Each laser shot ablates an amount of material fundamentally enabling depth profiling. The amount of material that is ablated and therefore the obtained depth resolution is influenced by the samples' properties, and the laser fluence [71]. Again, depth profiling can be carried out in different measurement modes each coming with unique advantages and disadvantages: a subsequent spot-scan on the same position, a subsequent line-scan on the same position, and subsequent images. When performing depth profiles, the energy distribution within a laser beam has to be considered. Within Nd:YAG lasers (conventionally used for LA-ICP-MS and LIBS), a Gaussian energy distribution within the beam-profile is observed. Therefore, observed craters are not perfectly cylindrical and flat-bottomed after a laser ablation process. This leads to so-called crater effects and smearing of the depth profile when analyzing thick samples [72, 73]. The influence of crater effects can be reduced by analyzing subsequent line-scan with overlapping laser shots on the same position. Nevertheless, with this approach the depth resolution is limited. For optimal results, the measurement mode as well as measurement parameters have to be optimized with respect to the investigated material and the necessary depth resolution and sensitivity.

By combining both imaging and depth profiling, the 3D information of a sample can be obtained. Even though time-consuming, this approach can offer great insight and benefits when it comes to material characterization and analysis.

3.2   Multivariate Statistics

In general, multivariate statistics involves data evaluation strategies where not only one variable is used to model a certain property but rather multiple input variables are used. This approach offers many advantages, even though coming with a more complicated data evaluation [74]. In many analytical techniques just one signal is detected. Thus, the analyte concentration and measured signal is correlated by establishing an univariate calibration function (e.g. Lambert-Beer law in atomic absorption spectroscopy). However, as LIBS is a spectroscopic method detecting light at different wavelengths, each detected intensity can be used as an input variable for data evaluation. Therefore, LIBS can highly benefit from multivariate data evaluation strategies [75]. Figure 3.3 schematically illustrates the difference between univariate and multivariate data evaluation from LIBS data. In this example, for the univariate calibration model only the sodium emission signal is used as an input variable to model the sodium concentration whereas for the multivariate approach additional emission signals originating from the investigated polymer sample are added to improve the performance of the evaluation.

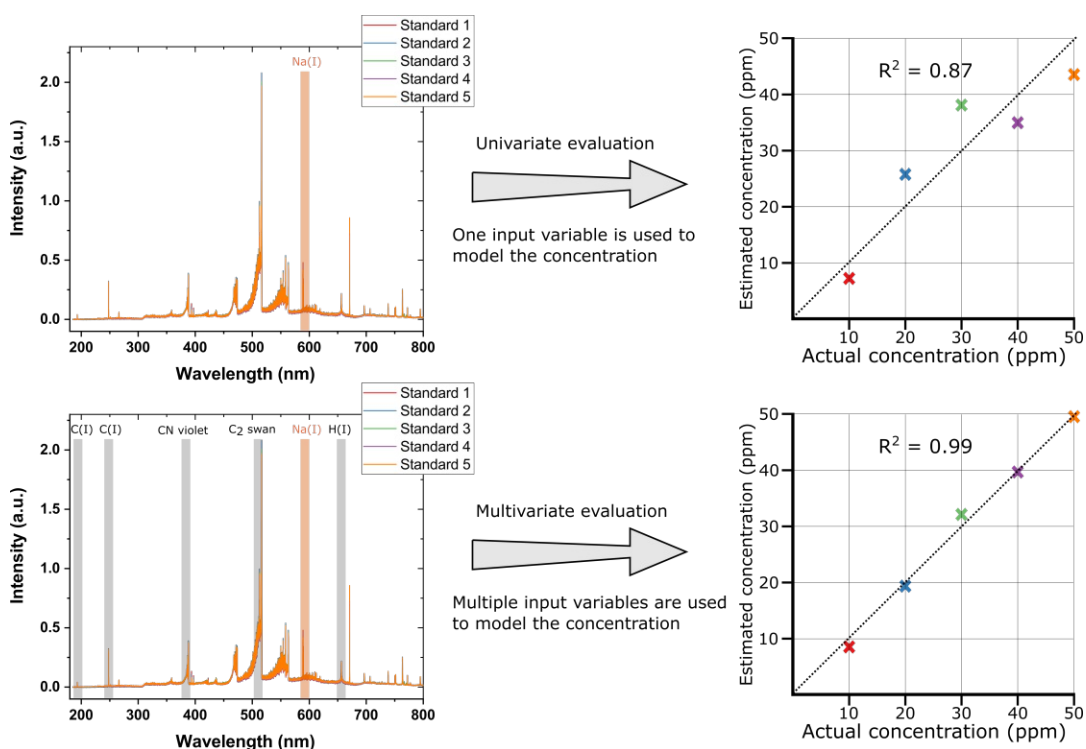FIGURE 3.3: Schematic example of univariate and multivariate data evaluation for the determination of the sodium concentration in polymer standards. Univariate data evaluation uses only one input variable (the sodium emission signal) to built a statistical model whereas multivariate data evaluation uses additional information (polymer-specific emission signals) from the LIBS spectrum as input variables to improve the performance.

Another field of application that greatly benefits from multivariate data evaluation strategies is sample identification, discrimination and classification. LIBS has already been reported in the literature to perform polymer classification. The classification of polymers from LIBS data can usually not be achieved by simply evaluating the presence or absence of an emission signal, instead the whole LIBS spectrum must be considered and small differences in obtained LIBS spectra have to be evaluated to accomplish classification and discrimination of different polymers. Therefore, LIBS spectra with a high signal-to-noise ratio (SNR), which is usually obtained by accumulating multiple spectra, is favourable. Until now, published papers only reported the classification of bulk samples where multiple spectra can easily be accumulated.

When it comes to classification of LIBS data, several multivariate methods have been applied in the literature. These methods range from simple Principal Component Analysis (PCA) [76] to more sophisticated methods such as Random Decision Forest (RDF) [77], Artificial Neural Networks (ANN) [78] and other machine learning approaches [79].

Multivariate data evaluation approaches can not only enable classification and discrimination of LIBS data but can also be used to enhance the performance of quantification approaches. Nevertheless, it should be mentioned, that multivariate data evaluation strategies are complex mathematical procedures which come with many prerequisites that have to be fulfilled. Therefore, a careless use of these tools may yield poor results [80]. Properly applied, multivariate analysis of LIBS data for quantification has found its way in the LIBS literature [81, 82]. Applied tools for multivariate calibration models include Principal Component Regression (PCR) [83], Partial Least Squares (PLS) [84], or Random Decision Forest (RDF) based calibration methods [85].

In this work, we use LIBS combined with multivariate statistics to develop a method for spatial resolved classification of different polymers by evaluating single-shot LIBS data. The developed approach was also used for an application in the field of cultural heritage science allowing a combined spatial resolved classification of contemporary art materials consisting of different polymers and inorganic pigments. Multivariate approaches applied in this work include: PCA, RDF, and k-means classification.

Besides classification of polymers, multivariate methods for the quantification of unknown polymer types or polymer types with an unknown composition where conventional matrix-matched quantification is not feasible were developed and evaluated. Therefore, a library of in-house prepared standards of 8 different polymer types was built and analyzed. This approach allowed to compare the performance of different approaches for the quantification in polymers were matrix-matched standards are not available.

3.3   Accelerated Stress Tests

Nowadays, electronic devices are often employed in fields where a high reliability is required. Therefore, estimating the life-time and possible failure mechanisms of electronic devices is crucial to assure a safe application. The investigation of polymer degradation, which is often linked to failure of the encapsulation material of electronic devices, is usually carried out by performing accelerated stress tests, that allow to observe alteration of these highly inert samples in a reasonable time [86, 87, 88].These stress tests often include harsh conditions such as elevated temperature, exposure to UV-radiation as well as exposure to corrosive gases. To investigate the capabilities of LA-ICP-MS and LIBS for the investigation of polymer degradation, various accelerated stress tests of different polymeric samples were carried out.

In this work, the ability of LIBS to detect changes in the polymeric network and oxidation of the sample was investigated. Oxidation of the sample should be observable by an increase of the observed oxygen emission signal in the LIBS spectrum. Additionally, polymer-specific signals that allow LIBS to distinguish between different polymer types are investigated for the detection of alterations in the polymeric network. Besides characterizing the degradation of the polymer, changes in the uptake behavior of inorganic species can be investigated simultaneous using LIBS. If the sensitivity of LIBS for inorganic species is not sufficient, a tandem LA-ICP-MS/LIBS system can be employed which to detect inorganic species with the ICP-MS. The most important characteristic LA-ICP-MS and LIBS offer, is the possibility to analyze depth profiles. Therefore, degradation behavior and uptake of inorganic species can be investigated in relation to the sample depth.

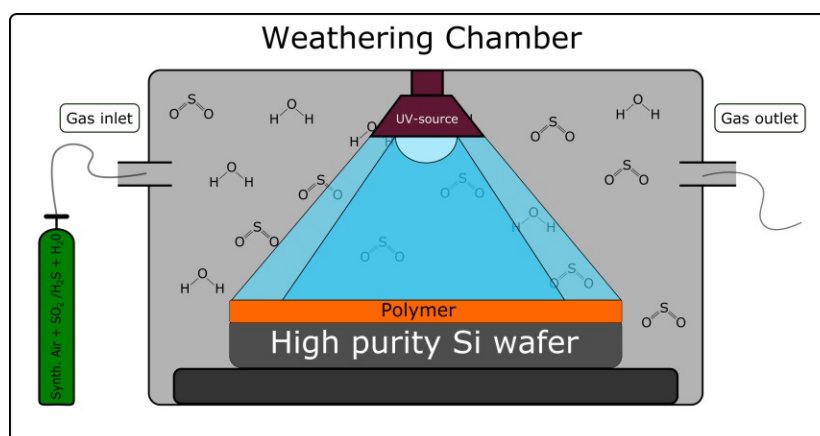FIGURE 3.4: Schematic drawing of the weathering chamber and weathering conditions used in this work.

Various different sample types, such as materials from the field of cultural heritage science, high-performance polymers employed in the semiconductor industry or polymers often found in the field of microplastics characterization were investigated. These samples were exposed to a wide range of different

ageing conditions in accelerated stress tests. These conditions include exposure to UV-radiation as well as exposure to various combinations of corrosive gases such as O_3, SO_2, and H_2S in a weathering chamber. These ageing conditions were used to investigate not only degradation of the polymer but also the influence of polymer degradation on the uptake of sulfur species. A schematic drawing of the employed chamber is shown in Figure 3.4. Another approach included an ageing procedure where samples where exposed to a combination of UV-radiation and HNO_3 with a consecutive exposure to artificial seawater containing heavy metals. In this case, the degradation of the polymer was investigated with a simultaneous characterization of the uptake of the heavy metals.

References

[1]   *Plastics Europe. Plastics - the facts 2019.* Tech. rep. 2019.

[2]   Güneri Akovalı. *Polymers in Construction.* en. iSmithers Rapra Publishing, 2005.

[3]   Shafferina Dayana Anuar Sharuddin et al. "A review on pyrolysis of plastic wastes". en. In: *Energy Conversion and Management* 115 (May 2016), pp. 308–326. DOI: 10.1016/j.enconman.2016.02.037.

[4]   Matthew Cole et al. "Microplastics as contaminants in the marine environment: A review". en. In: *Marine Pollution Bulletin* 62.12 (Dec. 2011). Number: 12 Reporter: Marine Pollution Bulletin, pp. 2588–2597. DOI: 10.1016/j.marpolbul.2011.09.025.

[5]   Noriyuki Kinjo et al. "Epoxy Molding Compounds as Encapsulation Materials for Microelectronic Devices". en. In: *Speciality Polymers/Polymer Physics.* Ed. by Yu. K. Godovsky et al. Advances in Polymer Science. Reporter: Speciality Polymers/Polymer Physics. Springer Berlin Heidelberg, 1989, pp. 1–48.

[6]   Atsuhito Hayakawa et al. "Epoxy resin composition for semiconductor encapsulation". Pat. US5739186A. Inventors: _:n2270 Issue: US5739186A. Apr. 1998.

[7]   Hideaki Sasajima et al. "New Development Trend of Epoxy Molding Compound for Encapsulating Semiconductor Chips". en. In: *Materials for Advanced Packaging.* Ed. by Daniel Lu and C.P. Wong. Cham: Springer International Publishing, 2017, pp. 373–419. DOI: 10.1007/978-3-319-45098-8_9.

[8]   John W. Osenbach. "Corrosion-induced degradation of microelectronic devices". en. In: *Semiconductor Science and Technology* 11.2 (Feb. 1996). Publisher: IOP Publishing, pp. 155–162. DOI: 10.1088/0268-1242/11/2/002.

[9]   Jan C. J. Bart. *Additives in Polymers: Industrial Analysis and Applications.* en. Google-Books-ID: ONIx_UDsl_EC. John Wiley & Sons, Apr. 2005.

[10] N. Heigl et al. "Near Infrared Spectroscopy for Polymer Research, Quality Control and Reaction Monitoring". EN. In: *Journal of Near Infrared Spectroscopy* 15.5 (Oct. 2007). Publisher: SAGE Publishing, pp. 269–282.

[11] Robin Lenz et al. "A critical assessment of visual identification of marine microplastic using Raman spectroscopy for analysis improvement". In: *Marine Pollution Bulletin* 100.1 (Nov. 2015). Number: 1 Reporter: Marine Pollution Bulletin, pp. 82–91. DOI: 10.1016/j.marpolbul.2015.09.026.

[12]   Rohit Bhargava, Shi-Qing Wang, and Jack L. Koenig. "FTIR Microspec-
        troscopy of PolymericSystems". en. In: *Liquid Chromatography / FTIR
        Microspectroscopy / MicrowaveAssisted Synthesis*. Advances in Polymer
        Science. Berlin, Heidelberg: Springer, 2003, pp. 137–191. DOI: 10.1007/
        b11052.

[13]   Andrea Käppler et al. "Identification of microplastics by FTIR and Raman
        microscopy: a novel silicon filter substrate opens the important spectral
        range below 1300 cm-1 for FTIR transmission measurements". en. In:
        Analytical and Bioanalytical Chemistry 407.22 (Sept. 2015), pp. 6791–6801.
        DOI: 10.1007/s00216-015-8850-8.

[14]   Charles A. Wilkie. "TGA/FTIR: an extremely useful technique for studying
        polymer degradation". In: *Polymer Degradation and Stability* 66.3 (Dec.
        1999). Number: 3 Reporter: Polymer Degradation and Stability, pp. 301–
        306. DOI: 10.1016/S0141-3910(99)00054-3.

[15]   M. Celina et al. "FTIR emission spectroscopy applied to polymer degrada-
        tion". en. In: *Polymer Degradation and Stability* 58.1 (Jan. 1997), pp. 15–
        31. DOI: 10.1016/S0141-3910(96)00218-2.

[16]   Liang Li. *MALDI Mass Spectrometry for Synthetic Polymer Analysis*. en.
        John Wiley & Sons, Oct. 2009.

[17]   Raquel Rial-Otero et al. "A Review of Synthetic Polymer Characterization
        by Pyrolysis–GC–MS". en. In: *Chromatographia* 70.3 (Aug. 2009), pp. 339–
        348. DOI: 10.1365/s10337-009-1254-1.

[18]   Joseph D. Menczel and R. Bruce Prime. *Thermal Analysis of Polymers:
        Fundamentals and Applications*. en. Google-Books-ID: qEuQDwAAQBAJ.
        John Wiley & Sons, Apr. 2009.

[19]   Xiaoyan Liu and Weidong Yu. "Evaluating the thermal stability of high
        performance fibers by TGA". en. In: *Journal of Applied Polymer Science*
        99.3 (2006), pp. 937–944. DOI: 10.1002/app.22305.

[20]   H. Medhioub et al. "Towards a structural characterization of an epoxy
        based polymer using small-angle x-ray scattering". In: *Journal of Ap-
        plied Physics* 101.4 (Feb. 2007). Publisher: American Institute of Physics,
        p. 043509. DOI: 10.1063/1.2511890.

[21]   Chang-Sik Ha and Joseph A. Gardella Jr. "X-ray Photoelectron Spec-
        troscopy Studies on the Surface Segregation in Poly(dimethylsiloxane) Con-
        taining Block Copolymers". In: *Journal of Macromolecular Science, Part C*
        45.1 (Jan. 2005). Publisher: Taylor & Francis _eprint: https://doi.org/10.1081/MC-
        200045810, pp. 1–18. DOI: 10.1081/MC-200045810.

[22]   David W. Hahn and Nicoló Omenetto. "Laser-Induced Breakdown Spec-
        troscopy (LIBS), Part II: Review of Instrumental and Methodological
        Approaches to Material Analysis and Applications to Different Fields". en.
        In: *Applied Spectroscopy* 66.4 (Apr. 2012). Number: 4 Reporter: Applied
        Spectroscopy, pp. 347–419. DOI: 10.1366/11-06574.

[23] David W. Hahn and Nicoló Omenetto. "Laser-Induced Breakdown Spectroscopy (LIBS), Part I: Review of Basic Diagnostics and Plasma–Particle Interactions: Still-Challenging Issues Within the Analytical Plasma Community". EN. In: *Applied Spectroscopy* 64.12 (Dec. 2010). Number: 12 Reporter: Applied Spectroscopy, 335A–366A.

[24] Richard E. Russo et al. "Laser Ablation in Analytical Chemistry". In: *Analytical Chemistry* 85.13 (July 2013). Number: 13 Reporter: Analytical Chemistry, pp. 6162–6177. DOI: 10.1021/ac4005327.

[25] Nicole L. LaHaye et al. "The effect of laser pulse duration on ICP-MS signal intensity, elemental fractionation, and detection limits in fs-LA-ICP-MS". en. In: *Journal of Analytical Atomic Spectrometry* 28.11 (2013). Publisher: Royal Society of Chemistry, pp. 1781–1787. DOI: 10.1039/C3JA50200G.

[26] A. De Giacomo et al. "ns- and fs-LIBS of copper-based-alloys: A different approach". en. In: *Applied Surface Science*. Photon-Assisted Synthesis and Processing of Functional Materials 253.19 (July 2007), pp. 7677–7681. DOI: 10.1016/j.apsusc.2007.02.037.

[27] Maximilian Bonta et al. "Elemental mapping of biological samples by the combined use of LIBS and LA-ICP-MS". In: *Journal of Analytical Atomic Spectrometry* 31.1 (2016). Publisher: Royal Society of Chemistry, pp. 252–258.

[28] Kiran Subedi, Tatiana Trejos, and José Almirall. "Forensic analysis of printing inks using tandem Laser Induced Breakdown Spectroscopy and Laser Ablation Inductively Coupled Plasma Mass Spectrometry". en. In: *Spectrochimica Acta Part B: Atomic Spectroscopy* 103-104 (Jan. 2015), pp. 76–83. DOI: 10.1016/j.sab.2014.11.011.

[29] Benjamin T. Manard et al. "Laser ablation – inductively couple plasma – mass spectrometry/laser induced break down spectroscopy: a tandem technique for uranium particle characterization". en. In: *Journal of Analytical Atomic Spectrometry* 32.9 (Aug. 2017). Publisher: The Royal Society of Chemistry, pp. 1680–1687. DOI: 10.1039/C7JA00102A.

[30] Claude [Hrsg Phipps. *Laser ablation and its applications*. eng. New York, NY: Springer, 2007.

[31] L. Jolivet et al. "Review of the recent advances and applications of LIBS-based imaging". en. In: *Spectrochimica Acta Part B: Atomic Spectroscopy* 151 (Jan. 2019), pp. 41–53. DOI: 10.1016/j.sab.2018.11.008.

[32] R. Sattmann et al. "Laser-Induced Breakdown Spectroscopy for Polymer Identification". EN. In: *Applied Spectroscopy* 52.3 (Mar. 1998), pp. 456–461.

[33] Ke Liu et al. "A review of laser-induced breakdown spectroscopy for plastic analysis". en. In: *TrAC Trends in Analytical Chemistry* 110 (Jan. 2019), pp. 327–334. DOI: 10.1016/j.trac.2018.11.025.

[34] A. Limbeck et al. "Methodology and applications of elemental mapping by laser induced breakdown spectroscopy". en. In: *Analytica Chimica Acta* 1147 (Feb. 2021), pp. 72–98. DOI: 10.1016/j.aca.2020.12.054.

[35] Camila Maione and Rommel Melgaço Barbosa. "Recent applications of multivariate data analysis methods in the authentication of rice and the most analyzed parameters: A review". In: *Critical Reviews in Food Science and Nutrition* 59.12 (July 2019). Publisher: Taylor & Francis _eprint: https://doi.org/10.1080/10408398.2018.1431763, pp. 1868–1879. DOI: 10.1080/10408398.2018.1431763.

[36] Gernot Friedbacher and Henning Bubert. *Surface and Thin Film Analysis: A Compendium of Principles, Instrumentation, and Applications*. en. Google-Books-ID: OfuRZG4OxOUC. John Wiley & Sons, Mar. 2011.

[37] Benoit Busser et al. "Elemental imaging using laser-induced breakdown spectroscopy: A new and promising approach for biological and medical applications". en. In: *Coordination Chemistry Reviews* 358 (Mar. 2018), pp. 70–79. DOI: 10.1016/j.ccr.2017.12.006.

[38] Jonathan N. Coleman et al. "Small but strong: A review of the mechanical properties of carbon nanotube–polymer composites". In: *Carbon* 44.9 (Aug. 2006). Number: 9 Reporter: Carbon, pp. 1624–1652. DOI: 10.1016/j.carbon.2006.02.038.

[39] D. Nabi Saheb and J. P. Jog. "Natural fiber polymer composites: A review". en. In: *Advances in Polymer Technology* 18.4 (1999). Number: 4 Reporter: Advances in Polymer Technology, pp. 351–363. DOI: 10.1002/(SICI)1098-2329(199924)18:4<351::AID-ADV6>3.0.CO;2-X.

[40] Norbert Eisenreich and Thomas Rohe. "Infrared Spectroscopy in Analysis of Plastics Recycling". en. In: *Encyclopedia of Analytical Chemistry*. American Cancer Society, 2006. DOI: 10.1002/9780470027318.a2011.

[41] Tom Learner and Getty Conservation Institute. *Analysis of Modern Paints*. en. Google-Books-ID: Ao5wcgaOmfIC. Getty Publications, 2004.

[42] Luis A. Escobar and William Q. Meeker. "A Review of Accelerated Test Models". In: *Statistical Science* 21.4 (2006). Publisher: Institute of Mathematical Statistics, pp. 552–577.

[43] S. Halim Hamid. *Handbook of Polymer Degradation*. en. Google-Books-ID: 2URZDwAAQBAJ. CRC Press, June 2000.

[44] Achim Göpferich. "Mechanisms of polymer degradation and erosion". en. In: *Biomaterials*. Polymer Scaffolding and Hard Tissue Engineering 17.2 (Jan. 1996), pp. 103–114. DOI: 10.1016/0142-9612(96)85755-3.

[45] Mathew C. Celina. "Review of polymer oxidation and its relationship with materials performance and lifetime prediction". en. In: *Polymer Degradation and Stability* 98.12 (Dec. 2013), pp. 2419–2429. DOI: 10.1016/j.polymdegradstab.2013.06.024.

[46] R Ramani and C Ranganathaiah. "Degradation of acrylonitrile-butadiene-styrene and polycarbonate by UV irradiation". In: *Polymer Degradation and Stability* 69.3 (Sept. 2000), pp. 347–354. DOI: 10.1016/S0141-3910(00)00081-1.

[47] Guirong Peng et al. "Degradation of polyimide film under vacuum ultraviolet irradiation". en. In: *Journal of Applied Polymer Science* 94.4 (Nov. 2004), pp. 1370–1374. DOI: 10.1002/app.20920.

[48] Kenneth Rasmussen et al. "Thermal And UV Degradation Of Polyimides And Silicones Studied In Situ With ESR Spectroscopy". en. In: (2009), p. 8.

[49] James J. Licari. *Coating materials for electronic applications: polymers, processing, reliability, testing*. William Andrew, 2003.

[50] G. Grundmeier, W. Schmidt, and M. Stratmann. "Corrosion protection by organic coatings: electrochemical mechanism and novel methods of investigation". In: *Electrochimica Acta* 45.15 (May 2000), pp. 2515–2533. DOI: 10.1016/S0013-4686(00)00348-0.

[51] P. A. Sørensen et al. "Anticorrosive coatings: a review". en. In: *Journal of Coatings Technology and Research* 6.2 (June 2009). Number: 2 Reporter: Journal of Coatings Technology and Research, pp. 135–176. DOI: 10.1007/s11998-008-9144-2.

[52] Oluwabunmi P. Abioye et al. "A Review Of Biodegradable Plastics In Nigeria". In: *International Journal of Mechanical Engineering and Technology (IJMET)* 9.10 (2018). Number: 10 Publisher: IAEME Publications.

[53] Aleksandra Wesełucha-Birczyńska et al. "Application of Raman spectroscopy to study of the polymer foams modified in the volume and on the surface by carbon nanotubes". en. In: *Vibrational Spectroscopy* 72 (May 2014), pp. 50–56. DOI: 10.1016/j.vibspec.2014.02.009.

[54] Neil J. Everall, John M. Chalmers, and Peter R. Griffiths. *Vibrational spectroscopy of polymers: principles and practice*. Wiley Chichester, 2007.

[55] C. Peike et al. "Non-destructive degradation analysis of encapsulants in PV modules by Raman Spectroscopy". en. In: *Solar Energy Materials and Solar Cells* 95.7 (July 2011), pp. 1686–1693. DOI: 10.1016/j.solmat.2011.01.030.

[56] Erwin Riedel and Christoph Janiak. *Anorganische Chemie*. ger. 2007.

[57] Dmitry R. Bandura, Vladimir I. Baranov, and Scott D. Tanner. "Detection of Ultratrace Phosphorus and Sulfur by Quadrupole ICPMS with Dynamic Reaction Cell". In: *Analytical Chemistry* 74.7 (Apr. 2002). Publisher: American Chemical Society, pp. 1497–1502. DOI: 10.1021/ac011031v.

[58] Noriyuki Yamada. "Kinetic energy discrimination in collision/reaction cell ICP-MS: Theoretical review of principles and limitations". en. In: *Spectrochimica Acta Part B: Atomic Spectroscopy* 110 (Aug. 2015), pp. 31–44. DOI: 10.1016/j.sab.2015.05.008.

[59] M Whitt et al. "Survey of heavy metal contamination in recycled polyethylene terephthalate used for food packaging". en. In: *Journal of Plastic Film & Sheeting* 29.2 (Apr. 2013). Publisher: SAGE Publications Ltd STM, pp. 163–173. DOI: 10.1177/8756087912467028.

[60] J. S. F. Pereira et al. "Evaluation of sample preparation methods for poly-mer digestion and trace elements determination by ICPMS and ICPOES". en. In: *Journal of Analytical Atomic Spectrometry* 26.9 (2011). Publisher: Royal Society of Chemistry, pp. 1849–1857. DOI: 10.1039/C1JA10050E.

[61] Isaac J. Arnquist et al. "A dry ashing assay method for the trace determi-nation of Th and U in polymers using inductively coupled plasma mass spectrometry". English. In: *Journal of Radioanalytical and Nuclear Chem-istry* 3.307 (2016), pp. 1883–1890. DOI: 10.1007/s10967-015-4343-7.

[62] Andreas Limbeck et al. "Recent advances in quantitative LA-ICP-MS analysis: challenges and solutions in the life sciences and environmental chemistry". en. In: *Analytical and Bioanalytical Chemistry* 407.22 (Sept. 2015), pp. 6593–6617. DOI: 10.1007/s00216-015-8858-0.

[63] J. El Haddad, L. Canioni, and B. Bousquet. "Good practices in LIBS analysis: Review and advices". In: *Spectrochimica Acta Part B: Atomic Spectroscopy* 101 (Nov. 2014). Reporter: Spectrochimica Acta Part B: Atomic Spectroscopy, pp. 171–182. DOI: 10.1016/j.sab.2014.08.039.

[64] Matthew W. Loewen and Adam J. R. Kent. "Sources of elemental frac-tionation and uncertainty during the analysis of semi-volatile metals in silicate glasses using LA-ICP-MS". en. In: *Journal of Analytical Atomic Spectrometry* 27.9 (2012). Publisher: Royal Society of Chemistry, pp. 1502–1508. DOI: 10.1039/C2JA30075C.

[65] J. Koch and D. Günther. "Femtosecond laser ablation inductively coupled plasma mass spectrometry: achievements and remaining problems". en. In: *Analytical and Bioanalytical Chemistry* 387.1 (Jan. 2007), pp. 149–153. DOI: 10.1007/s00216-006-0918-z.

[66] PaulJ Sylvester. "Matrix effects in laser ablation-ICP-MS". In: *Laser ablation ICP-MS in the earth sciences: Current practices and outstanding issues.* Vol. 40. Mineralogical Association of Canada, 2008, pp. 67–78.

[67] Natalia Miliszkiewicz, Stanisław Walas, and Anna Tobiasz. "Current ap-proaches to calibration of LA-ICP-MS analysis". en. In: *Journal of Analyt-ical Atomic Spectrometry* 30.2 (Jan. 2015). Publisher: The Royal Society of Chemistry, pp. 327–338. DOI: 10.1039/C4JA00325J.

[68] Gábor Galbács. "A critical review of recent progress in analytical laser-induced breakdown spectroscopy". en. In: *Analytical and Bioanalytical Chemistry* 407.25 (Oct. 2015), pp. 7537–7562. DOI: 10.1007/s00216-015-8855-3.

[69] Joachim Koch and Detlef Günther. "Review of the State-of-the-Art of Laser Ablation Inductively Coupled Plasma Mass Spectrometry". en. In: *Applied Spectroscopy* 65.5 (May 2011). Number: 5 Reporter: Applied Spectroscopy, 155A–162A. DOI: 10.1366/11-06255.

[70] Beatriz Fernández et al. "Direct analysis of solid samples by fs-LA-ICP-MS". en. In: *TrAC Trends in Analytical Chemistry* 26.10 (Nov. 2007), pp. 951–966. DOI: 10.1016/j.trac.2007.08.008.

[71] M. P. Mateo, J. M. Vadillo, and J. J. Laserna. "Irradiance-dependent depth profiling of layered materials using laser-induced plasma spectrometry". en. In: *Journal of Analytical Atomic Spectrometry* 16.11 (Nov. 2001). Publisher: The Royal Society of Chemistry, pp. 1317–1321. DOI: 10.1039/B104440K.

[72] Alexei Plotnikov et al. "Application of laser ablation inductively coupled plasma quadrupole mass spectrometry (LA-ICP-QMS) for depth profile analysis". en. In: *Journal of Analytical Atomic Spectrometry* 16.11 (Nov. 2001). Publisher: The Royal Society of Chemistry, pp. 1290–1295. DOI: 10.1039/B105441B.

[73] Alexei Plotnikov, Carla Vogt, and Klaus Wetzig. "An approach to the reconstruction of true concentration profile from transient signal in spatially resolved analysis by means of laser ablation ICP MS". en. In: *Journal of Analytical Atomic Spectrometry* 17.9 (Sept. 2002). Publisher: The Royal Society of Chemistry, pp. 1114–1120. DOI: 10.1039/B202258C.

[74] Desiré Luc Massart et al. *Handbook of chemometrics and qualimetrics.* Elsevier Science Inc., 1998.

[75] Tianlong Zhang, Hongsheng Tang, and Hua Li. "Chemometrics in laser-induced breakdown spectroscopy". en. In: *Journal of Chemometrics* 32.11 (2018). _eprint: https://onlinelibrary.wiley.com/doi/pdf/10.1002/cem.2983, e2983. DOI: 10.1002/cem.2983.

[76] V. K. Unnikrishnan et al. "Analytical predictive capabilities of Laser Induced Breakdown Spectroscopy (LIBS) with Principal Component Analysis (PCA) for plastic classification". en. In: *RSC Advances* 3.48 (2013), pp. 25872–25880. DOI: 10.1039/C3RA44946G.

[77] Liwen Sheng et al. "Classification of iron ores by laser-induced breakdown spectroscopy (LIBS) combined with random forest (RF)". en. In: *Journal of Analytical Atomic Spectrometry* 30.2 (2015). Publisher: Royal Society of Chemistry, pp. 453–458. DOI: 10.1039/C4JA00352G.

[78] Myriam Boueri et al. "Identification of Polymer Materials Using Laser-Induced Breakdown Spectroscopy Combined with Artificial Neural Networks". EN. In: *Applied Spectroscopy* 65.3 (Mar. 2011). Publisher: Society for Applied Spectroscopy, pp. 307–314.

[79] Yanwei Yang et al. "Application of Scikit and Keras Libraries for the Classification of Iron Ore Data Acquired by Laser-Induced Breakdown Spectroscopy (LIBS)". en. In: *Sensors* 20.5 (Jan. 2020). Number: 5 Publisher: Multidisciplinary Digital Publishing Institute, p. 1393. DOI: 10.3390/s20051393.

[80] A. Safi et al. "Multivariate calibration in Laser-Induced Breakdown Spectroscopy quantitative analysis: The dangers of a 'black box' approach and how to avoid them". In: *Spectrochimica Acta Part B: Atomic Spectroscopy* 144 (June 2018), pp. 46–54. DOI: 10.1016/j.sab.2018.03.007.

[81] Maximilian Bonta and Andreas Limbeck. "Metal analysis in polymers using tandem LA-ICP-MS/LIBS: eliminating matrix effects using multivariate calibration". en. In: *Journal of Analytical Atomic Spectrometry* 33.10 (2018). Publisher: Royal Society of Chemistry, pp. 1631–1637. DOI: 10. 1039/C8JA00161H.

[82] Rafael Hernández-García et al. "Quantitative analysis of Lead Zirconate Titanate (PZT) ceramics by laser-induced breakdown spectroscopy (LIBS) in combination with multivariate calibration". In: *Microchemical Journal* 130 (Jan. 2017), pp. 21–26. DOI: 10.1016/j.microc.2016.07.024.

[83] Sergey M. Zaytsev et al. "Comparison of single- and multivariate calibration for determination of Si, Mn, Cr and Ni in high-alloyed stainless steels by laser-induced breakdown spectrometry". en. In: *Journal of Analytical Atomic Spectrometry* 29.8 (2014). Publisher: Royal Society of Chemistry, pp. 1417–1424. DOI: 10.1039/C3JA50389E.

[84] Leticia Gómez-Nubla et al. "Analytical methodology to elemental quantification of weathered terrestrial analogues to meteorites using a portable Laser-Induced Breakdown Spectroscopy (LIBS) instrument and Partial Least Squares (PLS) as multivariate calibration technique". en. In: *Microchemical Journal* 137 (Mar. 2018), pp. 392–401. DOI: 10.1016/j.microc.2017.11.019.

[85] Ke Liu et al. "Quantitative analysis of toxic elements in polypropylene (PP) via laser-induced breakdown spectroscopy (LIBS) coupled with random forest regression based on variable importance (VI-RFR)". en. In: *Analytical Methods* 11.37 (2019). Publisher: Royal Society of Chemistry, pp. 4769–4774. DOI: 10.1039/C9AY01796H.

[86] M. Celina, K. T. Gillen, and R. A. Assink. "Accelerated aging and lifetime prediction: Review of non-Arrhenius behaviour due to two competing processes". en. In: *Polymer Degradation and Stability* 90.3 (Dec. 2005), pp. 395–404. DOI: 10.1016/j.polymdegradstab.2005.05.004.

[87] Mathew Celina et al. "Overview of accelerated aging and polymer degradation kinetics for combined radiation-thermal environments". en. In: *Polymer Degradation and Stability* 166 (Aug. 2019), pp. 353–378. DOI: 10.1016/j.polymdegradstab.2019.06.007.

[88] A. Hanif et al. "A Comprehensive Review Toward the State-of-the-Art in Failure and Lifetime Predictions of Power Electronic Devices". In: *IEEE Transactions on Power Electronics* 34.5 (May 2019). Conference Name: IEEE Transactions on Power Electronics, pp. 4729–4746. DOI: 10.1109/TPEL.2018.2860587.

4. Scientific Publications

This thesis is composed of 4 peer-reviewed publications and one submitted manuscript, which are all focused on the analytical challenges presented and discussed in Chapter 2. The first 3 publications are all in the field of spatially resolved analysis, the fourth publications is based on the investigation of polymer degradation and the topic of the fifth publication is quantitative trace metal analysis in polymers.

4.1   Article 1

The first publication is entitled "Spatially resolved polymer classification using laser induced breakdown spectroscopy (LIBS) and multivariate statistics". This article is, to the best of the authors knowledge, the first time that LIBS has been used for spatially resolved polymer classification. In this work, the applicability of LIBS to image the 2D distribution of two different polymer types (ABS nad PLA) within a sample was demonstrated using single-shot LIBS analysis. On the one hand, single-shot LIBS imaging provides fast measurement times but also increases the complexity of classification due to a lower SNR compared to accumulated spectra. Nevertheless, by using polymer specific LIBS signals as input variables for a PCA and proper standardization, the two different polymer types were accurately distinguished. The second application example presented in this work is based on the depth profiling of a polymeric multilayer system consisting of 4 layers of 3 different polymer types (PE, PAK and PVC) with a total thickness of 250 µm. For the analysis, the sample was ablated layer by layer with each layer covering an area of 1.5 mm x 1.0 mm. Due to lower SNR caused by crater effects typically occurring during depth profile measurements and a closer similarity in the LIBS spectra of the 3 polymers, classification was more challenging. PCA did not provide satisfying results and therefore, a more sophisticated method namely k-means clustering was employed. With this approach the differentiation of the 3 polymer types in the multilayer system was possible and the correct 3D distribution of the polymers within the sample was obtained.

Spatially resolved polymer classification using laser induced breakdown spectroscopy (LIBS) and multivariate statistics

Lukas Brunnbauer[a],[*], Silvia Larisegger[b], Hans Lohninger[a], Michael Nelhiebel[b], Andreas Limbeck[a],[**]

[a] *TU Wien, Institute of Chemical Technologies and Analytics, Getreidemarkt 9/164-IAC, 1060, Vienna, Austria*
[b] *KAI Kompetenzzentrum Automobil- und Industrieelektronik GmbH, Technologiepark Villach Europastraße 8, 9524, Villach, Austria*

A B S T R A C T

Synthetic polymers and plastics have become one of the most important materials in our modern world and everyday life with all kinds of applications mainly due to their wide range of excellent and tuneable properties. Several novel materials consisting of multiple different synthetic polymers or composite materials like natural-fiber-reinforced polymer composites have already been reported in literature. Additionally, materials consisting of multiple synthetic polymers already found their way in our daily lives (e.g. double-sided adhesive tape). With emerging materials consisting of different structured synthetic polymers, the need for analytical methods characterizing these kinds of sample also arises. Conventionally, analytical techniques such as FT-IR or Raman spectroscopy are used for polymer classification. Although, these techniques offer laterally resolved investigations they lack the possibility of analyzing depth profiles. In this work, we present laser induced breakdown spectroscopy (LIBS) as a novel and powerful analytical method for spatially resolved polymer classification. As a feasibility study, two exemplary structured synthetic polymer samples (2D structured and multilayer system) have been analyzed using LIBS and the spatial distribution of 5 different synthetic polymers, namely acrylonitrile butadiene styrene (ABS), polylactic acid (PLA), polyethylene (PE), polyacrylate (PAK) and polyvinylchloride (PVC) have been successfully classified using multivariate statistical approaches (principal component analysis (PCA) and k-means clustering). Spatially resolved classification results were validated by comparing the obtained distribution of the 2D structured sample to the elemental distribution of a contamination present in one of the synthetic polymers. Classification of the polymeric multilayer system was validated by comparing the obtained results to a microscopic cross-section. It was shown that LIBS cannot only be used to investigate 2D structured polymer samples but also for direct analysis of depth profiles. Besides synthetic polymer classification, LIBS provides simultaneous analysis of the elemental composition of the sample, which increases the total amount of information accessible with only one measurement.

1. Introduction

Nowadays, synthetic polymers and plastics are widely used materials with a broad range of applications in all kind of industries. The main reason for the popularity of synthetic polymers in our modern world is the large variety of properties these synthetic materials have to offer. In 2016 335 million tonnes of plastic have been produced [3], which is already getting close to the 1630 million tonnes of worldwide steel production [4]. Recently materials consisting of multiple organic species, especially natural-fiber-reinforced polymers or composites made of polymers and various allotropes of carbon (e.g. carbon nanotubes) have been investigated due to their superior properties compared to normal polymers [1,2,5]. Additionally, self-assembled layers consisting of different synthetic polymers have been reported in literature [6]. Also in the field of conservation and restoration of artworks the knowledge about the distribution of different kinds of polymeric binder materials is of great interest [7]. With more and more materials consisting of different structured synthetic polymers, the need for

analytical methods characterizing the spatial distribution of different synthetic polymers within one sample arises.

For classification of synthetic polymer samples, traditionally FT-IR spectroscopy or Raman spectroscopy is used [8–11]. These techniques offer spectral fingerprints for different polymers, which allow polymer identification. Combining FT-IR or Raman spectroscopy with microscopy, lateral distribution of multiple synthetic polymers within a sample can be investigated [12]. However, these techniques lack the inherent possibility of investigating depth profiles of layered systems and offer only information about the sample surface.

Laser induced breakdown spectroscopy (LIBS) is a laser assisted spectroscopic method which gives mainly elemental information about the investigated sample [13,14]. In LIBS, a laser beam is focused on the sample surface ablating material and forming a laser induced plasma. In this plasma, the ablated material is atomized, excited and ionized. When the excited states decay, radiation is emitted which is collected and analyzed [15,16]. Therefore, LIBS enables elemental bulk analysis but also mapping as well as depth profiling of elemental distributions

within a sample. For a more detailed introduction to LIBS see Cremers et al. [15]. As the recording of broadband LIBS spectra offers simultaneous multi-element analysis, multivariate data evaluation strategies are very common in the LIBS community [17,18].

LIBS offers direct access to analyzing the common major components of polymers namely carbon, hydrogen, nitrogen and oxygen and additionally molecular emission bands like the C_2 swan band, CN violet band [19] or OH band [20]. Recently several papers have been published showing the capabilities of LIBS combined with different multivariate statistical approaches for fast and reliable polymer classification [21,22]. Various approaches of using PCA for polymer classification have been published [23,24] whereas Banaee et al. used discriminant function analysis (DFA) for classification [25]. Also artificial neural networks have been applied for polymer classification using LIBS [26]. The capabilities and advantages of employing femtosecond lasers on LIBS polymer classification was investigated by Junjuri et al. [27]. However, in those previous studies only bulk polymer samples were analyzed and classified with LIBS.

LIBS has been used recently for imaging experiments as well as the investigation of depth profiles of elemental distributions. With lateral resolutions ranging from the low μm up to several hundred μm range and fast measurement times, LIBS is a very promising technique for imaging [28–31]. Additionally analyses of depth profiles have also been reported in literature [32,33].

In this work, the possibility of spatially resolved analysis and polymer classification using LIBS was combined and applied for the first time to a laterally structured polymer sample as well as a sample consisting of a layered system of different synthetic polymers. It was shown that LIBS cannot only be used to identify and correctly classify bulk polymer samples where spectra from multiple laser shots were accumulated but it can be used to image the lateral structure of different polymers using single shots. Multivariate statistical approaches (principal component analysis (PCA) and k-means clustering) were used to correctly map the structured polymer samples. Additionally LIBS was used to investigate a depth profile of a polymer multi-layer system.

2. Experimental

2.1. Chemicals

Polyethylene (PE), polyacrylate (PAK) and polyvinylchloride (PVC) were obtained from Acros Organics (Geel, Belgium). 3D printable polymers acrylonitrile butadiene styrene (ABS) and polylactic acid (PLA) were obtained from RS Components (Corby, United Kingdom). High purity n-doped Si wafer obtained from Infineon Austria AG (Villach, Austria) were used as substrate materials for the analysis.

2.2. Sample preparation

1. 2D structured samples

A structured sample consisting of ABS and PLA was prepared using a commercially available 3D printer (Ultimaker, Geldermalsen, The Netherlands). The structured sample shows the logo of the TU Wien. The letters "T" and "U" are made of PLA whereas the substrate material is made of ABS. The sample was smoothened using SiC abrasive paper (Struers GmbH, Austria) to decrease surface roughness which might cause problems with the laser focusing. After smoothening the surface, a pre-ablation step was used to clean the sample by removing surface contaminations introduced by the sample preparation steps.

2. Layered polymer sample

For a polymer layer system, commercially available double-sided adhesive tape (Tesa, Norderstedt, Germany) was used. The double-sided adhesive tape consists of a four-layer-system: PE liner, PAK

adhesive layer, PVC support and a second PAK adhesive layer with a total thickness of 250 μm. The thickness was determined using a profilometer (DektakXT, Bruker, Massachusetts, USA). The double-sided tape was applied with the PE liner to an n-doped Si wafer obtained by Infineon Austria AG (Villach, Austria), which was used as a substrate material for the analysis.

2.3. LIBS measurement

LIBS experiments were carried out using a commercially available LIBS J200 system (Applied Spectra, Inc, Fremont, CA). A frequency quadrupled Nd:YAG laser operating at a wavelength of 266 nm with a 5 ns pulse duration was used for ablation and excitation. Emitted radiation after each laser pulse was collected using two different collection optics connected to optical fibres: one collection optic optimized for UV-light and a second collection optic for the remaining part of the spectrum. The collected light was analyzed using a Czerny-Turner spectrometer with 6 channels covering a total wavelength range from 188 to 1048 nm. LIBS data was recorded using Axiom 2.0 software provided by the manufacturer.

LIBS parameters (laser energy, gate delay, atmosphere and laser spotsize) were optimized in preliminary experiments for best classification results for each sample. Optimizing the gate delay was a trade-off between short gate delays resulting in increased emission intensities of the elements carbon, oxygen and hydrogen and longer gate delays improving the signal-to-noise ratio especially in the wavelength range of the C_2 swan band. Table 1 shows the used LIBS parameters.

For laterally resolved polymer classification, the 3D printed sample was analyzed using line-scan patterns with a laser beam diameter of 100 μm and a distance of 100 μm between each line. The prepared sample was analyzed using 115 parallel line-scans with a length of 16.5 mm each. Obtained data was imported to Epina ImageLab 2.97 (Retz, Austria) which was used for further data treatment. Images were created using the recorded data of one laser pulse as one pixel.

The depth profile of the polymer multi-layer system was recorded by analyzing consecutive layers until full penetration through the sample was achieved. Each layer covered an area of 1.5 mm × 1 mm and was analyzed using 10 parallel line-scans with a distance of 100 μm between each line. Obtained data of each layer was imported to Epina ImageLab 2.97 to create classification maps of each layer. The resulting images were combined to a 3D map using Fiji with BoneJ plugin [34,35].

3. Results and discussion

In this work 5 different polymers (ABS, PLA in a lateral structured sample and PE, PAK, PVC in a layered sample) in two structured samples were analyzed and classified. Fig. 1 shows selection of emission signals (C(I) emission at 247.88 nm, C_2 swan band and H(I) emission at 656.28 nm) present in all 5 investigated polymers. All 5 polymer

Table 1
LIBS parameters.

Laser system	
Laser output energy [mJ]	3.8
Laser spotsize [μm]	100
Laser repetition rate [Hz]	10
Laser beam geometry	circular
Stage scan-speed [mm/s]	1
Atmosphere	Argon
Laser wavelength [nm]	266
Spectrometer system (Czerny-Turner)	
Detection channels	6
Detector	CCD
Gate delay [μs]	0.3
Gate width [ms]	1.05
Covered wavelength range [nm]	188–1048
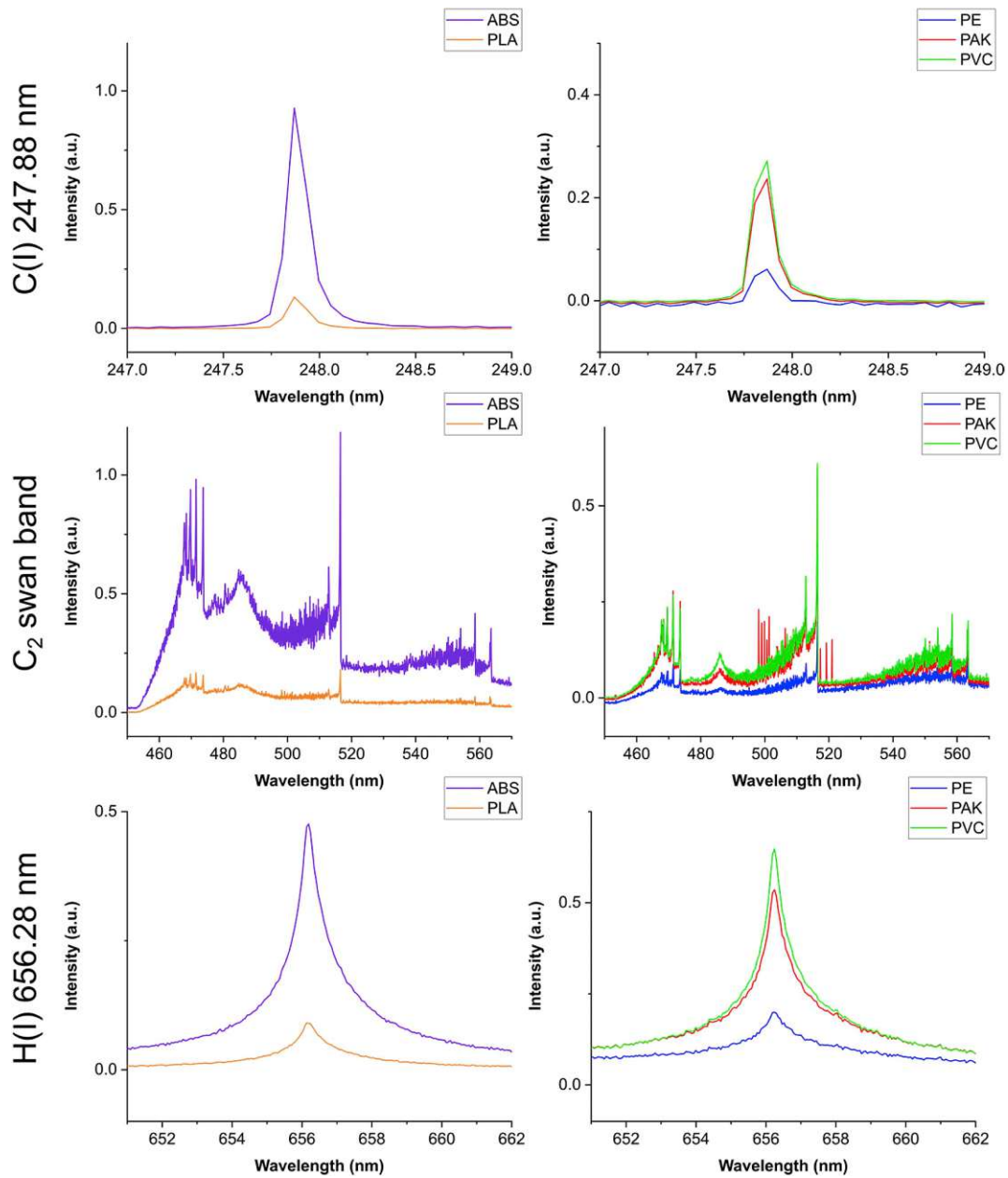
Fig. 1. Selected spectral LIBS features of the 5 investigated polymers.

Table 2
Integrated emission signals.

Emission signal	Integrated wavelength range [nm]
C (I)	192.59–193.43
C (I)	247.49–248.48
CN violet band	387.36–388.64
C_2 swan band Δv -1	473.22–474.29
C_2 swan band Δv 0	516.17–516.73
C_2 swan band Δv + 1	562.99–563.91
H (I)	650.21–663.67
O (I)	776.56–778.42

samples show more or less the same emission signals but with varying intensities and ratios between each polymer. For multivariate data evaluation and polymer classification, an extended selection of

emission signals originating from the polymers was used. The selected signals include atomic and molecular emission signals from major polymeric components, namely carbon, hydrogen and oxygen. Signals from inorganic additives, which may be present in polymeric samples were not used for polymer classification. By using only emission signals originating from the polymers itself, polymer classification independent of additives should be assured. The integrated wavelength ranges listed in Table 2 were used as variables for the following multivariate data evaluation.

3.1. 2D structured sample

To compensate shot-to-shot variations and surface roughness, each spectrum was standardized (mean = 0, standard deviation = 1) prior to further data treatment. For data evaluation of the 3D printed sample representing the logo of the TU Wien, principal component analysis

Table 3

Explained variance of each PC for the data of the 2D structured sample. Bold PCs are used for the Score-Plot.

Principal Component	Explained Variance [%]
1	**81.33**
2	**6.05**
3	5.59
4	2.58
5	2.11
6	1.49
7	0.53
8	0.32

(PCA) was calculated with all obtained spectra using the integrated emission intensities listed in Table 2 as variables. Background correction was performed using the mean value of 5 neighboring pixels of the detector when integrating each emission signal. All variables were standardized prior to calculating the PCA. Variance explained by each principal component is shown in Table 3. The score-plot of PC1 (81.33%) and PC2 (6.05%) (Fig. 2 a)) reveals two main clusters in the data being separated mainly by the first principal component, which corresponds well with the high amount of explained variance of the first principal component. As shown in Fig. 3 c), both investigated polymers can be also distinguished by their Na content. Therefore, the data of the score plot was colored using the Na-emission signal (589.0 nm) as a threshold to distinguish between the two clusters. The distribution of the Na signal intensity is shown in Fig. 4. A threshold of 800 cts was selected to distinguish spectra of the two polymers. In the score plot, all spectra with a Na signal less than 800 cts are colored violet representing PLA and all spectra with a Na signal more than 800 cts are colored orange representing ABS. Loadings plot (Fig. 2 b)) show the influence of each of the 8 variables on the principal components. As expected, a high correlation of the three variables of the C_2 swan band as well as the two carbon atomic emission signals is observed. Additionally the oxygen emission signal is negatively correlated to all other variables and shows a high contribution to distinguish the two polymers using the first principal component.

Fig. 3 a) shows a microscope picture of the analyzed area of the sample prepared via 3D printing. Plotting the score of the first principal component of the PCA of each spectrum as one pixel results in an image with 17 250 pixels and shows very good laterally resolved classification of the two polymers. To get a smooth result, the color between each pixel and its surrounding pixels was interpolated (Fig. 3 b)). As the used ABS contains Na-contaminations, this property was used to confirm the classification results and to show the capabilities of LIBS for elemental analysis. The elemental map of Na (589.00 nm) is shown in Fig. 3 c) for

comparison of the results. Pearson correlation coefficient (PCC) between the Na signal and the score of the first principal component was calculated to assess the similarity between the two images resulting in PCC = 0.8065. As the distribution of Na is not a perfect reference to assess the polymer distribution due to inhomogeneity in the Na-distribution, the deviation of the observed PCC value from 1 is explained. Nevertheless, correct classification of the two polymers is confirmed.

3.2. Depth profiling of a polymer multi-layer system

In this next section, the results of the depth profiling of a polymer multi-layer system of a double-sided adhesive tape applied to an n-doped silicon wafer are shown. The sample consists of a four-layer-system: PE liner, PAK adhesive layer, PVC support and a second PAK adhesive layer with a total thickness of 250 μm. The polymer multi-layer system was analyzed layer by layer. Full penetration of the sample was achieved after 53 ablated layers which was indicated by an increase of the silicon emission line at 288.17 nm. With a total thickness of 250 μm of the sample, an ablation rate of around 4.7 μm per layer was calculated. For data evaluation, data of all analyzed layers was merged into one dataset. To minimize the influence of crater effects, from each layer the first and the last line-scan as well as the first and the last shot of each line-scan was excluded from the following data analysis procedure. Influences of potential defocusing effects on the obtained spectra were compensated by standardizing each spectrum (mean = 0, standard deviation = 1). Emission signals listed in Table 2 were integrated as previously described and obtained variables were standardized. These variables were used for the following classification.

In a first step, similar to the 2D structured sample, PCA was calculated using the dataset of the polymer multi-layer sample. Corresponding score and loadings plots are shown in Fig. 5 and the explained variance by each PC is listed in Table 4. The score plot reveals only two clusters as opposed to the three different polymers present in the investigated sample. PAK and PVC could not be fully distinguished by PCA. Spectral features shown in Fig. 1 show a high similarity between PAK and PVC and as described later, different aspects in depth profiling may increase the difficulty of the classification task and therefore, PCA becomes insufficient for classification. For more satisfying results, a non-linear classification model, namely k-means clustering was applied to the dataset.

As the double-sided adhesive tape consists of three different polymers (PE liner, PAK adhesive layer and PVC substrate layer), k-means algorithm was executed to classify each spectrum of the dataset as one of three classes. After classification, images of the distribution of the three clusters were generated for each analyzed layer of the sample. The images representing the distribution of the three classes in each layer
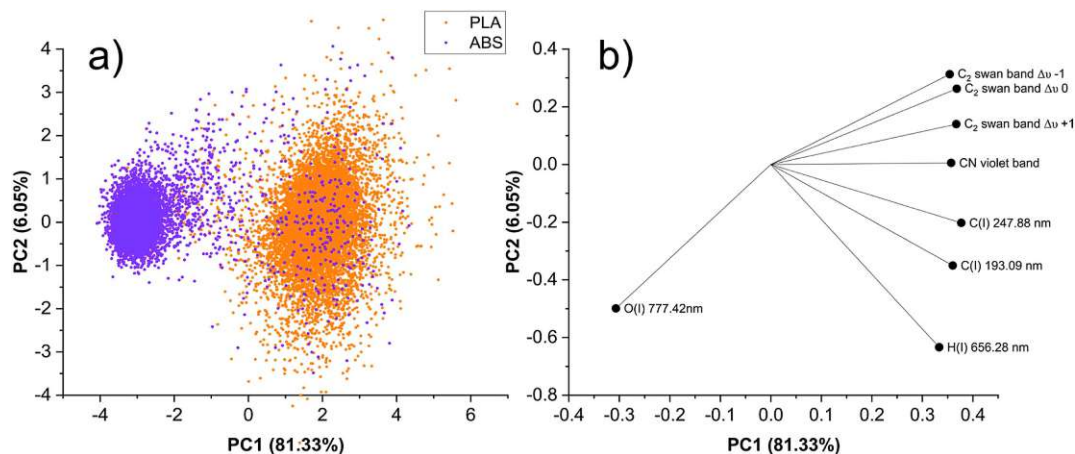

Fig. 2. a) Score-plot and b) Loadings-plot of the PCA revealing two clusters in the data of the 2D structured sample. Spectra were colored using Na signal as a cut-off between the two different classes.
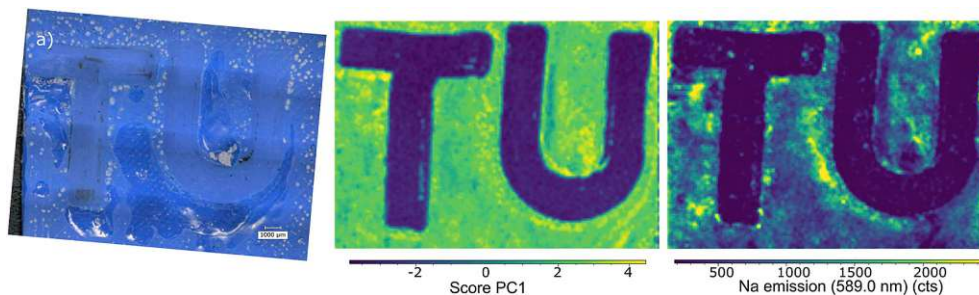
Fig. 3. a) Microscope picture of the analyzed 3D printed sample consisting of ABS and PLA, b) Polymer classification results by plotting the score of the first principal component of the PCA, c) Na distribution map for confirmation of the polymer classification results.
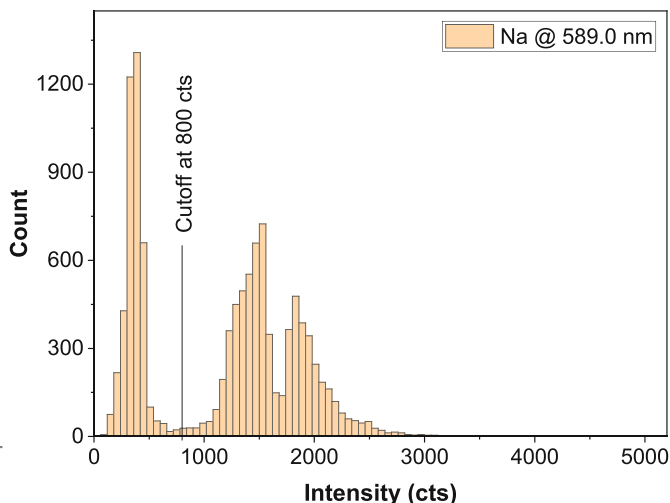
Fig. 4. Intensity distribution of Na signal (589.0 nm) of the 2D structured sample with the marked cut-off to distinguish between ABS and PLA.

Table 4
Explained variance of each PC for the data of the multilayer sample. Bold PCs are used for the Score-plot.

Principal Component	Explained Variance [%]
1	**39.99**
2	**17.88**
3	12.5
4	9.37
5	7.88
6	6.28
7	3.34
8	2.75

The quality of the classification result was assessed by comparing the obtained distribution to the microscopic cross section shown in Fig. 7. In the first PAK layer and the PVC substrate layer, the classification results show 98%–100% correctly classified spectra. The obtained thicknesses in the first two layers are in very good agreement (47 μm PAK and 75 μm PVC) with the obtained thicknesses from the microscope (47 μm PAK and 70 μm PVC). After the PVC layer, the classification result decreases slightly but still stays in the order of 90% correctly classified spectra per layer and the obtained thicknesses from the LIBS depth profile show a slight deviation (80 μm PAK and 44 μm PE) from the measured thicknesses from the microscope picture (64 μm PAK and 69 μm PE). This slight decrease of the classification results may be explained by uneven ablation of the sample causing a smearing of the polymers present in each layer. In a depth of 150 μm and lower, defocusing effects which may not be compensated by standardizing the obtained data and the enhanced distance of the laser induced plasma to the collection optics may affect the classification results negatively. Additionally, polymers may become translucent for the laser wavelength at a certain thickness causing a combined ablation

were merged into a 3D model made of 13 × 8 × 53 voxels (Fig. 6 a)). It should be mentioned that the z-axis was stretched by a factor of 10 for better presentation of the data. As the distribution of the three polymers in the layered sample is known, the three different polymers could be assigned to the three different classes. Additionally the contributions of each polymer to each layer was calculated and is shown in Fig. 6 b). The obtained results show the spatial classification representing the expected distribution of PAK, PVC and PE in the double-sided adhesive tape as shown in the microscopic cross-section in Fig. 7. It should be mentioned that for the measurement of the depth profile, the double-sided adhesive tape was applied to the Si-wafer the other way around.

Fig. 5. a) Score-plot and b) Loadings-plot of the PCA of the multilayer sample revealing only two of the expected three different polymers. PAK and PVC cannot be distinguished by PCA.
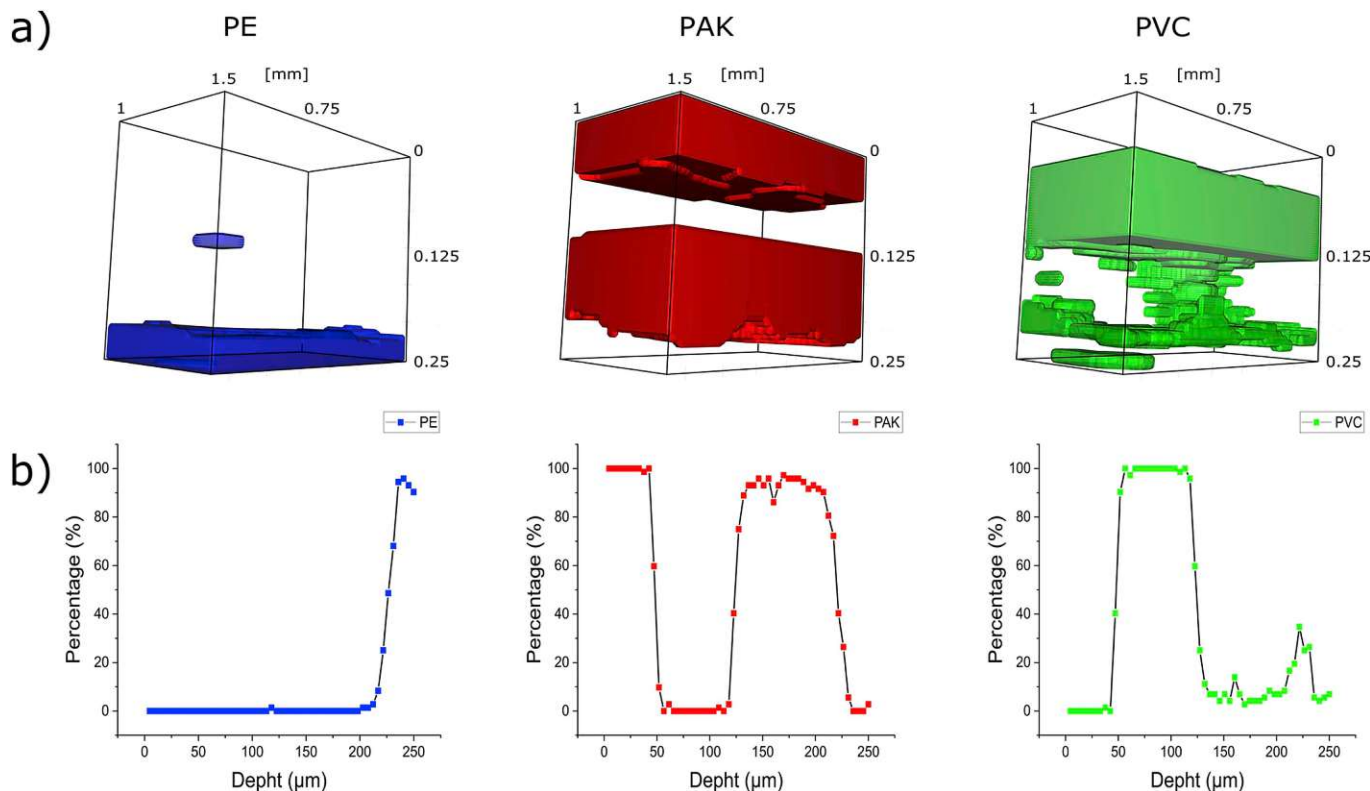
Fig. 6. a) Spatial distribution and b) depth profile of the percentage of each polymer in each of the analyzed layers of the double-sided adhesive tape.
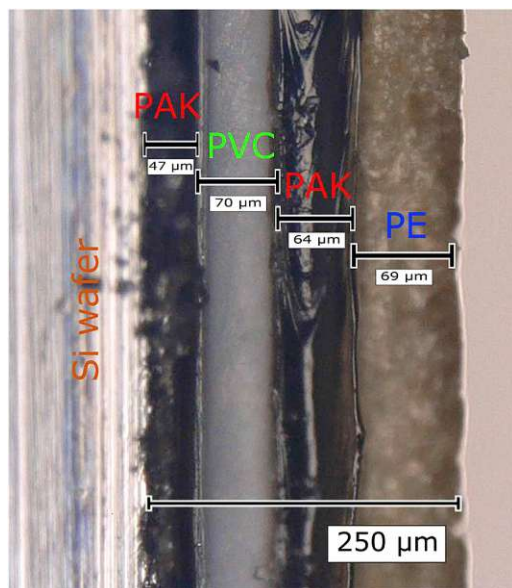
Fig. 7. Microscopic cross-section of the double-sided adhesive tape on a Si-wafer.

and excitation of the currently investigated and the underlying polymer layer. This effect can also lead to blurring of the depth profile. The observed deviation in the thickness of the PE layer can be explained by incomplete evaluation of the depth profile: the depth profile was stopped when an increase in the Si-signal was observed. Uneven abla-tion and therefore full penetration of the sample on certain spots may have caused an early abortion of the measurement. Nevertheless, a clear classification of the layered sample was achieved.

4. Conclusion

In this study, the capabilities of LIBS for spatially resolved polymer classification was shown using two structured samples consisting of different polymers. A 2D structured sample was imaged and the polymer distribution was successfully classified using PCA. The ob-tained distribution of the two polymers present in the sample was va-lidated by comparing the obtained image of the polymer distribution to a contamination present in one of the two polymers. A high Pearson Correlation Coefficient (PCC) of 0.8065 confirmed a good agreement between the two images and therefore, the laterally resolved polymer classification was confirmed. Besides imaging of a 2D structured polymer samples, also the capabilities of investigating depth profiles of samples consisting of layered systems of multiple different polymers using LIBS was shown successfully. The obtained 3D distribution of the different polymers present in the multilayer sample was compared to a microscopic cross-section of the investigated sample. The sequence of the different layers present in the sample was correctly classified and also the thickness of each layer is in good agreement with the micro-scopic cross-section. The presented results indicate that the conven-tional way of using LIBS for elemental analysis and elemental mapping can be extended to different fields where the qualitative distribution of different polymers is of interest. One of the most promising ways to improve especially depth profiling is refocusing the laser on the sample surface after each ablated layer. This may help not only with uneven ablation, which causes blurring of the depth profile but also with more reproducible LIBS spectra as the distance between the plasma and the collection optics stays constant throughout the complete measurement.

Declaration of competing interest

There are no conflicts of interest to declare.

Acknowledgments

References

[1] D.N. Saheb, J.P. Jog, Natural fiber polymer composites: a review, Adv. Polym. Technol. 18 (1999) 351–363, https://doi.org/10.1002/(SICI)1098-2329(199924) 18:4<351::AID-ADV6>3.0.CO;2-X.

[2] J.N. Coleman, U. Khan, W.J. Blau, Y.K. Gun'ko, Small but strong: a review of the mechanical properties of carbon nanotube–polymer composites, Carbon 44 (2006) 1624–1652, https://doi.org/10.1016/j.carbon.2006.02.038.

[3] PlasticsEurope, (n.d.). https://www.plasticseurope.org/en/resources/publications/ 395-plastics-facts-2017 (accessed June 12, 2019).

[4] World Steel in Figures 2017, (n.d.). http://www.worldsteel.org/media-centre/ press-releases/2017/world-steel-in-figures-2017.html (accessed June 12, 2019).

[5] J. Holbery, D. Houston, Natural-fiber-reinforced polymer composites in automotive applications, JOM 58 (2006) 80–86, https://doi.org/10.1007/s11837-006-0234-2.

[6] M. Böltau, S. Walheim, J. Mlynek, G. Krausch, U. Steiner, Surface-induced structure formation of polymer blends on patterned substrates, Nature 391 (1998) 877, https://doi.org/10.1038/36075.

[7] R. Mazzeo, E. Joseph, S. Prati, A. Millemaggi, Attenuated Total Reflection–Fourier transform infrared microspectroscopic mapping for the characterisation of paint cross-sections, Anal. Chim. Acta 599 (2007) 107–117, https://doi.org/10.1016/j. aca.2007.07.076.

[8] R. Bhargava, S.-Q. Wang, J.L. Koenig, FTIR microspectroscopy of PolymericSystems, Liq. Chromatogr. FTIR Microspectrosc. MicrowaveAssisted Synth. Springer Berlin Heidelberg, Berlin, Heidelberg, 2003, pp. 137–191, , https:// doi.org/10.1007/b11052.

[9] A. Cincinelli, C. Scopetani, D. Chelazzi, E. Lombardini, T. Martellini, A. Katsoyiannis, M.C. Fossi, S. Corsolini, Microplastic in the surface waters of the Ross Sea (Antarctica): occurrence, distribution and characterization by FTIR, Chemosphere 175 (2017) 391–400, https://doi.org/10.1016/j.chemosphere.2017. 02.024.

[10] U.P. Agarwal, S.A. Ralph, FT-Raman spectroscopy of wood: identifying contributions of lignin and carbohydrate polymers in the spectrum of black spruce (picea mariana), Appl. Spectrosc. 51 (1997) 1648–1655, https://doi.org/10.1366/ 0003702971939316.

[11] R. Lenz, K. Enders, C.A. Stedmon, D.M.A. Mackenzie, T.G. Nielsen, A critical assessment of visual identification of marine microplastic using Raman spectroscopy for analysis improvement, Mar. Pollut. Bull. 100 (2015) 82–91, https://doi.org/10. 1016/j.marpolbul.2015.09.026.

[12] J.V. Gulmine, P.R. Janissek, H.M. Heise, L. Akcelrud, Polyethylene characterization by FTIR, Polym. Test. 21 (2002) 557–563, https://doi.org/10.1016/S0142- 9418(01)00124-6.

[13] D.W. Hahn, N. Omenetto, Laser-induced breakdown spectroscopy (LIBS), Part I: review of basic diagnostics and plasma–particle interactions: still-challenging issues within the analytical plasma community, Appl. Spectrosc. 64 (2010) 335A–366A.

[14] D.W. Hahn, N. Omenetto, Laser-induced breakdown spectroscopy (LIBS), Part II: review of instrumental and methodological approaches to material analysis and applications to different fields, Appl. Spectrosc. 66 (2012) 347–419, https://doi. org/10.1366/11-06574.

[15] D. Cremers, L. Radziemski, Handbook of Laser Induced Breakdown Spectroscopy, Wiley, 2006.

[16] A.W. Miziolek, Progress in fieldable laser-induced breakdown spectroscopy (LIBS), Gener. Spectrosc. Technol. V, International Society for Optics and Photonics, 2012, p. 837402, , https://doi.org/10.1117/12.919492.

[17] J. El Haddad, L. Canioni, B. Bousquet, Good practices in LIBS analysis: review and advices, Spectrochim. Acta Part B At. Spectrosc. 101 (2014) 171–182, https://doi. org/10.1016/j.sab.2014.08.039.

[18] P. Pořízka, J. Klus, E. Képeš, D. Prochazka, D.W. Hahn, J. Kaiser, On the utilization of principal component analysis in laser-induced breakdown spectroscopy data analysis, a review, Spectrochim. Acta Part B At. Spectrosc. 148 (2018) 65–82, https://doi.org/10.1016/j.sab.2018.05.030.

[19] S.J. Mousavi, M. Farsani, S. Darbani, A. Mousaviazar, M. Soltanolkotabi, A. Eslami Majd, CN and C2 vibrational spectra analysis in molecular LIBS of organic materials, Appl. Phys. B 122 (2016), https://doi.org/10.1007/s00340-016-6371-6.

[20] C.G. Parigger, G. Guan, J.O. Hornkohl, Measurement and analysis of OH emission spectra following laser-induced optical breakdown in air, Appl. Opt. 42 (2003) 5986–5991, https://doi.org/10.1364/AO.42.005986.

[21] J.M. Anzano, C. Bello-Gálvez, R.J. Lasheras, Identification of polymers by means of LIBS, in: S. Musazzi, U. Perini (Eds.), Laser-Induc. Breakdown Spectrosc. Theory Appl. Springer Berlin Heidelberg, Berlin, Heidelberg, 2014, pp. 421–438, , https:// doi.org/10.1007/978-3-642-45085-3_15.

[22] R. Sattmann, I. Monch, H. Krause, R. Noll, S. Couris, A. Hatziapostolou, A. Mavromanolakis, C. Fotakis, E. Larrauri, R. Miguel, Laser-induced breakdown spectroscopy for polymer identification, Appl. Spectrosc. 52 (1998) 456–461.

[23] V.K. Unnikrishnan, K.S. Choudhari, S.D. Kulkarni, R. Nayak, V.B. Kartha, C. Santhosh, Analytical predictive capabilities of laser induced breakdown spectroscopy (LIBS) with principal component analysis (PCA) for plastic classification, RSC Adv. 3 (2013) 25872–25880, https://doi.org/10.1039/C3RA44946G.

[24] M. Bonta, A. Limbeck, Metal analysis in polymers using tandem LA-ICP-MS/LIBS: eliminating matrix effects using multivariate calibration, J. Anal. At. Spectrom. 33 (2018) 1631–1637, https://doi.org/10.1039/C8JA00161H.

[25] M. Banaee, S.H. Tavassoli, Discrimination of polymers by laser induced breakdown spectroscopy together with the DFA method, Polym. Test. 31 (2012) 759–764, https://doi.org/10.1016/j.polymertesting.2012.04.010.

[26] M. Boueri, V. Motto-Ros, W.-Q. Lei, Qain-LiMa, L.-J. Zheng, H.-P. Zeng, JinYu, Identification of polymer materials using laser-induced breakdown spectroscopy combined with artificial neural networks, Appl. Spectrosc. 65 (2011) 307–314.

[27] R. Junjuri, M.K. Gundawar, Femtosecond laser-induced breakdown spectroscopy studies for the identification of plastics, J. Anal. At. Spectrom. (2019), https://doi. org/10.1039/C9JA00102F.

[28] L. Jolivet, M. Leprince, S. Moncayo, L. Sorbier, C.-P. Lienemann, V. Motto-Ros, Review of the recent advances and applications of LIBS-based imaging, Spectrochim. Acta Part B At. Spectrosc. 151 (2019) 41–53, https://doi.org/10. 1016/j.sab.2018.11.008.

[29] R.R.V. Carvalho, J.A.O. Coelho, J.M. Santos, F.W.B. Aquino, R.L. Carneiro, E.R. Pereira-Filho, Laser-induced breakdown spectroscopy (LIBS) combined with hyperspectral imaging for the evaluation of printed circuit board composition, Talanta 134 (2015) 278–283, https://doi.org/10.1016/j.talanta.2014.11.019.

[30] M. Bonta, J.J. Gonzalez, C. Derrick Quarles, R.E. Russo, B. Hegedus, A. Limbeck, Elemental mapping of biological samples by the combined use of LIBS and LA-ICP-MS, J. Anal. At. Spectrom. 31 (2016) 252–258, https://doi.org/10.1039/ C5JA00287G.

[31] B. Busser, S. Moncayo, J.-L. Coll, L. Sancey, V. Motto-Ros, Elemental imaging using laser-induced breakdown spectroscopy: a new and promising approach for biological and medical applications, Coord. Chem. Rev. 358 (2018) 70–79, https://doi. org/10.1016/j.ccr.2017.12.006.

[32] T.O. Nagy, U. Pacher, A. Giesriegl, M.J.J. Weimerskirch, W. Kautek, Depth profiling of galvanoaluminium–nickel coatings on steel by UV- and VIS-LIBS, Appl. Surf. Sci. 418 (2017) 508–516, https://doi.org/10.1016/j.apsusc.2016.12.059.

[33] G.S. Senesi, G. Nicolodelli, D.M.B.P. Milori, O. De Pascale, Depth profile investigations of surface modifications of limestone artifacts by laser-induced breakdown spectroscopy, Environ. Earth Sci. 76 (2017) 565, https://doi.org/10. 1007/s12665-017-6910-4.

[34] J. Schindelin, I. Arganda-Carreras, E. Frise, Fiji: an open-source platform for biological-image analysis, Nat. Methods 9 (2012) 676–682.

[35] M. Doube, M.M. Kłosowski, I. Arganda-Carreras, F.P. Cordelières, R.P. Dougherty, J.S. Jackson, B. Schmid, J.R. Hutchinson, S.J. Shefelbine, BoneJ: free and extensible bone image analysis in Image, Bone 47 (2010) 1076–1079, https://doi.org/10. 1016/j.bone.2010.08.023.

4.2   Article 2

As the applicability of spatially resolved classification of polymers was confirmed in the first published article, this approach was used for an application example from the field of cultural heritage science. In the work "Multivariate analysis and laser-induced breakdown spectroscopy (LIBS): a new approach for the spatially resolved classification of modern art materials" LIBS was used to classify modern art materials. The investigated modern art materials consist of two components: a polymeric binder and inorganic pigments. The main goal of this work was to perform a simultaneous classification of 3 polymers and 9 inorganic pigments. Besides the classification of the polymers using polymer specific emission signals, elemental fingerprinting was used to identify the inorganic pigments. The elemental fingerprinting approach is based on the presence of unique elements in each inorganic pigment enabling the differentiation. To evaluate this approach, LIBS spectra of pure inorganic pigments and polymeric binders were recorded. Using a PCA, all investigated polymers and inorganic pigments were discriminated by their LIBS spectrum. However, the main challenge of this work turned out to be the classification of combinations of polymers and inorganic pigments. LIBS is a technique which is very prone to so-called matrix-effects meaning that the absolute signals observed are depending on the samples' constituents. Usually, the classification of polymers is based on small changes of polymer specific signals. When different inorganic pigments are present within a polymer, matrix-effects may also cause small variations of polymer specific signals making the classification task more challenging. Therefore, a Random Decision Forest (RDF) was used for the classification of polymer and inorganic pigments combination. RDF is a machine learning approach using a training data set to build a classification model. In this work, a RDF was trained using LIBS spectra from all investigated pigment/polymer combinations. With this approach a satisfying classification was achieved. Using the RDF it is also possible to perform laterally resolved classification.

References

1. Giakoumaki A, Melessanaki K, Anglos D. Laser-induced breakdown spectroscopy (LIBS) in archaeological science - applications and prospects. Anal Bio Chem. 2007;387:749−60.

2. Melessanaki K, Mateo M, Ferrence SC, Betancourt PP, Anglos D. The application of LIBS for the analysis of archaeological ceramic

and metal artifacts. Appl Surf Sci. 2002;197-198:156−63. 3. Maravelaki-Kalaitzaki PN. Innovative techniques for the characterization of encrustation on Pentelic marble from the Parthenon, chapter in "Cultural heritage conservation and environmental impact assessment by non-destructive testing and micro-analysis". 2005;135−148.

4. Corsi M, Crisoforetti G, Palleschi V, Salvetti A, Tognoni E. A fast and accurate method for the determination of precious alloys caratage by laser induced plasma spectroscopy. Eur Phys J. 2001;13:373−7.

5. Grolmusová Z., Mináriková L., Rakovský J., Čermák P., Veis P., Elementar LIBS. Analysis of biological samples. Proc of Contr Papers, 2009;Part III:189−192.

6. Colao F, Fantoni R, Lazic V, Morone A, Santagata A, Giardini A. LIBS used as a diagnostic tool during the laser cleaning of ancient marble from Mediterranean areas. Appl Phys A Mater Sci Process. 2004;79(2):213−9.

7. Roy A. Artists' pigments, vol. 2.Washington DC: National Gallery of Art; 1993.

8. Fitzhugh E. Artists' pigments, vol. 3. Washington DC: National Gallery of Art; 1997.

9. Learner T. Analysis of modern paints. The Getty Conservation Institute, 2004.

10. Learner T. Modern paints uncovered. The Getty Conservation Institute, 2008.

11. Sattmann R, Monch I, Krause H, Noll R, Couris S, Hatziapostolou A, et al. Laser-induced breakdown spectroscopy for polymer identification. Appl. Spectr. 1998;52(3):456−61.

12. Brech F, Cross L. Optical microemission stimulated by a ruby laser. Appl Spectr. 1962;16:59.

13. Anabitarte F, Cobo A. Lopez-Higuera J.M., Laser-induced breakdown spectroscopy: fundamentals, applications, and challenge, ISRN Spectroscopy, 2012.

14. Musazzi S, Perini U. Laser-induced breakdown spectroscopy, theory and applications. Opt Sci. 2014.

15. Bonta M, Limbeck A. Metal analysis in polymers using tandem LA-ICP-MS/LIBS: eliminating matrix effects using multivariate calibration. J Anal At Spectrom. 2018;33:1631−7.

16. Rai S, Rai AK. Characterization of organic materials by LIBS for exploration of correlation between molecular and elemental LIBS signals. AIP Adv. 2011;042103.

17. Borgia I, Burgio LMF, CorsoM, Fantoni R, Palleschi V, Salvetti A, et al. Self-calibrated quantitative elemental analysis by laserinduced plasma spectroscopy: application to pigment analysis. J Cult Herit. 2000;1:S281−6.

18. Gornushkin IB, Smith BW, Nasajpour H, Winefordner JD. Identification of solid materials by correlation analysis using a microscopic laser-induced plasma spectrometer. Anal Chem. 1999;71(22):5157−64.

19. Jolivet L, Leprince M, Moncayo S, Sorbier L, Lienemann C-P, Motto-Ros V. Review of the recent advances and applications of LIBS-based imaging. Spectr Acta Part B: Atom Spectr. 2019;151: 41−53.

20. Sarmiento A, Pérez-Alonso M, Olivares M, Castro K, Martínez- Arkarazo I, Fernández LA, et al. Classification and identification of organic bindingmedia in artworks by means of Fourier transform infrared spectroscopy and principal component analysis. Anal Bioanal Chem. 2011;399:3601−11.

21. Unnikrishnan VK, Choudhari KS, Kulkarni SD, Nayak R, Kartha VB, Santhosh C. Analytical predictive capabilities of laser induced breakdown spectroscopy (LIBS) with principal component analysis (PCA) for plastic classification. RSC Adv. 2013;3:25872−80.

22. Musumarra G, Fichera M. Chemometrics and cultural heritage. Chem Intel Lab Syst. 1998;44:363−72.

23. Breiman L. Random forests. Mach Learn. 2001;45(1):5−32.

24. Anghelone M, Jembrih-Simbürger D, Schreiner M. Identification of copper phthalocyanine blue polymorphs in unaged and aged paint systems by means of micro-Raman spectroscopy and randomforest. Spectr Acta Part A: Mol Biomol Spectr. 2015;149:419−25.

25. Sheng L, Zhang T, Niu G, Wang K, Tang H, Duan Y, et al. Classification of iron ores by laser-induced breakdown spectroscopy (LIBS) combined with random forest (RF). J Anal At Spectrom. 2015;30:453−8.

26. Qi J, Zhang T, Tang H, Li H. Rapid classification of archaeological ceramics via laser-induced breakdown spectroscopy coupled with random forest. Spectr Acta Part B: Atom Spectr. 2018;149:288−93.

27. Tropsha A, Gramatica P, Gombar VK. The importance of being earnest: validation is the absolute essential for successful application and interpretation of QSPR models. QSAR Comb Sci. 2003;22:69−77.

28. Grégoire S, Boudinet M, Pelascini F, Surma F, Detalle V, Holl Y. Laser-induced breakdown spectroscopy for polymer identification. Anal Bionanal Chem. 2011;400:3331−40.

29. Hufnagl B, Steiner D, Renner E, Loder MGJ, Laforsch C, Lohninger H. A methodology for the fast identification and monitoring of microplastics in environmental samples using random decision forest classifiers. Anal Methods. 2019;11:2277−85.

30. Miziolek AW, Palleschi V, Schechter I. Laser induced breakdown spectroscopy: Cambridge University; 2006.

4.3 Article 3 (Review-Article)

The third publication entitled "Methodology and applications of elemental mapping by laser induced breakdown spectroscopy - a review" is a review article focusing on spatially resolved analysis using LIBS. In the first part of the review, instrumental requirements are discussed for successful LIBS imaging experiments. The second part gives an introduction on chemometric approaches which are beneficial for LIBS imaging. The third part discusses published application examples of LIBS based imaging in fields such as: life science, geoscientific studies, cultural heritage studies and materials science.

Review

Methodology and applications of elemental mapping by laser induced breakdown spectroscopy

A. Limbeck [a, *], L. Brunnbauer [a], H. Lohninger [a], P. Pořízka [b], P. Modlitbová [b], J. Kaiser [b], P. Janovszky [c, d], A. Kéri [c, d], G. Galbács [c, d]

[a] TU Wien, Institute of Chemical Technologies and Analytics, Technische Universität Wien, Getreidemarkt 9/164, 1060, Vienna, Austria
[b] Central European Institute of Technology (CEITEC) Brno University of Technology, Purkyňova 656/123, 612 00, Brno, Czech Republic
[c] Department of Inorganic and Analytical Chemistry, University of Szeged, Dóm Square 7, 6720, Szeged, Hungary
[d] Department of Materials Science, Interdisciplinary Excellence Centre, University of Szeged, Dugonics Square 13, 6720, Szeged, Hungary

HIGHLIGHTS

- Elemental imaging using LIBS.
- LIBS instrumentation - technical requirements for imaging applications.
- Strategies for advanced data processing.
- Selected applications in life sciences, geoscientific studies, cultural heritage studies and materials science.

GRAPHICAL ABSTRACT
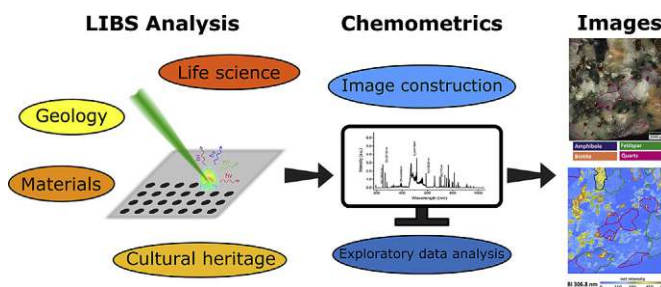
ABSTRACT

In the last few years, LIBS has become an established technique for the assessment of elemental concentrations in various sample types. However, for many applications knowledge about the overall elemental composition is not sufficient. In addition, detailed information about the elemental distribution within a heterogeneous sample is needed. LIBS has become of great interest in elemental imaging studies, since this technique allows to associate the obtained elemental composition information with the spatial coordinates of the investigated sample. The possibility of simultaneous multi-elemental analysis of major, minor, and trace constituents in almost all types of solid materials with no or negligible sample preparation combined with a high speed of analysis are benefits which make LIBS especially attractive when compared to other elemental imaging techniques. The first part of this review is aimed at providing information about the instrumental requirements necessary for successful LIBS imaging measurements and points out and discusses state-of-the-art LIBS instrumentation and upcoming developments. The second part is dedicated to data processing and evaluation of LIBS imaging data. This chapter is focused on different approaches of multivariate data evaluation and chemometrics which can be used e.g. for classification but also for the quantification of obtained LIBS imaging data. In the final part, current literature of different LIBS imaging applications ranging from bioimaging, geoscientific and cultural heritage studies to the field of materials science is summarized and reviewed.

* Corresponding author.
E-mail address: andreas.limbeck@tuwien.ac.at (A. Limbeck).

Contents

1. Introduction

In the last century, atomic spectroscopy has been used for the analysis of almost all elements in a wide variety of sample types. Motivation for the measurement of metals as well as non-metals in natural but also industrial samples was driven by their influence on sample behaviour and properties. Moreover, knowledge about prevailing trace element levels also provides information about origin, formation or degradation of environmental or geological samples. For example, there is a clear need to determine the concentration of toxic elements in environmental, medical, or biological samples. The ability to catalyse environmental, biological or technological processes is another important reason for the assessment of metal concentrations prevailing in respective samples. Studies related to the determination of sample age or provenance benefit from the measurement of elemental ratios. However, the application of trace element analysis is not limited to earth sciences and life sciences only. In the last decades, the measurement of sample composition, additive levels and elemental impurities have become important in the field of materials science. Primary goal of these efforts is to maintain or even improve the intended chemical, physical or mechanical product properties.

For many years, simple analysis of bulk concentrations was sufficient for sample characterization. At the same time, it has also become customary in many research fields to collect information about the elemental distribution within the investigated samples. For example, the spatially resolved analysis of essential metals (such as Cu, Zn, Fe, Mn, Mg, and others), metalloids or non-metals (like S, P, N and halogens) in thin sections of biological tissues has become a subject of great interest in life science studies. Elemental

maps are also of great importance in materials science, where typical applications include improvements in manufacturing and processing techniques such as deposition, diffusion or segregation processes, and coating or combustion procedures.

Thus, analytical techniques able to associate spatial coordinates to information on elemental composition are in high demand. Further requirements for appropriate methods include fast and simultaneous multi-elemental analysis of major, minor, and trace constituents, applicability for analysis of all kind of solid samples (conductive as well as non-conductive samples), no or negligible sample preparation, and no or minimal sample damage only. Since some types of environmental and biological, in particular medical samples are susceptible to vacuum, the method should work at ambient pressure to avoid unintended sample alterations.

In the last decades several analytical techniques capable of providing elemental imaging information have been employed for these purposes, including micro-X-Ray-Fluorescence-Analysis (μ-XRF), Electron Probe Micro Analysis (EPMA), Auger Electron Spectroscopy (AES), X-ray Photoelectron Spectroscopy (XPS), Secondary Ion Mass Spectroscopy (SIMS), Low Energy Ion Scattering (LEIS) and other synchrotron-based chemical imaging procedures [1]. Although each of these techniques has its own benefits (e.g. some are non-destructive (e.g. XRF), some are very surface sensitive (e.g. SIMS), and some provide also chemical information (e.g. XPS)), the method that complies with the requirements mentioned above to the largest extent is Laser Ablation-Inductively Coupled Plasma-Mass Spectrometry (LA-ICP-MS) [2]. Attributes that make this technique attractive for spatially resolved analysis of complex matrices such as geological, environmental, biological or technological samples are high sensitivity, wide linear dynamic range, fast

sample throughput, minimal sample preparation, minimal risk of sample contamination, and the ability to perform isotopic analyses. The steadily growing field of imaging applications include the characterization of advanced materials (e.g. metals, alloys, semiconductors, ceramic oxides, but also nitrides or carbides, composite materials) [3], the investigation of naturally occurring but also artificially introduced elements in hard and soft tissue material [4], but also geological samples such as rocks, minerals or meteorites [5].

Although LA-ICP-MS has become an established standard procedure for quantitative elemental mapping there still are three major limitations hampering the universal applicability of this method. Due to the transient nature of the signals produced in imaging experiments, the sequential operation mode of quadrupole and scanning sector field mass spectrometers (QMS and SFMS) does not permit the measurement of full mass spectra. Thus, a preliminary definition of the elements/isotopes of interest and therefore knowledge about sample composition is necessary prior to analysis. Moreover, in case of multi-element analysis the number of monitored m/z ratios is restricted when a certain degree in the quality of analysis (precision, accuracy, resolution) should be accomplished. A promising approach to overcome this limitation of QMS and SFMS instrumentation in imaging experiments is the use of a time of flight mass spectrometer (TOFMS), which provides access to full mass spectra and allows the identification of unknown sample constituents. However, independent from the applied type of mass spectrometer, LA-ICP-MS struggles with limitations in the sensitivity but also selectivity in the detection of most non-metals (such as S or P). The elements H, C, N and O, which are the major constituents of all organic compounds and thus all kinds of biological materials, and in addition also F for geological samples are not accessible at all. Finally, the aerosol generated during interaction of the focused laser beam with the sample must be transported from the ablation cell to the ICP-MS. Due to material losses in the transfer line, the efficiency of this transport step is always below 100%. Moreover, the wash out behaviour of the applied ablation cell determines the measurement time required for imaging experiments. With conventional ablation cells and QMS or SFMS instrumentation for samples in the mm x mm range, measurement times in the order of several hours are common. Combining the recently introduced rapid response cells with high repetition rate laser systems and ICP-TOFMS systems enables multi-elemental analysis of the same area in a fraction of that time. Nevertheless, even with these advanced ablation cells the repetition rates of commercial laser systems are not fully exploited.

Laser-induced breakdown spectroscopy (LIBS), another laser assisted technique used for elemental analysis, allows to overcome most of the main drawbacks of LA-ICP-MS. LIBS is also a microdestructive method which requires practically no sample preparation, works under ambient pressure conditions and can be used equally well for bulk measurements and spatially resolved investigations [6,7]. In addition to these useful features, which were also fulfilled by LA-ICP-MS, LIBS offers some unique advantages that make this technique especially attractive for imaging applications. Although the first ground-breaking works were published in the late 1990s [8,9], a prerequisite for the development of a large number of imaging applications was the continuous improvement of applied laser systems, spectrometers and detection units in the last two decades.

In the meanwhile, LIBS has attracted increasing attention in the field of imaging [10] since it enables extremely fast imaging experiments with pixel acquisition rates in the kHz range [11] and a spatial resolution down to some μm [12] with valuable und numerous developments and applications published by the group of Vincent Motto-Ros [13]. The lack of need for the transport of

ablated matter also eliminates carry-over and wash-out effects and transport efficiency is not an issue (even though with improved setups these effects are becoming less of an issue in LA-ICP-MS as transport efficiency improved from 40% in the beginning of ns-LA-ICP-MS to 80—90% in recent fs-LA-ICP-MS [14,15]).The ability to measure almost every element of the periodic table also including the elements H, C, N, O, and F which are not easily accessible by ICP-MS are further remarkable benefits of LIBS that are recognized in elemental imaging studies. Compared to alkali and earth alkali elements, which provide best detection limits, the sensitivity of non-metals is reduced. However, as these elements usually are main components this is not a limiting factor. In contrast to sequentially operating mass spectrometers, LIBS facilitates a simultaneous detection of the investigated wavelength range. Thus, with the collection of broadband spectra, no preliminary analyte selection is necessary and therefore, identification of prevailing elements can be done after the measurement. Additionally, statistical evaluation of broadband spectra is beneficial for sample classification. Moreover, LIBS spectra may also provide molecular information, which is useful especially in terms of polymer characterization and capabilities for stand-off analysis. Nevertheless, for some elements the sensitivity of LA-ICP-MS is still superior compared to LIBS enabling investigations with improved spatial resolution. Although the capabilities of LIBS for isotopic analysis have been demonstrated recently [16], LA-ICP-MS is still the method of choice for this special kind of analysis [17].

In Fig. 1, the basic concept of elemental mapping with LIBS is outlined. Within this review, a brief description of recent developments in instrumentation and technology is described. Different methodologies in terms of multivariate data processing, and calibration protocols for LIBS imaging are also discussed. The benefits of LIBS for spatially resolved analysis are presented by a selection of application examples from the fields of life sciences, geology and material sciences. Particular attention is paid to demonstrate the versatile character of LIBS, enabling the analysis of practically all kinds of solid samples without in-depth a priori knowledge of the sample composition. Finally, future prospects and potential applications of the technique are discussed.

2. Technical requirements

In order to be useful, LIBS imaging setups generally have to be designed and built specifically for the purposes of elemental imaging, due to a set of concomitant requirements that are usually demanded from conventional LIBS or LA-ICP-MS setups only separately. The primary reason for this is that not only the scanning laser ablation of the sample surface needs to be technically realized, but at the same time the plasma light also needs to be collected efficiently, therefore the optical and mechanical setup is more complicated than either in LIBS or LA-ICP-MS systems. The laser source, optical system, ablation chamber and the light detector all need to work concertedly to provide near ideal conditions for a fast, high-resolution, high-sensitivity LIBS imaging experiment. In the followings, we briefly overview the requirements set up by these conditions for the main components in the system. Readers interested in further technical details are kindly referred to reviews [13,18—22] and chapters in books [6,23—25] dedicated to LIBS instrumentation.

2.1. Laser source

The laser source has to be one that releases light pulses at a wavelength well absorbed by the sample material. The minimum pulse energy depends on the breakdown threshold (irradiance or power density needed to generate an LIB plasma) on the particular
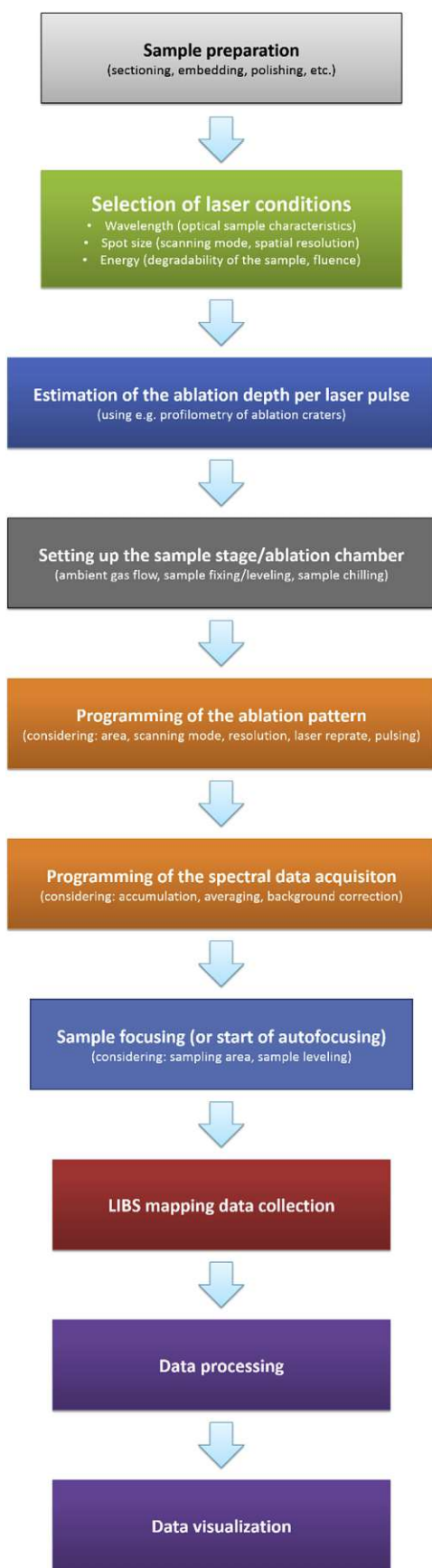
Sample preparation
(sectioning, embedding, polishing, etc.)

Selection of laser conditions
- Wavelength (optical sample characteristics)
- Spot size (scanning mode, spatial resolution)
- Energy (degradability of the sample, fluence)

Estimation of the ablation depth per laser pulse
(using e.g. profilometry of ablation craters)

Setting up the sample stage/ablation chamber
(ambient gas flow, sample fixing/leveling, sample chilling)

Programming of the ablation pattern
(considering: area, scanning mode, resolution, laser reprate, pulsing)

Programming of the spectral data acquisiton
(considering: accumulation, averaging, background correction)

Sample focusing (or start of autofocusing)
(considering: sampling area, sample leveling)

LIBS mapping data collection

Data processing

Data visualization

Fig. 1. A schematic flow chart of the preparatory and executive steps of 3D elemental mapping by LIBS.

sample. For most solids, GW/cm^2 irradiances are sufficient for this, which can already be achieved by using laser sources providing 10–100 mJ energy, 5–10 ns long pulses and a reasonable level of beam focusing. Since the spatial resolution of an imaging LIBS setup is always of primary importance, an advanced focusing optics is generally required anyway, which helps to keep the laser pulse energy requirement low. Good focusing, on the other hand, typically necessitates the laser source has a Gaussian intensity profile, as higher transversal modes can be less efficiently focused. It is also worth mentioning that flashlamp-pumped lasers often do not have the beam quality for tight focusing (e.g. 3–5 μm focal spots), unless they are built with an aperture-controlled resonator.

With regard to pulse energy, it is very important that the laser source provides an active control of the pulse energy and that the laser has ample reserve, in view of demanding samples with low absorbance. It should also be borne in mind that a high dynamic range (high contrast) attenuation of the primary laser beam (e.g. two orders of magnitude or more in energy) can usually only be achieved via the combination of at least two pulse energy control approaches (e.g. time-controlled active Q-switch, adjustable energy pumping source, rotatable polarizers, etc.) usually only available as options at a premium cost. We discuss further considerations related to both laser pulse energy and analytical spot size in the next section.

Meaningful laser wavelengths for LIBS purposes are typically in the UV or in the NIR range, especially for biological samples, where the selection should be based on the consideration of multiple factors. These include, but are not limited to the followings: *i)* the absorbance of the sample needs to be high at the chosen wavelength (to the benefit of sensitivity), *ii)* NIR wavelength, when combined with ns pulse duration, usually gives the best sensitivity in LIBS measurements, due to strong plasma heating which is proportional with λ^3, *iii)* UV wavelengths should always be preferred when spatial resolution is more important than sensitivity, as NIR laser ablation often generates strong thermal effects (charring) in the sample around the focal spot. However, wavelength is not an independent variable with laser sources. A certain laser type (active medium) will emit light at its characteristic fundamental wavelength and this can typically only be modified at a significant cost of pulse energy, also related to the regime of pulse duration (e.g. ns or fs). At present, most laser sources used in LIBS setups are still common solid-state lasers such as Nd:YAG or Nd:YLF. These lasers can offer high pulse energies only at their ca. 1064 nm fundamental wavelength and therefore other output wavelengths (532, 266 or 213 nm) are produced by employing nonlinear crystals, via the sum frequency generation technique, at a cost of 50–90% loss in pulse energy. Alternative laser sources are also available for LIBS use, such as excimer gas lasers, which can directly provide UV wavelengths (starting from 157 nm with an F_2 and up to 351 nm with a XeF medium), but they never really became widespread in analytical LIBS spectroscopy, due to their bulkiness and impracticality (e.g. frequent need for a refill of corrosive gases from gas tanks).

The selection of the laser source in terms of the pulse length regime (e.g. nanosecond(ns), picosecond(ps) or femtosecond(fs)) is also a subject of consideration. Apart from the significantly higher costs, fs pulses have been found to be advantageous from the point of view of a more stoichiometric ablation and therefore better analytical accuracy as well as a somewhat better spatial resolution (due to less debris around the crater caused by the smaller plasma plume). Please note though that smaller ablation spot size often also means smaller analytical LIBS signals. At the same time, ns pulses (assuming comparable irradiances) provide far better sensitivity, due to the higher mass of ablated material and more effective plasma heating/shielding. Thus, a fs laser source may only

be the better choice in an imaging LIBS setup, if the concentration of the analytes is high.

High repetition rate is a critical characteristic of laser sources suitable for LIBS imaging analysis, considering the large number of single point measurements to be performed during scanning. For example, a mapping task for an area of 1 cm^2 with a step size of 10 μm requires 1,000,000 measurements (without spot overlaps), which takes 13–27 h to complete with a laser operating only at the typical 10–20 Hz repetition rate. This measurement time is too long for many applications, where the use of lasers offering 1 kHz or higher repetition rates are required. In this respect, Q-switched diode pumped solid state (DPSS) lasers and fiber lasers, now becoming widely available commercially, have great potential. Typical Q-switched pulse energies of commercial lasers of these types are a few millijoules, although a tens of mJ fiber lasers and repetition rates in the hundreds of kHz range have already been reported [26]. Both DPSS and fiber lasers have superior beam quality, better stability and longer lifetime than conventional flashlamp-pumped Nd:YAG lasers, which convert to better spatial resolution, faster acquisition times and improved precision, thus at present these are the ideal, even if not yet widespread, laser sources for LIBS imaging analysis.

It also has to be added that while Ti:sapphire femtosecond laser sources are becoming more and more used in imaging LIBS setups due to their kHz-MHz range pulse repetition rates, high peak power and ultrashort pulses, they are actually not very good at producing single pulses [27]. They have difficulties with self-starting and stability, so they are very time-inefficient when it comes to single spot LIBS analysis (of course, these problems also affect fs LA systems). They are far more useful if trains of utrashort pulses need to be generated, which makes them most useful in continuous scan mode LIBS analysis (continuous line or area scans). For relevance of this in imaging LIBS, see section 2.5. On the other hand, DPSS lasers offer a good compromise between high repetition rate and reliable single-pulse operation; the achievable repetition rate with a DPSS is still quite high, typically some kHz.

Signal enhancement is always welcome in analytical spectroscopy, and LIBS elemental imaging is no exception. As is known from the literature, significant signal enhancement (up to ca. two orders of magnitude) can be achieved with the use of double-pulse or multi-pulse LIBS analysis (DP-LIBS and MP-LIBS) [19,28–33]. Although these approaches can be realized in several sophisticated optical configurations (e.g. with two lasers or a single laser, orthogonal/cross/colinear optical paths, delayed pulses, different pulse energy ratios, combination of IR/Vis/UV pulses etc.) when the analysis is carried out on a single spot, but the most practical one for LIBS elemental imaging is the colinear arrangement, which requires a special laser source that is capable of releasing a controlled burst of Q-switched pulses. Hence the use of the double-pulse approach in LIBS elemental mapping so far has been quite limited [34–37]. A drawback of the colinear DP-LIBS setup is that both pulses are ablative, which decreases the achievable depth resolution.

2.2. Laser focusing and light collection optics

Generally speaking, the optical setups used in LIBS instrumentation are quite diverse. Transmissive and reflective optical elements both in the laser beam focusing arm of the optical setup as well as in the light collection arm are equally used [24].

In an imaging setup, the beam guiding optics primarily should allow for a tight, variable spot-size focusing with a Gaussian intensity profile for the sake of high spatial resolution. Adequate focusing can principally be achieved by using a single "best form" lens, but for best results, a high numerical aperture lens (or a high

damage threshold microscope objective) is needed, which has to be illuminated as uniformly as possible, so often a beam expander is also required to be incorporated in the optical path. For the sake of variable spot sizes, a zoom optics is needed, with multiple further optical elements. All optical elements in the focusing system need to be anti-reflection coated in order to maximize the pulse energy available on the sample surface and to minimize back-reflection of laser light into the laser source. If such reflections are not avoided they could deteriorate the performance of the laser, thereby inducing a loss of beam and pulse quality eventually leading to fluctuations in the LIBS signal. In more sophisticated setups, a Faraday isolator (rotator) can also be used to eliminate the back-propagation of laser beam. The smallest laser spot in a LIBS setup ever achieved was 450 nm [38].

In LIBS elemental imaging, the analytical spot size has to be chosen so that one also considers the area of the scan, the laser pulse energy available and the information content to be obtained. Choosing a smaller spot size means more information, which may be a necessity for a largely heterogenous sample with very small features to be resolved, but it also brings about a largely extended analysis time (with non-overlapping spots, halving the spot diameter makes the duration of the scan four times as long). This may not be practical for large area scans. A too small spot size may also decrease the analytical signal, thus the SNR of the obtained image may suffer for low concentration analytes. This is further complicated by the fact that very small spot sizes (ca. 40 μm or less) are often produced in LIBS systems by a size aperture (pinhole) setup, which wastes much of the cross section of the laser beam, and hence there usually is a significant pulse energy loss with these settings. Since the signal in LIBS, within the same pulse duration regime, is more or less proportional to both the amount of ablated matter and the fluence, the loss of analytical signal can be dramatic. The possibility to use very small analytical spot sizes is a definite advantage of LA-ICP-MS over LIBS in elemental imaging, which is due to the fact that in the former, the laser ablation is only used as a means of sample introduction and it is the ICP plasma that is responsible for signal generation, plus of course MS detection has very good sensitivity. This is also the reason why e.g. a ns laser LA-ICP-MS system can work well with as low as 1 mJ pulse energy and like 5 μm spot size, whereas with a similar laser source, LIBS struggles with spot sizes below some 10 μm in diameter and/or less than 10 mJ pulse energy. The much smaller fluences used in LA-ICP-MS also cause less damage to the sample around the ablation crater. The bottom line is that in most of the cases, it is advisable to choose the maximum spot size that is sufficient to resolve sample features and to pay attention to the laser pulse energy delivered to the sample.

In most LIBS setups, spherical beam guiding optical elements are used which produce a circular spot, however some analytical advantages have been reported to be associated with the use of cylindrical lenses producing rectangular spots (e.g. Refs. [39,40]). These may also be used in imaging setups in order to ablate more material (e.g. in square-shaped spots as opposed to circular spots) with a same scanning step resolution, thereby achieving higher signals. Another interesting optical approach for laser beam focusing is the incorporation of a microlens array described by Sturm in Ref. [41] in a LIBS imaging setup.

The depth of focus (defined as the distance from the point of minimum beam diameter after focus to the position at which the area of the beam has doubled, characterized by the Rayleigh range) increases linearly with the wavelength and with the square of the ratio of the focal length to the input beam diameter at the focusing lens [6]. The calculation gives about 4 mm depth of focus for typical conditions (λ = 1064 nm, d = 12 mm, f = 120 mm). In an imaging application, it means that for practical samples with minimal

surface corrugations (<1 mm), a reasonably small area of interest (e.g. 1 cm^2) and minimal tilting (the sample is affixed in a holder in a position that the area of interest on the surface is nearly horizontal), there is usually no need for auto-focusing during scanning, as the sample surface will not move out of the depth of focus, and therefore the irradiance on the sample surface will stay acceptably stable, which is a pre-requisite for accurate and precise elemental mapping. This is fortunate from the point of view of scanning speed, as auto-focus optomechanisms are usually not speedy enough to keep the pace with the rate of data collection needed (>kHz). Nevertheless, an auto-focus feature (based on e.g. time-of-flight measurements from a supporting beam of diode laser pulses or on a camera image) is very useful, because it makes the bringing of the starting spot into focus much easier. This additionally aids sample surface observation via a digital camera. It should also be mentioned that in contrast to surface measurements, the depth of focus requirements for depth-resolved analysis are more demanding. A small depth of focus is also preferred if the sample is a thin slice.

It should also be added that auto-focusing is typically only featured in commercial LIBS (and LA) instruments, but can not be expected to work equally well on all sample types. Typically, transparent samples give camera-based systems a hard time, and samples with strong specular reflection or very little scattering can easily mislead time-of-flight based systems. In addition to this, it can also cause similar problems if the optical characteristics of the sample show great variability within the mapped area.

A general optical alternative for rastering the beam across the sample surface instead of sample translation is steering the beam by a mirror system (driven by e.g. piezoelectric drives or galvo-scanners) and an *F*-theta lens. However, this arrangement is not practical in LIBS, because the emitted light from the plasma also needs to be collected and this would be very much complicated by the varying direction of the ablative beam during scanning.

The light collection optics should of course be optimized for maximum collection efficiency. First of all this means that the collection solid angle should be as large as possible/practical. Second, although the collection of the light emission by the plasma can be also effectuated from the side, but most light can be collected if the collection optics is uniaxial with the laser beam focusing optics („top view"). This is due to the fact, that breakdown plasmas always propagate outwards in the direction of the surface normal and in most setups, the direction of the laser beam is perpendicular to the sample surface. This arrangement however necessitates the optical separation of the forward propagating „monochromatic" laser light from the backward propagating plasma emission to be detected. The above requirements are best realized either by using a concave, collection mirror pierced for the focused laser beam or by using a telescope (e.g. Galilean) arrangement. The collected light, now collimated by the mirror, can then be focused onto the entrance slit (round or circular) of the spectrometer, preferentially using a reflective optical component again in order to avoid chromatic aberration. However ideal, this setup is rarely used in commercial LIBS imaging systems because the sample surface also needs to be observed with a high resolution digital camera prior to the measurement for the selection of the area of interest and sample documentation purposes. This can be done easiest if this third „observation beam" is collected uniaxially with the laser beam and the light collection is performed from the side on a different axis, at some cost of sensitivity. It should be mentioned that use of fiber optic cables to couple the emitted light into to the spectrometer is very practical from the point of view of system assembly, but it comes with significant further losses in sensitivity, especially in the UV range. This is caused by multiple problems associated with the process of coupling light into the fiber, limited transmission through the fiber and sub-optimal filling of the entrance slit with light, etc.

2.3. Ablation chamber and sample positioning

Employing an ablation chamber that is rarely used in conventional LIBS analytical measurements is hardly avoidable in imaging analysis. Although the use of an ablation chamber imposes certain limitations in sample size and shape, which necessitates some mechanical sample preparation, it is not a drawback since sample preparation is almost always involved with LIBS imaging anyway.

The ablation chamber also provides a possibility to perform plasma generation under an inert gas atmosphere with pressure and composition control. This can be beneficial with respect to *i)* enhancing the sensitivity by modifying plasma physics, *ii)* allowing the access of the VUV spectral region by purging oxygen and nitrogen from the optical path, *iii)* reducing gas-phase reactions in order to avoid some spectral interferences and *iv)* reducing the depositions and thermal effects on the sample surface thereby slightly improving spatial resolution. For example, it is well documented [42] that a decreased pressure (ca. 10 Torr) argon gas atmosphere generally gives the highest sensitivity in LIBS measurements, and the addition of He to the gas reduces the amount of debris produced during laser ablation, which can help increase the imaging resolution. The use of He as ambient gas is also beneficial when detecting nonmetallic elements, such as F and S, because the helium plasma has higher excitation potential than argon. Using a gas flow around the sample and in the chamber also helps to keep the window of the chamber clean of deposits, which would otherwise continuously decrease the transmission of the window, thereby leading to a decrease of the laser fluence reaching the sample surface and a decrease of the recorded emission signal. This is especially important in imaging applications, since a great number of laser pulses are delivered to the sample, so cleaning the chamber window after each few shots is not an option. As a rule of thumb, it is generally advisable to use a laser focusing optics in nanosecond LIBS at atmospheric pressure with a working distance of at least 10—20 mm in order to keep the optical elements at a safe distance from the ablation plume ejected from the sample surface and some of the gas reaction products - if the gas pressure is higher or a femtosecond laser source is used then the distance can be smaller, because these conditions produce a much smaller plasma. At the same time, this working distance will be higher if the ablation gas has a pressure significantly lower than atmospheric, the laser pulse energy is higher than usual or the samples vigorously get oxidized in the atmosphere, such as with polymers/organics, as the height of the plume will be larger. It also has to be considered that plasmas in argon are generally hotter and larger than those in helium, due to the higher thermal conductivity of the latter. It should also be noted that the purging of the ablation chamber with a gas flow ideally dictates to be performed at a volume rate which ensures the exchange of the gas between each laser shots. This, in turn, suggests that the volume of the chamber should be kept at a minimum — limited by the sample size and the chamber height (min. working distance), of course. The higher the laser repetition rate, the faster the gas exchange needs to be. The use of gas flow rates around 20 L/min are common.

A further device the use of which is crucial for a successful high repetition-rate scanning LIBS imaging application is a motorized, high-speed micropositioning two-axis (or if depth-resolved analysis is also planned, three-axis) translation stage that programmatically moves the sample under the focused laser beam. Needless to say that the linear resolution and the positional accuracy of these stages have to be in the sub-μm range, a value significantly smaller than the spatial resolution (analytical spot

size) aimed to be achieved, with a travel range that exceeds the lateral sample dimensions. In addition to this, the stage also needs to be very fast in *x-y* scanning speed, otherwise an ideally kHz-range repetition rate laser can not be exploited. As a numerical example, a fast precision translation stage with a 250 mm/s speed allows a 10 mm line to be scanned in 1/25 s. This speed can be exploited with a laser having 25 kHz repetition rate if a 10 μm spatial resolution is to be achieved. A Z-axis piezo translation stage, with a travel of, say, 500 μm is also necessary if depth-resolved analysis is planned (3D mapping). This limited travel range is sufficient for most such studies, considering the increasing difficulties in the efficient collection of light from an increasing depth ablation crater. It may also be added that the tilting of the sample surface (e.g. by employing a rotation stage working around either the *x* or *y* axis) can be used as an approach to enhance depth resolution [43]. Mounting the sample holder on a rotation stage also helps to ensure that the area of interest on the surface of the sample is horizontal for the scanning.

Considering the usual long time (several hours) needed for the imaging, the use of a thermostatable (cooling) sample holder should be considered in case of perishable (e.g. biological) samples. Without cooling, the microbiological degradation of the sample can cause analytical errors due to compositional changes (e.g. loss of volatiles) or phase transformations (e.g. liquefaction, thawing). Such sample holders are commercially available and are widely used in microscopy; the cooling is performed by a thermoelectric (TEC) device, supported by a recirculated fluid heat dissipation line.

The shape transformation or dimensional changes of the sample during the measurement time are also to be avoided. Flexible or mechanically not stable samples may not even be suitable for LIBS imaging. A common solution for fixing such samples is to embed them in a rigid polymer matrix, e.g. epoxy resin, and then cut the block at the right elevation to expose the desired cross section of the sample [44,45]. This approach has been long used in the field of microscopy and was taken over by the LA-ICP-MS and now by the LIBS imaging community. Another possibility to fix samples that are not rigid enough is to freeze them and keep them frozen during the whole measurement time by employing an above mentioned thermostable sample holder. It is worth mentioning though that local thawing of the sample and the production of water vapor under the action of the laser pulse is inevitable. This can complicate quantitative or 3D mapping measurements and the use of a dry purging gas becomes very important. Further details of the sample preparation of various applications can be found in section 4.

Last, but not least, the use of the ablation chamber is also preferred due to safety considerations — without an ablation chamber, the analysis of samples that impose chemical, radiological, or biological hazards is not advised.

2.4. Spectrometers and detectors

The dispersive optical arrangement of spectrometers used for elemental imaging is no different from regular LIBS analysis. The choice of the optical setup of the spectrometer is dictated by such features as spectral resolution, spectral coverage and sensitivity. Theoretically, no specific dispersive optical setup is preferred over the others in LIBS imaging, thus all major types of spectrometers (e.g. Czerny-Turner, Paschen-Runge, Echelle, etc.) are in fact used. It is mainly the type and characteristics of the photoelectric detector used what makes a difference in mapping.

Charge coupled devices (CCD) are common in LIBS. Linear or 2D CCD arrays, in an intensified (with a microchannel plate, MCP) or non-intensified form are mostly employed. Linear CCD arrays are mostly used in Czerny-Turner spectrometers, whereas CCD cameras can be found in Echelle spectrometers. Back-thinned, Si-based CCDs

provide low noise levels and good sensitivity in the UV−Vis−NIR range and can be efficiently synchronized with at least μs triggering accuracy and μs - ms range integration times, suitable for gated LIBS detection. The spectral resolution and sensitivity achievable depend on the optical setup of the spectrometer as well as the pixel resolution of the CCD array. Compact spectrometers incorporating linear CCD array detectors (having 2048 or 3684 pixels) typically provide good sensitivity, but the combination of spectral resolution (0.05−0.1 nm) and spectral coverage (100−150 nm) they offer is sub-optimal for LIBS detection, hence are preferred in portable and cost-conscious instruments. Echelle spectrometers with megapixel CCD cameras on the other hand can provide good spectral resolution (ca. 10−30 p.m.) along with a more or less complete UV−Vis spectral coverage, at the expense of some sensitivity.

A common problem with scientific CCD and intensified CCD (iCCD) detectors is their strongly limited read-out speed (after exposure, the pixels are read out in a serial fashion, which takes a long time), typically in the 1−100 Hz range (1−100 frames per second). This obviously is a serious drawback in LIBS imaging, which gives best performance at frequencies two to three orders higher (10−100 kHz). At present, the best promise for this field is the development of complementary metal-oxide semiconductor (CMOS) photosensor arrays. These devices have advanced read-out electronics and some of them already offer Gpixel/s read-out speeds, allowing for a sustained > kHz acquisition at their full megapixel resolution. At this speed, the camera's record length also becomes an issue, as a high-speed camera is preferred to be able to store all the frames in its on-board memory buffer, thereby requiring multi-GB memory. These CMOS cameras are now commercially available, but they are quite expensive, and have not made their way into the mainstream spectrometers, partially because of their somewhat reduced sensitivity compared to CCDs. Nevertheless, they definitely represent the future of LIBS imaging detectors. It is also worth mentioning that using photoelectron multiplier (PMT) detectors in discrete wavelength spectrographs, such as the Paschen-Runge arrangement, is a viable option for high speed LIBS imaging, but it is only feasible in industrial setups which work with a pre-defined set of analytical lines [24].

2.5. Data collection modes

Further consideration should also be given to the planning of LIBS data collection; in other words, the measurement pattern or data collection mode. This is the approach the system will follow to scan the rectangular analytical area on the sample surface. Essentially, two basic approaches are possible: step scan and continuous scan. Whether the former or the latter is better for a given mapping application strongly depends on the laser, optical setup, ablation stage available in the system and on the analyte concentration.

In step scan mode, the sample stage moves step by step from one measurement spot to the next. In each location, a full feature LIBS measurement (with autofocusing, cleaning shots, signal averaging or accumulation, double-or multi-pulsing, etc., if needed) is performed and the stage only moves on when LIBS data collection is completed. Step scan mode is therefore very adaptive and can be employed in any LIBS system. The cost of this flexibility is the very slow speed of mapping, which - in addition to the above features — is further decreased by the necessity to accelerate, decelerate and letting to stabilize the stage between locations (which is also influenced by the weight of the sample). One would think that this limits the usefulness of step scan mode to small area elemental imaging, but in actuality, its ability to optically follow the change in surface elevation becomes increasingly useful when larger areas are to be scanned. Users of scanning LIBS setups with conventional nanosecond laser sources can benefit the most from the step scan

mode data collection.

In continuous scan mode, the stage is continuously moving, and the laser is continuously firing at a calculated relative rate that allows the achievement of the required lateral imaging resolution (distance of measurement spots). Obviously, only single-shot analysis is possible in continuous scan mode − there can be no cleaning shot, no signal averaging or accumulation to improve sensitivity, etc. Should the sample surface move out of focus while translating, practically there is also no possibility to re-focus the optics. On the plus side, continuous scan mode is faster than step scan, while it is also easy on the laser and the stage. The extra speed of continuous scan mode can be best exploited, if the laser has a very high repetition rate, the sample surface is very smooth and levelled, and the analyte concentration is relatively high. That is also the reason why scanning LIBS systems built around a femtosecond laser usually force the use of the continuous scan mode.

The overall organization of the ablation pattern is the same in both scan modes: the area of interest on the sample surface is covered by „horizontal" or „vertical" lines closely spaced next to each other. In order to minimize stage movement and hence the total scanning time, the stage steps to the next line position at the end of a line, following basically a serpentine sequence („progressive scan"). It is also worth mentioning that there is some dispute in the LIBS and LA-ICP-MS elemental imaging literature about that whether the overlapping or non-overlapping analytical spots, assuming the same spot size, are better to use in the scans. As usual, the truth is that both approaches have their pros and cons, which are again related to the characteristics of the given LIBS instrumentation. Logically, non-overlapping spots generate less carry-over of ablated material from one spot to the other (from one pixel to the other in the elemental image), therefore tend to produce a sharper map that is a better reproduction of a highly heterogeneous sample composition. At the same time, overlapping analytical spots are claimed to carry the advantage to produce super-resolution images, which means that by using post-processing of measurement data, an elemental map with higher resolution than that possible by adjacent, but non-overlapping spots can be produced. Since more debris around ablation craters is generated with nanosecond pulses, large spot sizes and high pulse energies, therefore it is not surprising that femtosecond LIBS systems promote the use of scanning with overlapping spots. An additional factor in these systems is that the repetition rate of the laser is often so high that sometimes the sample translation stage can not keep up the pace with it (especially at larger spot sizes), so the use of non-overlapping spots is not really an option. At the same time, conventional nanosecond laser-based systems, which are slower to scan, but provide more flexible and more sensitive LIBS mapping, can be used with or without spot overlap.

2.6. Two- and three-dimensional mapping

3D representations of elemental distributions in solid samples by LIBS is recently becoming more and more popular, as they provide a more informative and visually appealing illustration of data. Since LIBS is a (micro) destructive analytical technique, depth-resolved (3D) elemental mapping can only be carried out in a sequential way, that is by repeating 2D scans over and over the same sample area. In these experiments, the depth resolution is basically defined by the depth of the ablation craters generated by each laser shot (= the thickness of the layer removed by a 2D scan). The 2D images are then stacked in order to get a 3D image. Assessment of the depth resolution can be experimentally done by ablating layered reference materials. Counting the number of repeated laser shots (N) needed to penetrate a layer of known thickness (d) in a reference material, to be determined by monitoring the analytical signal from an analyte characteristic of either the topmost layer or the layer below, is the basis of the calculation (depth resolution $= d/N$). The depth resolution can be controlled mainly by the laser fluence, spot size and the angle of incidence for the laser beam [43].

Unfortunately, the actual realization of 3D LIBS mapping with a reliable depth resolution is quite complicated, especially for larger cumulative depths (many layers). The root of many of these complications are shared with 3D LA-ICP-MS mapping, so in order to conserve space here, the interested reader is kindly referred to the LA-ICP-MS imaging literature (e.g. Refs. [4,46]). These complications include, among others, the followings: *i)* mapping via laser ablation leaves behind a roughened (crated- and debris-ridden) surface, where the overall height of corrugations (depth) can not be well defined (continuous scanning also suffers from the same problem, when the whole analytical area is considered); *ii)* the depth increase caused by each laser pulse becomes less and less as the ablation depth increases; *iii)* after each 2D scan, the sample stage is supposed to move the sample up into the depth of field (DOF) of the focused laser beam again, but it will not be easy for the autofocusing optical subsystem (either camera-based or time-of-flight distance measurement-based) to control this movement, with a roughened up analytical area (of course, the extent of these difficulties also depend on the optical system and the intended depth resolution); *iv)* the debris left behind in each area scan (it can not be completely avoided) will spread the ablated matter over onto adjacent craters, thereby „smearing" adjacent pixels of the elemental map generated (this effect will intensify with the ablation of each layer); *v)* signals collected during the depth-resolved elemental imaging of porous materials (e.g. polymers or layers with discontinuities) will also have contributions from underlying layers of the material, thus the interface between layers can not be correctly detected; *vi)* for heterogenous samples, the ablation rate can also vary from point to point. One consequence of these and other related complications is that only a few depth layers can be mapped − or in other words, the depth of the mapped sample volume should be practically much smaller than the side length of the surface area (unless very small areas are scanned).

2.7. Stand-off mapping

Stand-off LIBS analysis in single spots has been successfully demonstrated in the literature by many times, in several applications ranging from laboratory experiments to industrial monitoring, or from underwater archeology to planetary expeditions [19,22,47]. The tasks of focusing the laser beam over a distance and collecting the plasma emission with a telescopic optical system can be practically solved, as is also illustrated by the availability of several commercial LIBS measurement systems (see e.g. company websites of Applied Photonics, CEITEC and others). It is also known that the use of fs lasers in this scenario is especially advantageous, as the self-focusing filamentation of these laser beams make it easier to maintain the high fluence needed for plasma generation on the sample surface from a distance [27]. Rastering a laser beam over an analytical area is also a routine optical task, which can be done e.g. by galvo scanners. This can lead one to the conclusion that it is relatively straightforward to build a stand-off LIBS elemental mapping setup with analytical features comparable to those working in the lab.

In reality, there are several obstacles that need to be tackled for a successful stand-off LIBS imaging. First the sensitivity of a stand-off LIBS system is inherently much lower than that of conventional LIBS setups due to the very small light collection solid angle. If trace elemental mapping is to be attempted then this has to be compensated for by, e.g. increasing the size of the analytical spot

while keeping the laser fluence at the same level, but this will seriously deteriorate the spatial resolution of the elemental map and may need a very powerful laser. Another possibility is to use a non-conventional spectrometer which is far more sensitive – for example, interferometric spectrometers, such as the spatial heterodyne spectrometer (SHS) can boost sensitivity by a factor of 100 [48–50]. Second, any temporal or spatial fluctuations in the medium in which the laser pulse has to travel from the source to the sample will have an influence on the intensity or direction of the beam during scanning which can compromise the spatial resolution and the intensity of the elemental map obtained. Third, in stand-off analytical scenario, a clear view of the sample surface is needed, which typically also means that the sample is exposed to the influence of any environmental contaminations during the scanning time, which can easily be hours, and this may introduce spikes, glitches in the map recorded.

Table 1 offers an overview regarding commonly used laser parameters and instrumentation in various LIBS imaging applications.

3. Data processing of LIBS imaging

The following discussion applies to full LIBS spectra and not only selected wavelengths, as this is sometimes done to speed up the measuring process and to reduce memory requirements. While there is plenty of literature dealing with simple univariate approaches (an overview is given, for example, by Jolivet et al. [13] and by Zhang et al. [51]) we deliberately focus on multivariate methods which can clearly outperform conventional approaches both in accuracy and flexibility.

3.1. Conversion of 3D data

LIBS images form, as any other type of hyperspectral images, three-dimensional data sets (two spatial dimensions and one spectral dimension). However, most readily available chemometric methods work on two-dimensional data matrices which makes it necessary to convert the measured 3D data space into a 2D data space before applying multivariate statistical methods. The 3D to 2D conversion is done by means of serialisation: each pixel of the image is considered to be an independent sample [52]. Thus, all pixels of the image are arranged into a two-dimensional array, where the rows are the pixels and the columns are the intensities (Fig. 2). Of course, after applying the statistical toolset the processed data has to be transformed back to image coordinates. This way it is possible to present the processed data as images showing specific aspects of the original data.

There is one drawback to this approach: this transformation ignores the spatial relationship between neighbouring pixels because each pixel is treated independently. Thus special methods should be used to exploit spatial relationship as well. This can be done by performing, for example, texture analysis in parallel to hyperspectral analysis as it has been done with images obtained from the Mars rover Curiosity [53].

3.2. Automatic selection of spectral peaks

Given that full LIBS spectra have typically thousands of spectral peaks an automatic selection of peaks is more or less mandatory. Actually, one may have two goals when selecting spectral peaks: *i)* finding and identifying *all* peaks and *ii)* finding the important peaks which allows to solve a particular problem. Whether option *i)* or *ii)* is the best way to go depends on the type of the subsequent analysis. In the case of exploratory analysis one should use all peaks in order to avoid loss of information, and in the case of a specific classification task, for example, one wants to identify only those peaks which have the greatest contribution to the classification. In general, one should first identify all available peaks and use this set of peaks as the starting point for the next steps of the analysis. There are several methods, for example random forests, which provide an intrinsic selection of proper wavelengths.

One way to automatically select spectral peaks is to identify them by a method called image features assisted line selection (IFALS) [54]. IFALS performs a geometric analysis of the spectral curve which allows for detecting peaks in the spectral line. This method comes from machine vision where it is used in motion detection [55].

Another method is to correlate the spectral line with a small template peak while shifting the template peak along the spectral axis. Maxima of the correlation indicate the position of a spectral peak. This method is sensitive to peak width and may require running the algorithm several times with adjusted widths of the template peak. While the IFALS method is in general faster it exhibits some problems if peaks are driven into saturation (peaks are cut off and show a flat top). The correlation method is more reliable in such cases, given that the template width approximately matches the peak width of saturated peaks.

3.3. Pre-processing and scaling of the spectra

Depending on the multivariate methods applied during data analysis the scaling of spectra may be necessary or must not be applied at all [56,57]. In general, methods based on distances, such as hierarchical cluster analysis, must not be preceded by scaling operations, and methods based on variances, such as Principal Component Analysis (PCA), can use scaled data and might benefit from it.

The most often used scaling types are mean-centering and standardization. Mean-centering calculates the mean of the intensities of each wavelength and subtracts it from the corresponding intensities. This shifts the entire data cloud to the origin. Standardization mean-centers the data and then divides the individual variables by their respective standard deviation. Thus, the extent of the data space becomes comparable along all axes. Please note that standardization destroys the spectral correlation to some extent, a fact which might become important when a particular method requires the preservation of the spectral correlation (i.e. when applying an internal standard).

In many cases there is no clear rule when to apply which type of scaling. Thus, it is recommended to experiment with all three types of scaling (no scaling, mean-centering and standardization) to find out which approach fits best.

Pre-processing in LIBS-based hyperspectral imaging is straightforward and comparatively simple. Basically, two methods are often to be used: *i)* scaling the spectra to take care of varying experimental conditions during the measurement (which may take several hours if the image has a high spatial resolution). This can be easily achieved by, for example depositing a thin uniform layer of gold on the sample and using several of the gold lines as an internal standard to correct the spectra [58]; *ii)* In many situations, especially when the concentration of a particular analyte is low, noise acquired during the measurement of the data can become a considerable problem. Although many applications simply use spatial down-sampling approaches to reduce the spectral noise this approach is not recommended because information is destroyed (i.e. the spatial resolution decreases).

One of the methods to reduce noise without decreasing spatial resolution is to perform a principal component analysis, remove the components exhibiting low eigenvalues and back-transform the reduced set of principal components to the original data space. In this way it is possible to remove noise from the image data.

Table 1

Overview of used LIBS instrumentation in various imaging applications. Application fields LS: Life science, GS: Geoscientific studies, CH: Cultural heritage studies, MS: Materials science.

Laser Wavelength (nm)	Laser energy (mJ)	Pulse duration	Lateral Resolution (μm)	Detected Wavelength (nm)	Reference number
532/1064	30/80	ns	100	200–975	[37]
1064	–	ns	15	250–330	[52]
266	–	ns	100	185–1048	[83]
266	3.8	ns	100	185–1048	[84]
266	21.5	ns	40	185–1048	[113]
266	0.8	ns	25	315–350	[114]
266	15	ns	100	185–1040	[115]
532	–	ns	–	200-510/200-900	[116]
532	20	ns	100	270–1000	[118]
266	20	ns	150	187–1041	[119]
266/1064	10/100	ns	200	–	[120]
266	15	ns	–	–	[121]
1064	160	ns	100	200–1100	[122]
1064	90	ns	75	200–850	[123]
532	20	ns	100	240–940	[124]
532/1064	60/60	ns	–	240–860	[125]
1064	0.5	ns	12	315–345	[127]
1064	15	ns	100	315–350	[128]
1064	5	ns	100	286–320	[129]
1064	0.5	ns	40	315–350	[131]
1064	5	ns	–	282–317	[133]
1064	2	ns	50	190–230	[134]
532	–	ns	500	253–617	[137]
266/1064	10/90	ns	150	–	[138]
1064	70	ns		190–970	[139]
266	10	ns	500	–	[143]
532	20	ns	300	200–975	[144]
1064	35	ns	700	200–600	[145]
1064	0.5	ns	50	250-480/620-950	[146]
1064	–	ns	10	245-310/400-420	[147]
266	18	ns	100	240–800	[148]
1064	10	ns	90	270–330	[149]
1064	0.6	ns	15	190-230/250-335	[150]
1064	1	ns	10	–	[151]
1064	0.6	ns	10	150–250	[152]
213	–	ns	85	668–708	[153]
213	6	ns	50	284–333	[154]
1064	60	ns	250	220–800	[155]
266	6.75	ns	50	185–1050	[156]
1064/1064	50/10	ns	60	198-710/284-966	[157]
1064	1	ns	50	252–371	[158]
355	170	ns	700	360–800	[163]
355	170	ns	–	280–800	[164]
1064	50	ns	300000	240–340	[165]
1064	1.5	ns	8	200–1000	[166]
266	2.5	ns	80	180–1050	[167]
1064/1064	5.4/8.7	ns	20	190–900	[168]
1064	2	ns	6	130–777	[171]
1064	–	ns	100	186–1040	[172]
400	0.2	fs	6	–	[173]
1064	10	ns	30	190–210	[174]
532		ns	–	209-225/335-345	[175]
1064	0.6	ns	15	338–362	[176]
1064	1	ns	30	150–255	[177]
343	0.16	fs	75	390-403/452-500	[178]
266	8.4	ns	40	185–1048	[179]
532	20	ns	–	200–895	[180]
1064	3	ns	80	747–941	[181]
1064	65	Ns	0.67	200–980	[182]
532	120	Ns	1500	200–980	[183]
266	2	Ns	10	364–398	[184]
1064	100	Ns	800	258-289/446-463	[185]
266	2	Ns	25	–	[186]
266	2	Ns	25	272–775	[187]
532	2.9	Ns	130	187–1045	[188]
-	0.6	Ns	12	310–350	[189]

However, this approach has a big drawback: the principal components are sorted according to decreasing variance which might lead to the removal of valuable image information if the removed components contain useful information.

An alternative approach which uses basically the same idea but exploits a different weighting of the information content is maximum noise fraction (MNF) transform [59]. The basic idea behind MNF transform is to rotate the data space in a way that the
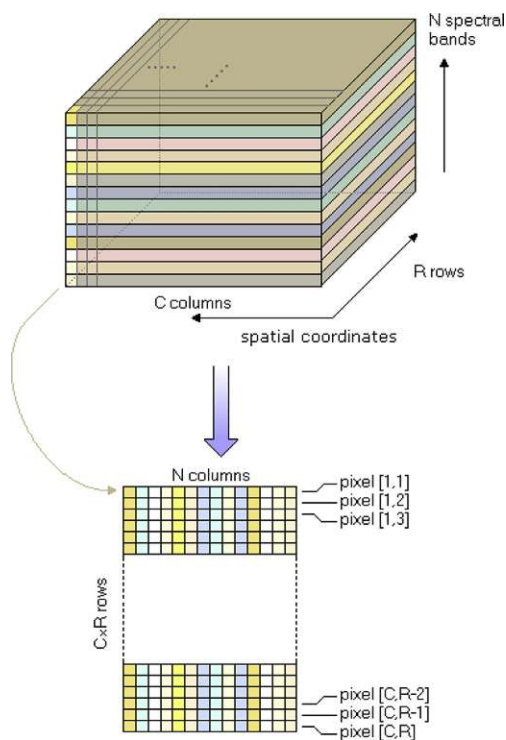
Fig. 2. The conversion from the 3D image space to the 2D analysis space.

signal to noise ratio is maximized along the new axis (instead of the variance in the case of PCA). The only problem with MNF is that it is necessary to correctly estimate the covariance structure of the noise. MNF transform works quite well if the structure of the noise is estimated correctly. If it is impossible or difficult to create a correct estimate of the noise structure, the results will be poor, resulting in artefacts which may hamper the following analysis of the image.

3.4. Data analysis

3.4.1. Exploratory analysis

Exploratory data analysis is a valuable toolset when just starting to get into the analysis of a largely unknown sample. All these methods are governed by the principle that the high-dimensional data space is projected onto a two dimensional space (i.e. the computer screen) in a way that the information contained in the high-dimensional data is largely conserved. The following section shortly discusses the most prominent methods used for exploratory purposes and gives some hints on introductory literature as well as on applications:

3.4.1.1. Principal component analysis (PCA) [37,52,60,61]. The basic idea of PCA [62] is the rotation of the *p*-dimensional coordinate system to achieve uncorrelated axes which show a maximum of variance of the data space. The maximizing of the variance is governed by the idea that the information content is proportional to the variance in a certain direction of the data space. This way it is possible to sort the resulting new (rotated) axes according to their information content. Without going into the mathematics of the PCA we can assume the first few components will show a big part of all available information. And indeed, PCA can be easily used to find spectrally similar regions of an image by looking at the score plots (Fig. 3).

3.4.1.2. Hierarchical cluster analysis (HCA). Hierarchical Cluster Analysis [64,65] generates dendrograms which depict the distances between individual spectra. The fundamental idea is that similar spectra show small distances in the *p*-dimensional data space and thus form clusters of neighbouring points in this space. There are several ways to create dendrograms which differ in the weighting of the inter-cluster vs. the intra-cluster distances (controlled by the Lance-Williams equation [66]). The resulting dendrograms can be quite different, not all of them being easy to interpret. A notably good choice is Ward's approach (which can also be covered by the Lance-Williams equation) [67]. The resulting dendrogram can be used to assign class numbers to all the spectra according to their mutual distance, thus effectively colouring chemically similar regions of a sample.

3.4.1.3. Similarity maps. Similarity maps [68,69] are basically maps which depict the spectral similarity of all spectra of an image to a reference spectrum. The reference spectrum may either be taken from the acquired image data or from a database. Thus, the user can quickly identify regions which are similar to a particular spot of the sample or similar to selected database spectrum. The spectral similarity can either be based on some kind of correlation or on some kind of spectral distance. Typical similarity measures are the Euclidean distance, the Mahalanobis distance [70], the Pearson's correlation coefficient, the spectral angle mapper [71] or spectral information divergence [72] (Fig. 4).

3.4.1.4. Vertex component analysis (VCA). The idea behind VCA is to resolve a linear mixture model in order to identify pure component spectra [73]. VCA is commonly used in endmember detection in geology and mineralogy and assumes that there are pure spectra of the searched components in the image. VCA operates on the raw data and its speed depends on the dimensionality of the data space. This automatically slows down VCA for full-scale LIBS spectra as these spectra have typical lengths of more than 10.000 intensity values.

3.4.1.5. Self-organizing maps (SOM). SOMs is a non-linear projection method which tries to segment images while maintaining topological relationships [74]. Thus, SOMs lend themselves to be used in imaging applications. SOMs have the advantage that the expected number of clusters has to be known (as opposed to, for example, *k*-means clustering).

Several applications have been published using SOMs. For example, Pagnotta et al. use SOMs to segment LIBS images of mortars [75], or Tang et al. use SOMs and *k*-means clustering to classify polymers [76] whereas Klus et al. used SOMs to study U-Zr-Ti-Nb in sandstone [77].

3.4.2. Classification

Classification methods are used when one wants to predict and assign the type of an unknown material. Classifiers are not "instant methods", in fact they have to be trained by known correct samples. This implies additional efforts, especially as far as the correctness of the training data is concerned (because wrongly labelled training data automatically lead to poor classification results). However, if the training sample is correct, classifiers usually deliver excellent results (assuming that the problem at hand can be solved at all).

Classification schemes can be grouped in linear and non-linear classifiers. In general, linear classifiers such as Partial Leas Squares Discriminant Analysis PLS/DA and Linear Discriminant Analysis (LDA) cannot solve non-linear problems, while non-linear classifiers will deliver solutions for both linear and non-linear cases. This does not automatically imply that one should always use non-linear classifiers, as non-linear classifiers tend to overfit
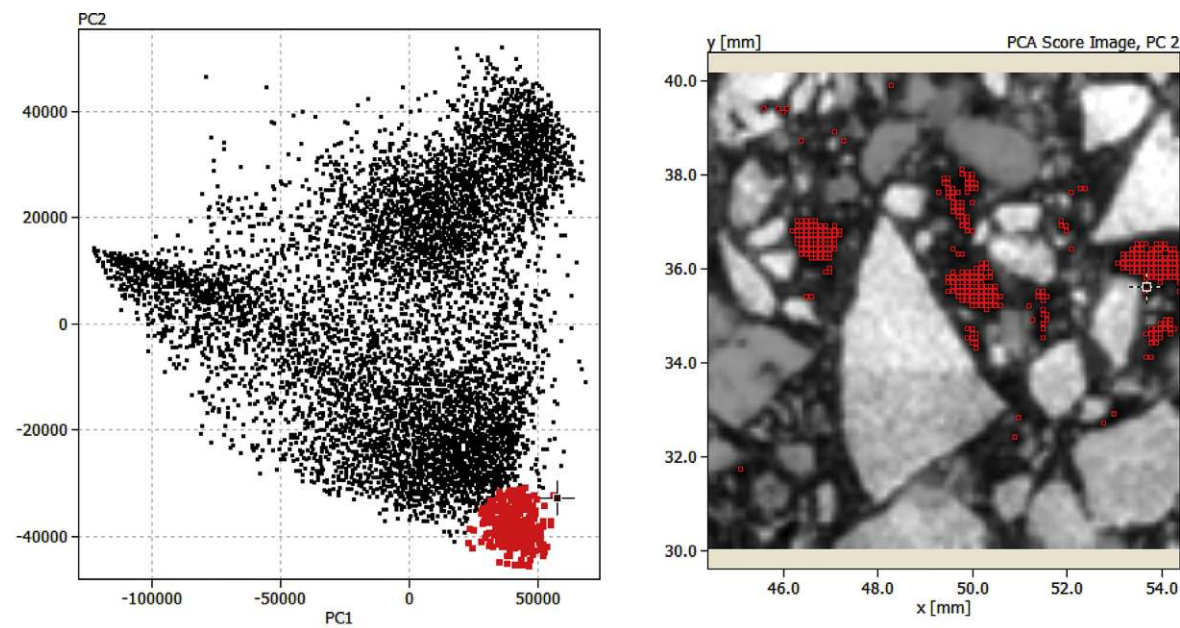
Fig. 3. Principal component analysis of the mean-centered LIBS spectra of a concrete sample. Left: score/score plot of the first two principal components. The cluster of spectra in the lower right corner has been marked. Right: the score image of the second principal component, displaying the marked pixels. The marked regions contain high concentration of calcium [dataset] [63].
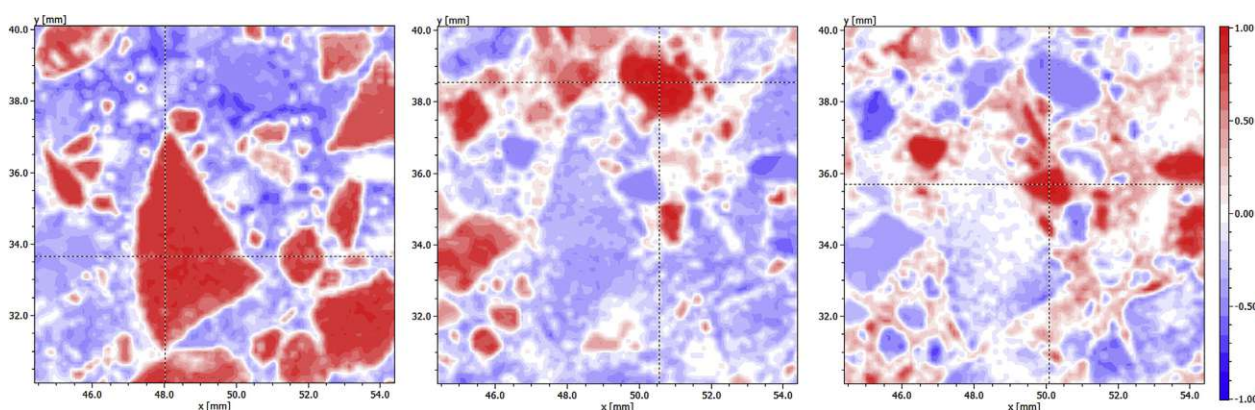

Fig. 4. Similarity maps of three different positions using the Pearson correlation of standardized spectra. Red areas indicate high spectral similarity to the location marked by the crosshair, blue areas indicate dissimilarity and white areas indicate indifferent areas (non-significant correlations). [dataset] [63].

the training data while with non-linear classifiers, this can be avoided if some requirements are met.

Most classifiers work best if configured as a binary classifier and some of the classification methods cannot be used for multi-class problems at all. In such cases it is recommended to generate binary indicator variables. Such indicator variables are derived from the class numbers by creating as many indicator variables as available classes. Each indicator variable is filled with a zero value for spectra which do not belong to the particular class and with a value of one if the spectrum belongs to this class. In this way the k-multiclass problem is transformed into k binary classification problems.

3.4.2.1. Linear Discriminant Analysis (LDA). One of the simplest linear classifiers is LDA [78]. LDA is based on a linear regression model which generates a linear surface in the p-dimensional space, effectively separating the two classes. Linear discriminant analysis suffers from the fact that multi-collinearity causes weakly

determined coefficients which can result in unstable class assignments. Further, in LDA the number of variables must be well below a third of the number of pixels, which might become a problem with small images. Thus, LDA is largely replaced by PLS/DA (see below).

3.4.2.2. Partial Least Squares discriminant analysis (PLS/DA). As mentioned above the instabilities of the regression coefficients can be avoided by using PLS/DA [79], which calculates the regression coefficients of the model by using PLS [80]. As PLS is not sensitive to multi-collinearity of the variables, it does not need more samples than the number of variables. PLS/DA is an almost perfect approach to linear classification of spectra obtained from images. However, PLS requires reducing the number of factors to an optimum amount otherwise it degenerates to LDA in the case of using all factors. The optimum number of factors is determined by cross validation.

3.4.2.3. Random forests (RF). RF is one of the newer methods introduced in the field of machine learning at the beginning of this century [81,82]. RFs have proven themselves as a very reliable and powerful tool both for classification purposes and for modelling approaches. The basic principle of RFs is the combination of many de-correlated decision trees which "vote" for the final outcome within the ensemble of trees. The voting can be performed in several ways, usually by majority voting in classification scenarios. Typically, between 50 and 150 trees are sufficient to solve most classification problems. Each of the decision trees is based on a random selection of variables thus avoiding any correlation between the trees. Random forests have successfully been used to classify LIBS images of modern art materials [83] or to discriminate various polymer samples [84].

3.4.2.4. K-nearest neighbours (kNN). Another non-linear classification method is kNN classification [85]. kNN is based on the idea that the k closest objects in the p-dimensional space determine the class of an unknown spectrum (by for example, majority voting). kNN is easy to use and to calculate, however it requires having a good and correct database of known spectra. Errors in the database automatically lead to misclassifications. Further the database should have built in some redundancy so that the data space is populated by at least 10 to 20 examples per class.

There are no exact rules of the selection of k, however an odd k in the range between 3 and 9 usually works best. For a particular classifier and a particular database k should be determined by means of cross validation. Theoretical considerations [64] show that the error of 1NN ($k = 1$) is less than twice the Bayes error - which makes kNN some kind of a benchmark. However, kNN suffers a lot from the curse of dimensionality [86] as the distances in a p-dimensional space become more and more similar with increasing p.

3.4.2.5. Support vector machine (SVM). SVM [87] is an intrinsically linear classifier which can be applied to non-linear problems by applying a transformation of the data space using for examples polynomials or Gaussian density functions [88]. It can be shown that SVMs can solve non-linear problems even without explicitly calculating the non-linear transformation (this is commonly called the "kernel trick"). The basic idea of an SVM is to find a discrimination surface of finite thickness (as opposed to PLS/DA which uses an infinitely thin separating plane) which is controlled by a few points at the border of this surface. These points are called "support vectors" because they control the location and orientation of the separating surface. An application of both SVM and kNN to classifier soft tissues is given by Li et al. [89].

3.4.2.6. Artificial neural networks (ANNs). ANNs comprise a family of diverse and partially unrelated methods whose applications span a vast range of fields from pattern recognition and associative retrieval to calibration tasks. A well-structured survey on these methods can be found, for example, in the book of Du and Swamy [90].

The main problems with the quantitative analysis of LIBS spectra are spectral overlapping, self-absorption and matrix effects resulting often in nonlinear relationships between quantities and the corresponding spectral signals. These nonlinear effects can be addressed by ANNs. While there are several applications of ANNs to the quantitative analysis of LIBS data [91] imaging related analysis based on ANNs is still in its infancy. An extensive overview on ANNs and LIBS including spectral imaging is given by Koujelev and Lui [92].

3.4.3. Calibration

Calibration based on LIBS data can become quite complex if the matrix shows extreme variability, as for example in geological or biological samples. In principle, the quantification of a particular chemical element is possible by setting up a univariate regression given that the matrix is well defined, and the used spectral lines do not interfere with other elements. However, this assumption proves to be not met in many practical cases. Thus, a multivariate approach is needed to account for matrix effects and interferences.

The classical approach would be Multiple Linear Regression (MLR). However, MLR suffers from multi-collinearity of the independent variables and requires the number of training samples to be at least three times higher than the number of used wavelengths. Although there are various variable selection techniques to keep this ratio within an acceptable range, a much better approach is to use Partial Least Squares (PLS) regression. Other possibilities are random forests, artificial neural networks and the Franzini-Leoni method [93].

3.4.3.1. Partial Least Squares (PLS). PLS is certainly the most common and most mature method [80] and the setup of a calibration model is straightforward: *i)* define the independent variables (i.e. use all available wavelengths), *ii)* define the target variable to be calibrated, *iii)* find the optimum number of factors by cross validation, and finally *iv)* store and apply the found model. A good comparison of univariate regression and PLS is given by Ref. [94].

3.4.3.2. Random forests (RF). Random Forests can be used in the same way as in classification scenarios. The only difference is the voting of the individual trees of the random forest. For regression (= calibration) purposes the outputs of the individual trees should be averaged (instead of majority voting). Random forests however have one problem: they cannot extrapolate. Thus, when using random forests, it is mandatory that the training data completely cover the calibration range in order to avoid any extrapolation. More details on random forests can be found in Ref. [95].

There are several papers using random forests for calibration purposes. Wang et al. used a combination of wavelet transform with random forests where wavelets were used for de-noising the data. The de-noised and optimized variables were then fed into a random forest-based model to determine metal concentrations in an oily sludge [96].

3.5. Image fusion

Image fusion is a technique which allows to combine two images of different spectral and spatial resolution into a single image. Normally an image with high spatial but low spectral resolution (typically a monochromatic or a colour photo of the sample) is combined with an image of high spectral but low spatial resolution (i.e. the LIBS-based image). This combination results in a crisp image of the sample which is coloured according to the elemental information obtained from the LIBS measurement.

More than 10 methods of image fusion have been published, from simple arithmetic multiplication of the two images, to spectral substitution-based techniques such as the Brovey transform [97], to sophisticated calculations based on principal components or wavelets [98]. For most purposes Brovey transform delivers a very good compromise, as it is fast and delivers nice images which retain the texture of the high-resolution photo while being coloured to indicate elemental constituents.

4. Applications

In the following chapter, selected LIBS imaging applications are

presented which highlight the benefits of this analytical technique. In particular, the possibility to detect all elements of the periodic table is represented with 52 different chemical elements being analyzed in the presented works. Moreover, capabilities for simultaneous multi-element analysis is demonstrated in numerous publications. In more than 10% of the discussed applications elemental distributions of 10 or more elements were measured. Additionally, elements which are not accessible or do not allow detection with a high sensitivity with other imaging techniques are often analyzed in LIBS applications. The most common detected elements in the presented compilation of applications include mainly light elements, alkali and earth alkali elements, and non-metals. Another main benefit of LIBS is the high speed of analysis, thus large sample areas (up to several cm^2) can be analyzed in a reasonable time. Table 2 gives an overview and summarizes LIBS imaging applications allowing to conclude on the advantages this techniques has to offer. A detailed discussion of the individual publications is provided in the following chapter.

4.1. Life science

The capability of LIBS to obtain spatially resolved multi-elemental images has received increased attention. Life science applications appear to be one of the most promising field for further development of LIBS-based imaging. In this review we summarize the current state-of-the-art together with the most recent and crucial research works related to elemental bio-imaging in individual life science applications. Mainly, we tend to emphasize technical aspects of the analysis including benefits of LIBS over other analytical techniques, evidence on laser-tissue interaction, etc.

Continuous improvements in LIBS lead to further establishment of the technology among its analytical counterparts; namely LA-ICP-MS which is still considered to be the reference to LIBS. LA-ICP-MS held its position for decades in bioimaging due to its higher sensitivity and spatial resolution [99—101]. Recently, LIBS has been narrowing the gap in terms of repetition rate, cost of analysis and instrumentation affordability when insufficient sensitivity seems to be an issue of the past. LIBS fully matured in plant bioimaging [44] and becomes a viable alternative in biomedical applications [45].

The contemporary LIBS literature reflects a wide range of bio-applications where various samples (soft/hard tissues, liquids, pathogens, etc.) are analyzed under various conditions. Several LIBS reviews dealing with the analysis of biological samples or, more exactly, with their bioimaging were already published, e.g. plant material analysis [102,103], plant bioimaging [44], agriculture and food analysis [104,105], preclinical applications and medical applications [13,45,106], and veterinary and livestock applications [106].

Here we focus solely on "solid" samples and thus skip any discussion over the analysis of algae [107], pathogens with emphasis on bacteria [108], or liquid samples of biological origin [106]. The analysis of homogenized pellets is not considered, despite this approach enables easier calibration and quantitative analysis [109]. But the process of pelletization loses any information on the original tissue composition and analyte distribution. Therefore, those biological materials and/or approaches for their analysis are out of scope of this review.

Numerous ways of sample pre-treatment leading to significantly different outcomes and limitations have been presented. It is noteworthy that the sample preparation process is crucial for successful analysis using LIBS [110] and must be optimized a priori. Unfortunately, there is no established protocol of biological tissue sample preparation for LIBS analysis. The plant tissues are either fixed on top of the epoxy or pressed onto a sticky tape; potentially, cryo-fixing via flash freezing was also introduced [44,111]. Hard tissues (e.g. bones and teeth) are non-demanding. Fixing them in epoxy seems to be an appropriate approach and their cutting and polishing is then straightforward.

Fixing soft tissues is a critical step in the analytical routine [112]. Most often the researchers choose between cryo-sections and formalin fixation and paraffin embedding (FFPE). The FFPE is a golden standard in clinical applications and pathological examination of a tissue when haematoxylin and eosin staining is concerned. Thus, adapting the LIBS methodology to fit this sample preparation seems adequate. The sample may then be measured in thin sections with thicknesses approximately 10 μm. Direct LIBS analysis of paraffin blocks is also possible when providing more material for ablation and, in turn, better sensitivity. However, evidence was found indicating that the FFPE preparation of a tissue leads to unwanted redistribution of the elemental content [112]. This raises further considerations when using FFPE in metallomics applications. It is advised to use other approaches too as references to check the correctness of the sample preparation.

The parameters involved in sample preparation and consecutive laser-matter interaction make the tissue ablation a complex phenomenon. Involved parameters have convoluted dependence on laser-ablation performance and the optimization process is, therefore, tedious, and lengthy. Successful implementations of LA-ICP-MS to individual applications (e.g. plants [101] and biomedical [99]) may serve as an inspiration for LIBS research and development efforts. Both techniques have already been utilized in tandem when complementing their benefits and increasing the range of detected elements [113]. Yet still, a potential of their joint utilization is mitigated by certain discrepancies in optimal settings of laser ablation parameters.

The quantitative analysis applied directly to bioimaging of heterogeneous samples attracts considerable attention. However, any success is limited due to the essence of laser ablation itself; the need for matrix-matched standards with similar physical and chemical properties is a persistent challenge. A comprehensive review summarizing individual efforts in quantification of LIBS and LA-ICP-MS images was recently delivered [109]. As in the case of sample preparation, works on LA-ICP-MS might be an interesting source of information for further development of LIBS methodology. Several approaches have been introduced to calibrate the LIBS system. Quantification analysis of plant tissues is centered around homogenization and pelletization [111]. In the case of soft tissues, the methodology is not straightforward and contains homogenization of the tissue, utilization of inkjets or agarose gels. The most promising method so far seems to be the use of epoxy mixtures [114]. Considering hard tissues, the calibration strategies are based on calcium-rich materials, including hydroxyapatite [115] or calcium oxalate [116]. Despite all the efforts, there is still a dire need to deliver a methodology enabling accurate quantification in direct imaging of bio-samples [109]. Finally, the use of calibration-free or C-Sigma methods [117] seems promising, yet still, their implementation to bioimaging is only foreseen.

In the following paragraphs, we overview papers dealing with the imaging of plant, soft, and hard tissues. The literature research of LIBS applications is extended with the discussion over utilized LIBS instrumentation and its performance. Unifying benefits of LIBS technique which make it especially attractive over LA-ICP-MS for the presented applications are typically faster throughput and, thus, larger imaged areas; measurement of inaccessible (e.g. O, N, H) or challenging (e.g. C, P, S) elements; simultaneous detection of all analytes with no need for preselection; etc.

Table 2
Overview of LIBS imaging applications.

Sample Material	Investigated Elements	Data Evaluation	Analyzed Area (mm^2)	Reference number
Minerals	U	Multivariate	225	[37]
Minerals	Al, C, Cd, Co, Cr, Fe, H, Mn, O, P, Sn, Ti	Multivariate	468	[52]
Cultural heritage samples	C, H, Na, O	Multivariate	128	[83]
Polymers	H, K, Na, O	Multivariate	190	[84]
Soft tissue	Fe, Gd, Na, Si	Univariate	–	[113]
Soft tissue	Ca, Co, Mn, Ni, Sr, V	Univariate	–	[114]
Hard tissue	C, Ca, Cl, Fe, H, K, Mg, Mn, Na, O, P, S, Sr, Zn	Univariate	4	[115]
Hard tissue	Cd, Te, Si	Univariate	900	[116]
Plant tissue	Al, Ba, C, Ca, Cu, Fe, H	Univariate	–	[118]
Plant tissue	Cd	Multivariate	–	[119]
Plant tissue	Li	Univariate	–	[120]
Plant tissue	Cd	Univariate	–	[121]
Plant tissue	K, Mn	Univariate	1.7	[122]
Plant tissue	Er, Y, Yb	Univariate	–	[123]
Plant tissue	Cr	Univariate	–	[124]
Plant tissue	Ca, Gd	Univariate	–	[125]
Soft tissue	Ca, Cu, Gd, Na	Univariate	2	[127]
Soft tissue	Ca, Fe, Gd, Si	Univariate	–	[128]
Soft tissue	Ca, Na	Univariate	–	[129]
Soft tissue	Fe, Mg, Si	Univariate	–	[131]
Soft tissue	Al, Cu, Fe Mg, Na, Si	Univariate	–	[133]
Soft tissue	Ba, Ca, Fe, Na, Sr	Univariate	–	[134]
Hard tissue	Al, Ca, Na, P	Univariate	–	[137]
Hard tissue	Fe, Si	Univariate	–	[138]
Soft tissue	Cd	Univariate	–	[139]
Immunoassay	Ag	Univariate	–	[143]
Immunoassay	Au, Eu, Nd, Pr, Yb	Univariate	–	[144]
Immunoassay	Ag, Al, Ca, Cu, Fe, Mg, Si, Zn	Univariate	–	[145]
Mine core	Al, Fe, Mg, Mn, Na, Si, Sr	Univariate	1600, 750	[146]
Speleothem	Al, Ca, Fe, K, Mg, Na, Si, Sr	Univariate	2000	[147]
Speleothem	Ca, Mg	Univariate	72	[148]
Shells	Cu, Mg, Pb, Si, Zn	Univariate	–	[149]
Minerals	Ce, Cu, Fe, La, Si, Y	Univariate	470	[150]
Minerals	Al, As, B, C, Ca, Cu, Fe, Mo, P, S, Si, Ti, Zn	Univariate	–	[151]
Mine core	F, O	Univariate	15, 200	[152]
Minerals	Al, Ca, Si	Univariate	16	[153]
Minerals	Al, Cu, Fe, Mg, P, Si	Univariate	0.6	[154]
Carbonaceous shale	Al, Ca, Fe, K, Mg, Na, Si	Multivariate	29	[155]
shale	Al, C, Ca, Fe, H, Mg, O, Si	Univariate	64	[156]
Ore	Al, Ca, Cr, Cu, F, Fe, K, Mg, Mn, Na, Ni, P, S, Si, Ti, Zr, Pd, Pt	Multivariate	10000	[157]
Minerals	Al, Ca, Cu, Fe, K, Mg, Na, Ni, Pd, Pt, S, Si	Univariate	1200	[158]
Cultural heritage samples	Al, Cu, Fe	Univariate	–	[163]
Cultural heritage samples	Al, Ca, Fe, K, Mg, Na, Si	Univariate	–	[164]
Cultural heritage samples	Ca, Mg, Si	Univariate	–	[165]
Cave walls	Mg, Si, Sr	Univariate	–	[166]
Cultural heritage samples	Al, C, Ca, Cu, Na, O, S, Si	Univariate	0.8	[167]
Limestone	C, Ca, Fe	Univariate	625	[168]
Steel	Al, Mn, N, O	Univariate	100	[171]
PCB	Al, Au, Ba, Ca, Co, Cu, Fe, K, Li, Mg, Mn, Na, Ni, Sb, Si, Sn, Ti, Zn, Pb	Multivariate	1200	[172]
Thin films	Ba, Cu, Mg, Mn, Y	Univariate	–	[173]
Composite material	C, Co, Cr, Fe, Ni, Si, W	Univariate	0.81	[174]
Catalyst	Pd, Pt, Rh	Univariate	345	[175]
Catalyst	Al, CN, Fe, Pd	Univariate	–	[176]
Catalyst	Al, C, Ni, S, V	Univariate	–	[177]
LLZO	Al, La, Li, Zr	Univariate	1.23	[178]
LLZO	La, Li, Fe, Zr	Univariate	–	[179]
LiCoO$_2$	Co, Li	Univariate	0.25	[180]
Concrete	Ca, Cl, Na	Univariate	0.04	[181]
Lithiated tungsten	Ar, Ca, H, K, Li, Na, O, W	Univariate	26.4	[182]
Lithiated tungsten	Li, Si, Ti	Univariate	–	[183]
Nuclear waste	Al, Ca, Eu, Fe, La, Mo, Nd, Pr, Sr, Zr	Univariate	1.9	[184]
Gunshot residues	Ba, Pb, Sb	Univariate	21450	[185]
Tablets	Fe, Ti	Univariate	4	[186]
Tablets	K, Mg, Na	Univariate	4	[187]
Solar cell material	Cu, Ga, In, Se	Univariate	6.6	[188]
Piezoelectric crystal	Ca, Zr	Univariate	225	[189]

4.1.1. Imaging of plant tissues

In the last two decades LIBS became an established analytical tool in the plant bioimaging. This issue has already been addressed in several studies and review publications [44,102,104,111]. It is noteworthy that we avoid any discussion of food analysis [104,105].

LIBS technique excels over other analytical techniques mainly in terms of affordable instrumentation enabling large-scale mapping. Such instrumentation provides reasonable analytical performance (sensitivity) and is, thus, a vital alternative in many applications. The imaging of macro- and micro-nutrients is a great added value

of LIBS when high number of whole plants (or their parts — roots, stems, leaves) are scanned. The control of nutrient contents is of paramount interest while plants suffer from various stress during growth, e.g. draught, insufficient sunlight, under- or over-fertilization, toxic environment. The latter then extends the number of applications into environmental monitoring and the uptake, accumulation and translocation of toxic and heavy metals.

The most recent bioimaging plant review [44] deals in great details with the novelty of using LIBS as a new instrumental method in the spatially resolved single/multi-element analysis of various plant samples. The paper comprehensively describes the analysis of various plant species, plant tissues as well as detection of different analytes as essential elements (K, Ca, Mg, P, Fe, Mn, Cu, and B), non-essential elements (Pb, Cd, Ag, Si, Li, Y, Yb, and Cr), several types of nanoparticles (silver, cadmium telluride, and photon-upconversion nanoparticles) or even pesticide (chlorpyrifos).

A recent work [118] studies the translocation of two types of cadmium telluride NPs (CdTe quantum dots and CdTe quantum dots cover by silica shell) together with free Cd (II) ions by using two different LIBS approaches. Selected plants (white mustard) were exposed to test compounds for 3 days, then the plants were washed, dried, epoxide glued onto glass slides, and then LIBS analysis was performed. Firstly, the whole plants were measured in a raster of spots with a 100 μm step (giving the lateral resolution). Then, only the important or somehow interesting plants parts where measured with the step 25 μm, in so-called micro-LIBS setting, to show exact place of cadmium bioaccumulation sites and to demonstrate different behaviour of cadmium in plants based on his source (see Fig. 5).

A recently published approach in LIBS plant analysis shows a spatially resolved root-rhizosphere-soil image in wider context of plant in its natural environment [119]. LIBS elemental images visualize the nutrient exchange in plant rhizospheres and organic/inorganic content in switchgrass. The live root sampling was demonstrated in plant analysis and the drill press for sectioning frozen stabilized soil. Multi-elemental images of roots (and rhizospheres) in surrounding soil for H, C, O, P, K, Ca, Mg, Fe, Si, Al, Mn, and Zn were shown with 100—150 μm lateral resolution. Based on

plotted maps and principal component data analysis the elements profiles in soil depending on their distance from roots could be assessed. This approach offers detailed information at the scale, which has clear implications for various soil/plant science challenges (e.g. phytoremediation or effects of fertilizers on agricultural yields).

The current state of the LIBS plant bioimaging can be summarized by the following highlights. In the last two decades LIBS plant analysis made a great step forward due to not only an improvement in LIBS instrumentation (sensitivity, speed, and spatial resolution of analysis) and in plant sample preparation, but mainly by using obtained LIBS maps in interdisciplinary research works [119], by involving of plant toxicity testing [120], and by searching for interesting and novel applications in imaging of Li in the plant leaves [121] and nanoparticle enhanced detection [122]. Recent work presents the possibility of in situ plant analysis in field conditions [123], 3D-model compilation of element distribution in leaves [123], and nanoparticles localization [124].

The best achieved spatial resolution in plant analysis has been recently improved to 25 μm [119], this value is already close to commonly used LA-ICP-MS spot sizes, where the lateral resolution is in the range of 1—500 μm [101]. Zhao et al. [122] demonstrated a novel idea of deposition Ag nanoparticle on the plant surface in order to achieve a sensitivity enhancement (limit of detection (LOD) for phosphorus were found to be improved by two orders of magnitude) in Nanoparticle Enhanced LIBS (NELIBS) experiments. Double pulse LIBS arrangement was employed as another way of signal enhancement [125]. Furthermore, the information on the spatial distribution of selected elements can be used as a valuable information showing the relationship between the exact location of an element and its effect. This effect could be negative (even toxic) - [122] as well as positive [126] for plant development, it depends on the chemical species of the element and its concentration, and also the type of monitored plant as the effects are specific to each organism.

4.1.2. Imaging of mammal tissues

4.1.2.1. Soft tissues. The LIBS technique repeatedly proved its bioimaging applicability for tracing uptake, transport, distribution, and bioaccumulation of macro- and micronutrients, nanoparticles, and non-essential elements in several organisms (mouse, human), organs (kidney, lung, skin), and diseased tissues (skin or lung tumours) as was summarized in three most recent reviews [13,45,106].

Elemental variations can be effectively used as an indicator of malignancy and to monitor its stage and progression. Therefore, the analysis of metallomes (metalloproteins, metalloenzymes and other metal containing biomolecules) undergoes intense research. The main research target of metallomics is the elucidation of metallomes' biological or physiological functions during physiological and pathological alterations of tissues. Incorporation of spectroscopic methods can fill knowledge gaps in these biological processes. Any changes in the elemental composition induce significant alteration of further tissues' growth, pathological processes, and even initiation and progression of a carcinoma.

The body of work published by the Vincent Motto-Ros' group bring tremendous progress in terms of spatial resolution and scale of the analysis; the distribution of elements in mouse kidneys [114,127—131], mouse tumours [132,133], and healthy human skin or human skin melanoma [134] was imaged. Outside of their works, the human malignant pleural mesothelioma (lung tumour) was investigated using LIBS multi-element mapping [113]. All these studies showed LIBS as an advanced analytical platform providing large-scale elemental imaging of heterogeneous sample surfaces. Also, the great accessibility for assessment of nanoparticles was
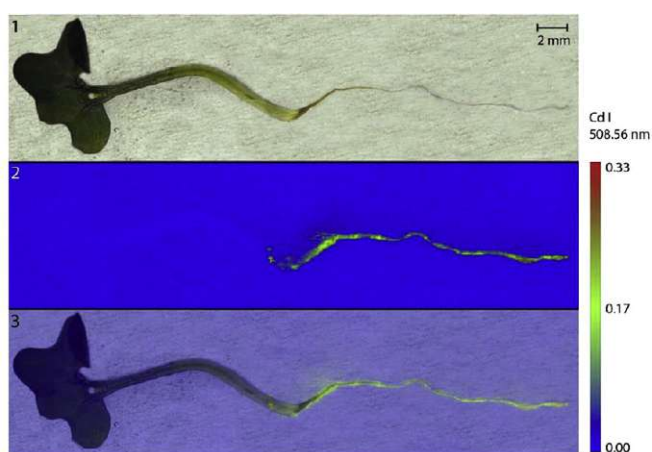

Fig. 5. Example of LIBS elemental images obtained for plants. 1. Photograph of Sinapis alba plant exposed to CdTe QDs at the nominal concentration 200 mM Cd before LIBS measurements. 2. LIBS maps constructed for Cd I 508.56 nm (spatial resolution of 100 μm). 3. Overlap of the original photograph of the plant with LIBS map. The scale shows the total emissivity of the selected emission lines [118]. Reprinted from "Detail investigation of toxicity, bioaccumulation, and translocation of Cd-based quantum dots and Cd salt in white mustard", 251, Pavlína Modlitbová, Pavel Pořízka,Sára Střítežská,Štěpán Zezulka, Marie Kummerová, Karel Novotný, Jozef Kaiser, 126174, 2020), with permission from Elsevier.

demonstrated by detection of gadolinium-based nanoparticles in mouse kidneys [130].

It is noteworthy that the sample preparation process is crucial for successful bioimaging in LIBS and has be to be optimized a priori for each experiment as summarized in review by Jantzi et al. [110]. There is no established way of soft tissue sample preparation for LIBS yet. Vincent Motto-Ross' group early stage research papers recommend the use of sample cryo-sections [128,129]. However, in their latter work improved detection was obtained by using epoxy fixing of samples after dehydration in a series of ethanol solutions [114,130], see Fig. 6. On contrary, Bonta et al. [113] compared the cryo-cutting and paraffin embedding after formalin fixation (the gold standard in histological tissue preparation) and found that paraffin fixation influences the distribution of certain elements. Moreover, the soft tissue sections were planted on silicon wafers instead of glass slides (as it is the most common), which led to improvement in sensitivity.

The thickness of the cross-section is of interest in order to supply sufficient amount of material for laser ablation and to reach satisfactory sensitivity. An effort is being invested in fitting laser spectroscopy to standard histological routines (to complement e.g. haematoxylin and eosin staining with minimum extra sample handling). However, the histology demands thinner sections (up to 5 μm) and laser-ablation demands more material in the interaction spot and thus thicker sections are preferable (from 10 μm).

Finally, the phenomenon of and parameters affecting the laser-tissue interaction are being extensively investigated. Detailed description of pulsed laser ablation of soft tissues is given elsewhere [135]. LIBS instrumentation and individual parameters were comprehensively summarized by Jolivet et al. [13].

4.1.2.2. Hard tissues. The pulsed laser ablation of hard tissues is less demanding in terms of analytical LIBS performance when compared to the case of soft tissues. Therefore, there are many pioneering works that utilized LIBS in the imaging of hard tissues (e.g. bone, teeth) where imaging was substituted with less demanding line scans. Former LIBS review publications have also mentioned the imaging of hard tissues (also referred as biominerals or calcified tissues) [102,106]. Another publication [136] brings a detailed review on the utilization of LIBS in the analysis of biominerals going well beyond the imaging point of view.

From the biological point of view, the imaging of biominerals targets wide selection of elements [136]. First, the major interest is in the detection of Ca and P forming the mineral phase and to macro elements such as C, O, N, and H relating the signal to organic phases (e.g. proteins). Detection of essential elements (Cu, Mn, I, Sr, Zn, etc.) indicates changes in the function of organs and nutrition. Finally, the uptake and accumulation of trace metals (Pb, Hg, Cd, As) shows potential malnutrition or long-term exposition to toxic environment.

The analysis of hard tissues may be divided into two main directions: *i)* monitoring of uptake and accumulation of various elements in tissues and *ii)* detection of qualitative difference between healthy and diseased tissue. The former case leads to nutrition habits or malnutrition when the cross-section of a tooth is imaged, e.g. the ratio of Sr/Ca was used to characterize a bear tooth [137]. The latter case, the imaging discovers correlations between the diseased tissue and increase/decrease in content of major or minor elements [138].

4.1.2.3. Tag-LIBS. Recently, traditional optical and spectroscopic methods evaluating the immunoassay results (absorbance, fluorescence, and luminescence) are being complemented with laser-ablation based spectroscopy methods [44]. Spectroscopic techniques are adapted to standard routines and benefit the researcher with an alternative insight. Apart from the simple label readout, accurate qualitative and quantitative chemical (i.e., elemental or molecular) information is obtained.

The utilization of NPs across various applications has also influenced the LIBS community. NPs are vitally used for signal enhancement in the laser ablation of selected analytes. LIBS was already used as a readout method for NP-based labels in the so-
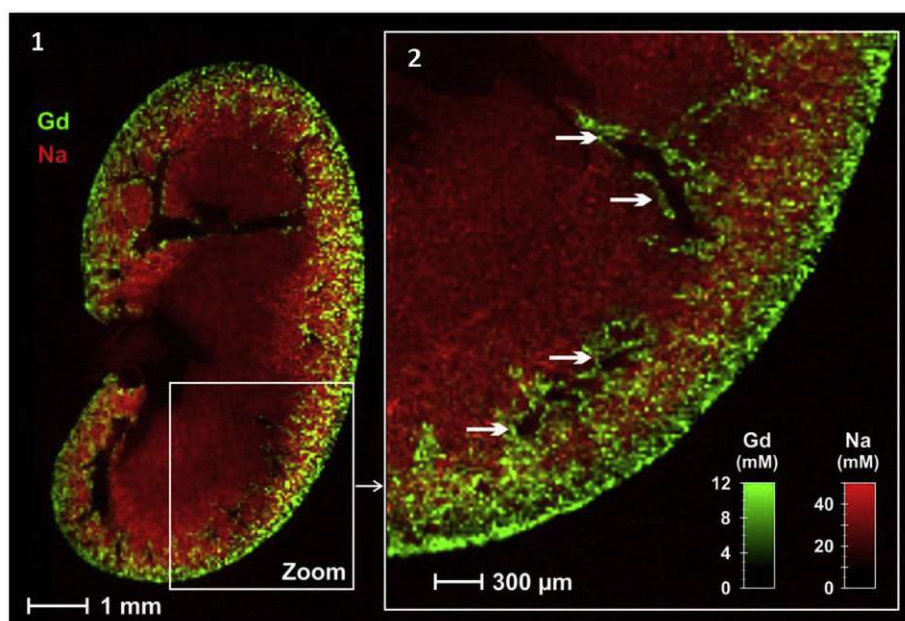
Fig. 6. Example of LIBS elemental images obtained for soft tissues. 1) Gadolinium (green) and sodium (red) distributions in a coronal murine kidney section, 24 h after gadolinium nanoparticle administration (spatial resolution of 40 μm). 2) Magnification of the image presented in (1.) in an adjacent section with 20 μm resolution. The white arrows indicate regions that are lacking in tissue, corresponding to blood vessels and collecting ducts [114]. Reprinted by permission from Springer Nature: Springer Nature, Scientific Reports, Laser spectrometry for multi-elemental imaging of biological tissues, L. Sancey et al., 2020.

called Tag-LIBS; which was introduced almost a decade ago [139]. Ovarian cancer biomarker CA-125 conjugated with silica microparticles reached ppb-level limits of detection. From this success, several patents stemmed [140,141].

The concept of Tag-LIBS is straightforward: the proteins (biomarkers) within the tissue are selectively bonded to metallic nanoparticles. The sample is then scanned, and the LIBS signal of NPs is imaged. Then, the distribution of targeted proteins (e.g. cancer) is imaged indirectly through the presence of NP-signal. The biggest advantage is that the NPs may be engineered in various way in order to be strictly specific to selected protein [142]. Such concept has a great potential in large-scale analysis of cancerous tissues when it could circumvent the relatively poor limits of detection of LIBS technique. However, intense research and sample pre-treatment optimization is needed prior the full exploitation of the Tag-LIBS.

LIBS was further developed as a vital readout technique for various pathogens and proteins. Metallothionein was deposited on a polystyrene microtiter plate and detected via its conjugation with Cd-containing quantum dots [143]. Au and Ag NP labels were examined from the bottom of a standard 96-well microtiter plate; a sandwich immunoassay for human serum albumin using streptavidin-coated Ag NP labels was developed [144]. Most recently, LIBS was implemented for the analysis of lateral-flow immunoassays with Au NPs labelled *Escherichia coli* [145]. Fluorescence and atomic absorption spectrometry were typically provided as reference techniques.

4.2. Geoscientific studies

Investigation of the distribution of different elements within rocks, sediments, corals, and shell samples offers insights into past, present, and future development of the climate. As mappings of large areas, desirable with resolution in the low μm range, is often necessary, LIBS is a very promising technique for paleoclimate studies as it offers very fast mappings [146]. Cáceres et al. [147] report the possibility to perform megapixel elemental images of different large samples such as speleothems (calcium carbonate cave deposits) and corals (calcium carbonate skeletons) using LIBS. This study presents the advantages of mapping large areas with a high lateral resolution for paleoclimate studies.

Speleothems were also investigated using LIBS by Ma et al. [148] that report the distribution of relative elemental concentrations of major, minor as well as trace elements. The list of investigated elements includes Ca, Na, Mg, Al, Si, K, Fe and Sr. By evaluating compositional correlations, mineral phases within the speleothems were identified. In the work of Hausmann et al. [149], Mg and Ca concentration ratios were mapped in shell carbonate, which is a type of sample often used in paleoclimatic and environmental studies. This work mainly focused on the development of an automated, high-throughput LIBS system for the analysis of these types of samples.

Fabre et al. [150] evaluated the use of LIBS for spatially resolved mineral characterization. Different phases of the investigated minerals were analyzed within a 5 cm^2 sample area with a lateral resolution of 15 μm. This study demonstrated the advantages of LIBS when it comes to mapping of large sample areas. Additionally, they also reported the detection of some rare earth elements (La and Y) in LIBS imaging experiments using a laser spot size of 10 μm. Challenges in the data evaluation of megapixel elemental images of complex multi-phase samples were also addressed. Imaging of rare earth elements in minerals was shown to be possible by combining LIBS with plasma-induced luminescence (PIL) by Gaft et al. [151]. For the detection of elements that are relevant to mineralogy (e.g. S, P, As, B, C or Zn) and have strong emission lines in the vacuum ultraviolet (VUV) wavelength range, Trichard et al. [152] reported the use of a VUV probe during mapping in a mining ore under ambient conditions. They achieved a detection limit of 0.2 wt% for sulfur in a single-shot configuration. In the work of Quarles et al. [153], the unique ability of LIBS to detect F was used to map F in bastnäsite mineral. Additionally, quantitative results were obtained by using in-house prepared standards based on NIST SRM 120c.

3D elemental distributions of rare earth elements in the mineral Bastnäsite were reported by Chirinos et al. [154], who used a combined setup incorporating LIBS and LA-ICP-MS. They revealed that new possibilities can be achieved by this combination, such as an expanded dynamic range or the joint 2D/3D visualization of elements and isotopes. Such a setup enables the detection of each element with the more suitable technique, which was demonstrated via the example of calcium: LIBS has a high sensitivity for Ca whereas LA-ICP-MS suffers from interferences due to which usually the less abundant isotope ^{44}Ca has to be measured.

In order to boost sensitivity, a double-pulse LIBS system was employed by Klus et al. [37] for the high resolution mapping of uranium distribution in sandstone-hosted uranium ores. Different data-evaluation strategies were also investigated in this work. Moncayo et al. [52] demonstrated the applicability of PCA for dataset reduction and for the exploration of megapixel elemental maps of a turquoise sample. Shale samples were imaged in a study conducted by Xu et al. [155]. In this study, the existence of a local thermodynamic equilibrium (LTE) was assessed and confirmed on the mapped area of the sample. As electron density and excitation temperature was also confirmed on the mapped area, a linear conversion of emission line intensities to concentrations was performed. Prochazka et al. used a combination of double-pulse LIBS with high resolution X-ray computer tomography to provide volumetric information of the elemental distribution in minerals [35]. Another study on shale samples was carried out by Jain et al. [156]. In this work, shale samples taken at various depths were analyzed and mapped using LIBS. Using the unique feature of LIBS to detect C and H, it was possible to detect and map these elements. Additionally, quantitative results for these elements were obtained by characterizing some of the samples using CHN-analysis and using these as calibration standards for LIBS.

As LIBS usually allows detection of emission signals over a broad spectral range, multivariate data evaluation strategies are commonly employed, which support not only elemental mapping but also spatially resolved sample classification. Meima et al. [157] investigated the applicability of a spectral angle mapper (SAM) algorithm for the laterally resolved classification of different minerals in ore samples. Several base metal sulfides, rock-forming minerals, accessory minerals, as well as several mixed phases making up the main borderline between different mineral grains were successfully classified in the recorded images. Rifai et al. [158] used PCA for the identification of different minerals in a platinum-palladium ore. With this approach, seven different minerals were identified and correlated with the generated maps. Quantitative multiphase mineral identification was also carried out by Haddad et al. [159] using a multivariate curve resolution − alternating least square (MCR-ALS) method. Obtained results were evaluated and in good agreement to conventional EDS-SEM analysis. Therefore, LIBS proves to be a very useful tool for mineral identification in mining operations as it can be employed in an online-setup.

The EU regularly updates its list of critical raw materials (CRM) and their governance levels. These strategic documents list a number of inorganic elements and materials, which are highly demanded by current industrial technologies, but for which the supply is limited within the EU [160]. The high demand for some of these elements and materials already increased their price on the market, which in turn made mining and metallurgical processing of

their ores economical in a significantly lower concentration than before. Consequently, assessment or re-assessment of geological formations potentially containing these elements/materials is in progress everywhere in the EU. Considering that some of the elements on these CRM lists are light elements (e.g. Be, Li, B, F) that are not easy to detect by other techniques, LIBS has a great prospect in these explorations. For example, Fig. 8, shows LIBS elemental maps of a granitoid rock sample for Be, studied by Jancsek et al. [161]. The map reveals that out of the four mineral grain types studied, Be and Bi is present in the highest concentration in biotite and amphibole, which suggests that mainly these minerals should be mined. Such LIBS imaging carried out by portable, stand-off instrumentation has the potential to be able to seriously speed up the assessment of the supplies (see Fig. 7).

4.3. Cultural heritage studies

LIBS imaging experiments can provide important information about art or historical items. Elemental fingerprints can be used for provenance studies and to assess the authenticity of samples. This information can be well augmented by elemental imaging data that can shed light on the fabrication process of the artefacts. One of the first applications of LIBS imaging in the field of cultural heritage science was presented at the first LIBS Conference in the year 2000 by Corsi et al. [162] investigating the elemental distribution of a roman fresco by analysing a 11x11 grid on the sample. As LIBS also offers remote analysis, historical objects can be analyzed directly in museums without bringing the sample to the laboratory. Grönlund et al. [163,164] were the first to report remote imaging of cultural heritage objects using a fully mobile LIDAR system operating at a wavelength of 355 nm mounted on a Volvo F610 truck. In this work, the spatial arrangement of different metal plates was identified over a distance of 60 m. In a study by Fortes et al. [165], elemental images of the façade of a cathedral in Malaga were recorded using a portable LIBS system. This data allowed the evaluation of Si/Ca and Ca/Mg intensity ratios and hence the identification of construction materials.

Alterations of cave walls, which poses a challenge when it comes to preservation of cave art, were investigated by Bassel et al. [166]. In this study, mainly coralloid formations were investigated using a portable instrument for spot measurements in the cave but imaging experiments were also carried out in the laboratory. Major elements (Si, Al, Fe, Ca, Mg, Na, K) as well as minor and trace elements

(Li, Rb, Sr, Ba) were detected.

While the use of portable LIBS systems allow analysis of samples that otherwise would not be possible as the sample can not be brought into a laboratory, these systems usually come with some limitations compared to more sophisticated lab-based LIBS systems. These limitations usually involve sensitivity and spectral or lateral resolution. Double-pulse or tandem LA-ICP-MS/LIBS instrumentation, which are only available in more sophisticated setups, can also be used to improve the quality of analysis.

Syta et al. [167] reported the combined use of LIBS and LA-ICP-MS imaging to investigate medieval Nubian objects with displaying specific blue paintings whether they are Egyptian blue ($CaCuSi_4O_{10}$) or lapis lazuli ($Na_{8-10}Al_6Si_6O_{24}S_{2-4}$). By elemental mappings of cross-sections of various samples and using Na and Cu as elemental markers, the identification of these two inorganic pigments was achieved. Weathering of historical limestone samples from Italian urban environments were investigated by Senesi et al. [168] using double-pulse LIBS 3D imaging. The double-pulse approach allowed for high resolution and 3D elemental mappings of a degradation layer present on the investigated weathered limestone. A decrease of Al, Fe, Si and Ti line intensities and an increase of Ca line intensity with depth in the degradation layer was found and was ascribed to decreased atmospheric pollution effects at greater depths.

Bulk classification of various materials relevant for the field of cultural heritage has already been performed in several works [169,170]. In the work of Pagnin et al. [83] the capabilities of LIBS for the spatially resolved classification of contemporary art materials consisting of inorganic pigments and organic binder materials was investigated. A multivariate classification model was established that allows the classification of mixtures of 9 different inorganic pigments and 3 different organic binders. The developed classification model was used for the laterally resolved classification of these materials within a structured sample (Fig. 9).

4.4. Materials science

Materials science uses and develops a range of materials. These materials can vary widely in their chemical composition, as they include e.g. alloys, steel, ceramics, glasses, polymers as well as composites. All these materials must comply with criteria set up for their physical and chemical properties for their successful application — whether these criteria are met or not is often tested by homogeneity and chemical composition analysis. Therefore,
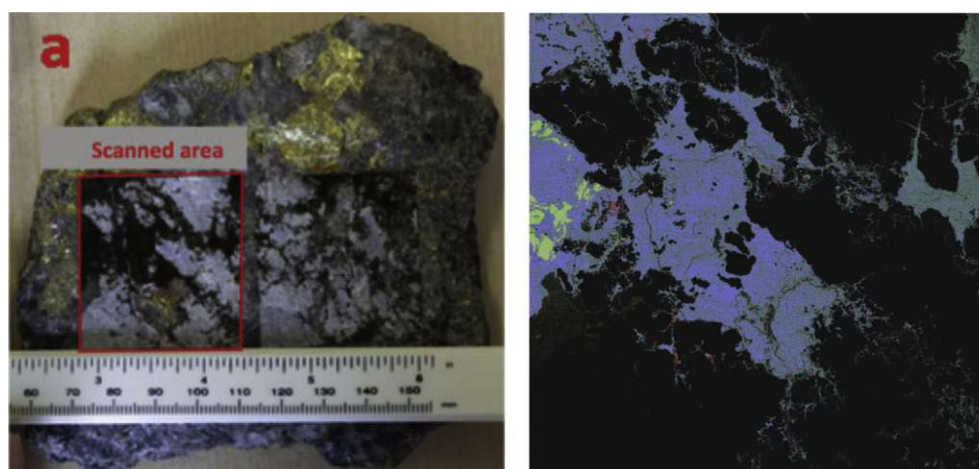

Fig. 7. Chemical mapping of an area of 40 × 40 mm², composed of 1602 × 1602 pixels, on the rough surface of the rock, showing the spatial distribution of Fe (green), Cu (blue), Zn (red), Ca (cyan), Ag (magenta) and Al (yellow). The dark area corresponds to the absence of LIBS signal in the crystalline mineral (silicates) under our experimental conditions. The spatial resolution (laser spot size and step size) is 50 μm [146]. Reprinted from Spectrochimica Acta Part B: Atomic Spectroscopy, Volume 150, K. Rifai et al., LIBS core imaging at kHz speed: Paving the way for real-time geochemical applications, 2018, with permission from Elsevier.
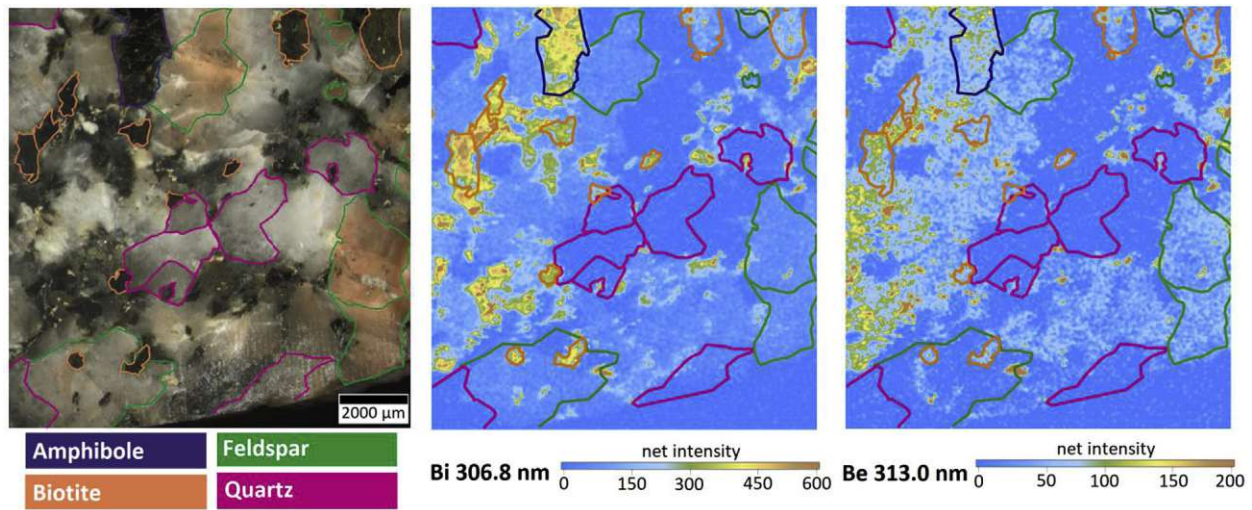
Fig. 8. Light microscope (on the left) and LIBS chemical imaging (on the right) of a granitoid sample taken from Mórágy, Hungary. Location of the four mineral grain types (quartz, feldspar, biotite, and amphibole) in the rock are indicated by coloured contour lines [161].
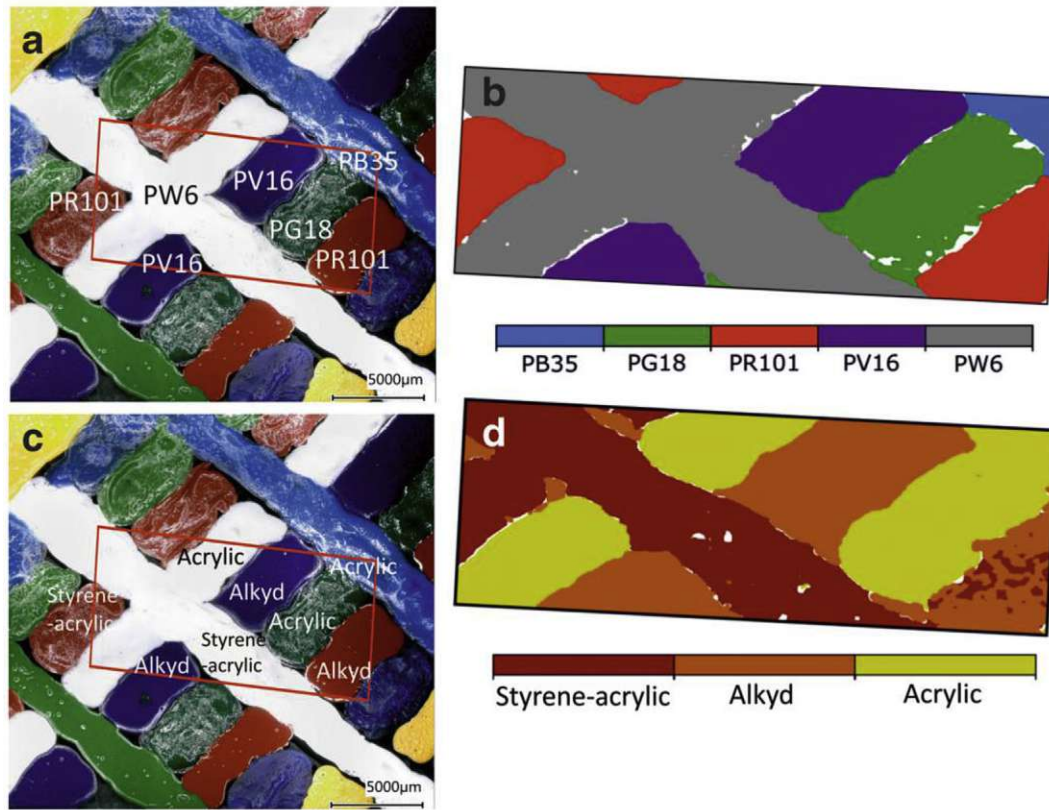

Fig. 9. Laterally resolved classification of contemporary art materials using LIBS. a) microscope image with marked distribution of different inorganic pigments, b) predicted distribution by a random decision forest of the distribution of inorganic pigments, c) microscope image with marked distribution of organic binder materials and d) predicted distribution by a random decision forest of the distribution of organic binder materials [83]. Reprinted by permission from Springer Nature: Springer Nature, Analytical and Bioanalytical Chemistry, "Multivariate analysis and laser-induced breakdown spectroscopy (LIBS): a new approach for the spatially resolved classification of modern art materials", L. Pagnin et al., 2020.

elemental imaging techniques such as LIBS are very useful to investigate novel materials, derived information is often very useful for further improvement of material properties as well as for the monitoring of production/synthesis procedures.

Alloys, or eminently steel, are amongst the most widely applied materials and are therefore of great interest for research. In the work of Bette et al. [171] LIBS elemental imaging was performed for the first time with repetition rates of 1000 Hz. In this work, steel samples were analyzed with a special focus on detecting non-metallic inclusions such as sulfur and phosphorus.

Recycling of electronical waste is becoming more and more important. Mappings of printed circuit boards were carried out by

Carvalho et al. [172]. LIBS data combined with multivariate data evaluation strategies (PCA) was used to investigate metal distributions within the boards. The authors were able to identify and map 18 elements within the sample. The described results are valuable for the research of new recycling strategies for electronic waste.

Bulk materials are often covered with thin films to enhance their physical and/or chemical properties. Thin films of copper, as well as $YBa_2Cu_3O_7$ (YBCO) - a high-temperature superconducting material - were investigated in the study of Ahamer et al. [173]. A fs-LIBS system was employed to perform high resolution elemental and molecular imaging of the thin film. Composite wear-resistance coatings made of 1560 nickel alloy reinforced with tungsten carbide was analyzed by Lednev et al. [174]. In this work, LIBS was used for 3D imaging experiments with a special focus on the analysis of C and Si which were not detectable with SEM/EDX. Besides C and Si, also Fe, Ni, Cr, W and Co were detected with LIBS.

Heterogeneous catalysis is a field important for various applications in the chemical industry or e.g. in the exhaust systems of cars. Mesoporous alumina is often used as a support. Investigation of the lateral distribution of the active material across the surface of the catalyst, but also of contaminations in the mesoporous alumina in spent catalysts offers an important insight into catalytic processes. Compared to EPMA, which is conventionally used for elemental mappings in the field of catalysis, LIBS enables analysis of light elements. LIBS imaging experiments were already conducted in 1999 in this field by Lucena et al. [175], who investigated the distribution of platinum group metals (PGMs) in car catalysts. Trichard et al. [176] use LIBS for the quantitative imaging of Pd in catalysts. In their follow-up work [177] Trichard et al. reported successful quantitative imaging in heterogeneous catalyst samples impregnated up to 53 days with asphaltenes. LIBS was not only able to detect S, C and Al, but also Ni and V, which are only present in the trace (ppm) range. By transforming the 2D maps to 1D profiles, transport mechanisms of the investigated materials within the alumina substrate were assessed.

With the strongly going industrial application of Li-ion batteries, a lot of research focuses on developing novel materials which could improve the performance of these batteries. Hou et al. [178] investigated LLZO ($Li_7La_3Zr_2O_{12}$), a promising novel material for a solid-state electrolyte, by using fs-LIBS to perform 3D elemental analysis with a special focus on elemental ratios of Li/La, Zr/La and Al/La. The reported depth resolution was an impressive 700 nm. Interface formation between a Li electrode with an LLZO electrolyte were investigated by Rettenwander et al. [179] using LIBS imaging combined with other analytical techniques. LIBS images revealed the formation of a Li deficient interlayer at the interface. Li-ion cathode material $LiCoO_2$ was analyzed by Imashuku et al. [180]. Li/Co ratios were quantified and investigated in cycled cathode materials. Even though the precision of obtained quantitative results is not comparable to conventional X-Ray Absorption

Spectroscopy (XAS), LIBS results can still be used to obtain semi-quantitative results.

Concrete is one of the most important construction materials for roads, bridges, tunnels, buildings, etc. hence the monitoring of the degradation and changes of its properties is crucial. For example, the distribution of various species harmful to concrete, such as Cl^-, Na^+, SO_4^{2-}, is of great interest as it can promote the assessment of the expected lifetime of the structures. As these species are only harmful if they are present in specific phases within concrete, the differentiation between the cement phase and agglomerates is also necessary. Gottlieb et al. [181] reported the use of LIBS in combination with an expectation-maximization (EM) algorithm for the cluster analysis of different phases present in concrete. This approach made it possible to exclude non-relevant aggregates from the analysis area.

The uses of polymers ranges from packaging over composite to construction materials. In some applications, polymers are used as a bulk material, however, materials consisting of multiple polymer layers are also often used in e.g. food packaging. A study demonstrating the capabilities of LIBS to map the distribution of different polymers within a sample was carried out by Brunnbauer et al. [84]. 2D mappings as well as 3D depth-profiling of structured polymer samples were carried out and the distribution of the different polymer types present in the sample were classified using multivariate statistical methods.

Due to its ability to perform remote analysis, LIBS inherently has advantages over other techniques when analysing dangerous or hazardous materials, for example in nuclear applications. Li et al. [182] and Hai et al. [183] carried out studies regarding the Experimental Advanced Superconducting Tokamak (EAST) fusion reactor located in Hefei, China. In the first study by Li et al., 2D analysis as well as depth profiling of Li on a W wall employed in the EAST fusion reactor as a plasma facing material (PFM). Hai et al., recorded distribution of impurities (H, O, Ar, K, Na, and Ca) on lithiated tungsten employed in reactor walls. Investigations regarding nuclear waste using LIBS were carried out by Wang et al. [184] with a special focus on the long-term migration of Mo, Ca, Sr, Al, Fe and Zr and various rare-earth elements.

Lately, LIBS imaging has also found its way into forensic science, where López-López et al. [185] et al. successfully employed LIBS mapping experiments for the visualization of gunshot residues. In this work, elemental markers such as Pb, Sb and Ba were used to investigate the distribution of residues as a function of their distance from clothing targets.

Pharmaceutical tablet coatings were investigated using 3D depth profiling by Zou et al. [186]. In this work, coating thickness, coating uniformity as well as contaminations were analyzed in various tablets. Coating thickness and uniformity was characterized using Ti as an elemental marker. Additionally, Fe was detected as a contamination. In a follow-up work by Smith et al. [187], hyperspectral imaging was used to investigate minor elements present in

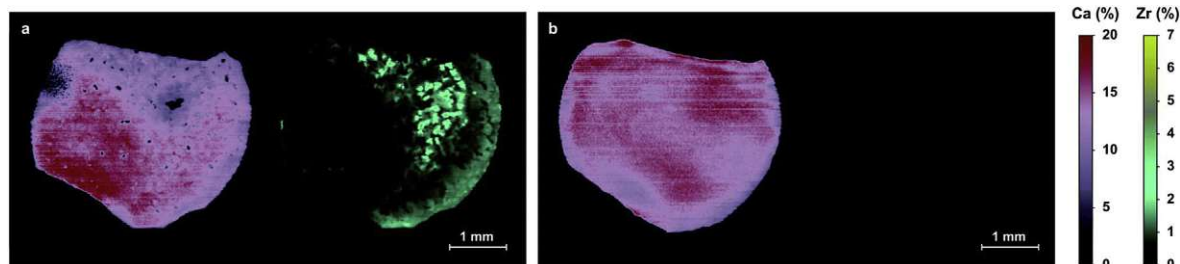**Fig. 10.** LIBS transversal chemical imaging for Ca and Zr obtained on the two cross sections of a 3-mm wide fiber pulled at 6 mm h^{-1} and located at (a) z = 19 mm and (b) z = 27 mm [189]. Reproduced from by permission of The Royal Society of Chemistry, CrystEngComm. 21, Lead-free piezoelectric crystals grown by the micro-pulling down technique in the BaTiO3−CaTiO3−BaZrO3 system, P. Veber et al., 2019.

tablet coatings such as Na, Mg and K. Additionally, PCA was employed and successfully used for the classification of 4 different tablet coatings.

The capabilities of LIBS for the investigating the composition of solar cells was reported by Lee et al. [188]. In this work, the composition of a commercial Cu(In,Ga)Se2 solar cells module was mapped. Obtained results were in good agreement with conventionally used SIMS analysis making LIBS a promising tool in quality control in the solar cells industries as analysis times could be reduced significantly.

In the work of Veber et al. LIBS was used as an analytical tool to investigate elemental distributions of Ca and Zr in lead-free piezoelectric crystals grown by the micro-pulling down technique [189]. Longitudinal LIBS analysis was in good agreement with EPMA analysis and was able to reveal inhomogeneities of Zr especially at high pulling speeds. Additionally, cross-sections of pulled fibres revealed elemental segregation at the core (Fig. 10).

5. Conclusion

LIBS is gaining more and more attention in the field of elemental imaging, mainly due to its ease of use in terms of sample preparation, speed of analysis and simple instrumentation compared to similar techniques. However, recently these advantages have become also accessible with LA-ICP-MS using laser-ablations systems with fast washout cells and modern ICP-TOF-MS instrumentation. Nevertheless, compared to this advanced approach LIBS offers some unique benefits such as access to the whole periodic table of elements and the possibility to collect elemental and molecular information simultaneously. In addition, LIBS instrumentation is usually significantly cheaper than LA-ICP-MS Thus, applications become feasible which could not be addressed with other elemental imaging techniques, some prominent examples have been presented within this review.

Despite the general applicability of LIBS there are still some limitations which hamper the usefulness for challenging research tasks. In particular, to fully exploit the multi-element capabilities of this technique the measurement of broadband spectra is obligatory. However, to ensure selective analysis the presence of spectral interferences must be avoided, necessitating also requirements regarding spectral resolution. Unfortunately, most instruments enable either the collection of broadband spectra with rather low resolution or the analysis of small wavelength sections with high resolution. Consequently, the development of LIBS spectrometer which enable the simultaneous measurement of the whole spectral range (approximately from 200 to 1000 nm) with high resolution is aimed for.

Another weakness of current LIBS instrumentation is the sometimes insufficient sensitivity, thus measurements require the use of increased laser beam diameters to enable reliable analyte detection, and thereby imaging applications which need a high spatial resolution are disabled. A common solution to improve the sensitivity of analysis is the use of ICCD detectors or novel developments such as sCMOS detectors, enabling LIBS measurements with significantly improved detection limits. But usually with these advanced detectors only a certain spectral range can be covered, disabling the coincident detection of emission lines from different wavelength ranges. Even though, recording of high-resolution LIBS spectra with excellent sensitivity can be already achieved by combining an Echelle spectrometer with several ICCD detection units, ongoing improvements in LIBS instrumentation are demanded which will most probably allow for higher sensitivity at a lower price point in the future.

Besides instrumental developments, novel approaches such as Tandem LA-ICP-MS/LIBS, LIBS/Raman or double-or multi-pulse LIBS are promising to enhance the performance of LIBS [190] as well. In the case of Tandem LA-ICP-MS/LIBS, trace elements can be detected with the high sensitivity of ICP-MS and LIBS is used for the analysis of minor and major components as well as e.g. H, C, N and O making it a very versatile tool for multi-element imaging. The applicability of this Tandem approach for the investigation of tissue thin cuts [113] and archaeological samples [167] have been published recently. Hybrid LIBS/Raman systems have been recently reported in literature [191]. With this setup complementary information obtained from Raman spectroscopy was combined with LIBS data and used e.g. to improve classification of polymers [192] and analysis of forensic samples such as pigments and inks [193]. This combination is very promising to solve difficult classification tasks which seem to become more and more important. Double-pulse LIBS uses two consecutive laser pulses increasing the plasma temperature and reducing the atmospheric pressure and number density. This approach is especially interesting for applications which demand quasi non-destructive sample analysis such as valuable art work or heritage samples. With the use of a fs-laser for the ablation step only a minimum of sample material is consumed, which is efficiently atomized and excited with the second pulse from a ns-laser. This allows in particular significant improvements in the spatial resolution of analysis as a result of the enhanced sensitivity [120,138].

The progress of various chemometric approaches useful for LIBS data evaluation is also remarkable and may help advancing the establishment of LIBS as an elemental imaging technique, which is also capable of chemical sample classification. Here, especially the advantage of broadband LIBS spectra should be mentioned. Improvements of automatic peak detection combined with multivariate evaluation methods may enable fast and superior data evaluation strategies taking advantage of the information present in broadband LIBS spectra compared to simple univariate evaluations where only one emission signal from the spectrum is used. Nevertheless, due to the fast advancements in multivariate data evaluation strategies such as machine learning, algorithms are often used as black-boxes, often leading to misinterpretation of results. Therefore, expertise in this field could be very valuable for LIBS.

At the same time, some aspects of LIBS elemental mapping — most notably quantification - remain to be challenging. In this field, novel approaches such as multivariate calibration or calibration-free quantitation may prove to be useful tools.

Declaration of competing interest

The authors declare that they have no known competing financial interests or personal relationships that could have appeared to influence the work reported in this paper.

Acknowledgments

References

[1] G. Friedbacher, H. Bubert, Surface and Thin Film Analysis: A Compendium of Principles, Instrumentation, and Applications, John Wiley & Sons, 2011.

[2] R.E. Russo, X. Mao, H. Liu, J. Gonzalez, S.S. Mao, Laser ablation in analytical chemistry—a review, Talanta 57 (2002) 425–451, https://doi.org/10.1016/S0039-9140(02)00053-X.

[3] A. Limbeck, M. Bonta, W. Nischkauer, Improvements in the direct analysis of advanced materials using ICP-based measurement techniques, J. Anal. At. Spectrom. 32 (2017) 212–232, https://doi.org/10.1039/C6JA00335D.

[4] A. Limbeck, P. Galler, M. Bonta, G. Bauer, W. Nischkauer, F. Vanhaecke, Recent advances in quantitative LA-ICP-MS analysis: challenges and solutions in the life sciences and environmental chemistry, Anal. Bioanal. Chem. 407 (2015) 6593–6617, https://doi.org/10.1007/s00216-015-8858-0.

[5] M.E. Shaheen, J.E. Gagnon, B.J. Fryer, Femtosecond (fs) lasers coupled with modern ICP-MS instruments provide new and improved potential for in situ elemental and isotopic analyses in the geosciences, Chem. Geol. 330–331 (2012) 260–273, https://doi.org/10.1016/j.chemgeo.2012.09.016.

[6] D.A. Cremers, L.J. Radziemski, Handbook of Laser-Induced Breakdown Spectroscopy, John Wiley & Sons, 2013.

[7] A.W. Miziolek, V. Palleschi, I. Schechter, Laser Induced Breakdown Spectroscopy, Cambridge University Press, 2006.

[8] J.M. Vadillo, S. Palanco, M.D. Romero, J.J. Laserna, Applications of laser-induced breakdown spectrometry (LIBS) in surface analysis, Fresenius' J. Anal. Chem. 355 (1996) 909–912, https://doi.org/10.1007/s0021663550909.

[9] T. Kim, C.T. Lin, Y. Yoon, Compositional mapping by laser-induced breakdown spectroscopy, J. Phys. Chem. B 102 (1998) 4284–4287, https://doi.org/10.1021/jp980245m.

[10] V. Piñon, M.P. Mateo, G. Nicolas, Laser-induced breakdown spectroscopy for chemical mapping of materials, Appl. Spectrosc. Rev. 48 (2013) 357–383, https://doi.org/10.1080/05704928.2012.717569.

[11] H. Bette, R. Noll, High speed laser-induced breakdown spectrometry for scanning microanalysis, J. Phys. Appl. Phys. 37 (2004) 1281–1288, https://doi.org/10.1088/0022-3727/37/8/018.

[12] D. Menut, P. Fichet, J.-L. Lacour, A. Rivoallan, P. Mauchien, Micro-laser-induced breakdown spectroscopy technique: a powerful method for performing quantitative surface mapping on conductive and nonconductive samples, Appl. Optic. 42 (2003) 6063–6071, https://doi.org/10.1364/AO.42.006063.

[13] L. Jolivet, M. Leprince, S. Moncayo, L. Sorbier, C.-P. Lienemann, V. Motto-Ros, Review of the recent advances and applications of LIBS-based imaging, Spectrochim. Acta Part B At. Spectrosc. 151 (2019) 41–53, https://doi.org/10.1016/j.sab.2018.11.008.

[14] S.J.M.V. Malderen, A.J. Managh, B.L. Sharp, F. Vanhaecke, Recent developments in the design of rapid response cells for laser ablation-inductively coupled plasma-mass spectrometry and their impact on bioimaging applications, J. Anal. At. Spectrom. 31 (2016) 423–439, https://doi.org/10.1039/C5JA00430F.

[15] C.C. Garcia, H. Lindner, K. Niemax, Transport efficiency in femtosecond laser ablation inductively coupled plasma mass spectrometry applying ablation cells with short and long washout times, Spectrochim. Acta Part B At. Spectrosc. 62 (2007) 13–19, https://doi.org/10.1016/j.sab.2006.11.005.

[16] A.A. Bol'shakov, X. Mao, J.J. González, R.E. Russo, Laser ablation molecular isotopic spectrometry (LAMIS): current state of the art, J. Anal. At. Spectrom. 31 (2016) 119–134, https://doi.org/10.1039/C5JA00310E.

[17] J.D. Woodhead, M.S.A. Horstwood, J.M. Cottle, Advances in isotope ratio determination by LA–ICP–MS, Elements 12 (2016) 317–322, https://doi.org/10.2113/gselements.12.5.317.

[18] F.J. Fortes, J. Moros, P. Lucena, L.M. Cabalín, J.J. Laserna, Laser-induced breakdown spectroscopy, Anal. Chem. 85 (2013) 640–669, https://doi.org/10.1021/ac303220r.

[19] D.W. Hahn, N. Omenetto, Laser-induced breakdown spectroscopy (LIBS), Part II: review of instrumental and methodological approaches to material analysis and applications to different fields, Appl. Spectrosc. 66 (2012) 347–419, https://doi.org/10.1366/11-06574.

[20] G. Galbács, A critical review of recent progress in analytical laser-induced breakdown spectroscopy, Anal. Bioanal. Chem. 407 (2015) 7537–7562, https://doi.org/10.1007/s00216-015-8855-3.

[21] C. Pasquini, J. Cortez, L.M.C. Silva, F.B. Gonzaga, Laser induced breakdown spectroscopy, J. Braz. Chem. Soc. 18 (2007) 463–512, https://doi.org/10.1590/S0103-50532007000300002.

[22] J. Laserna, J.M. Vadillo, P. Purohit, Laser-induced breakdown spectroscopy (LIBS): fast, effective, and agile leading edge analytical technology, Appl. Spectrosc. 72 (2018) 35–50, https://doi.org/10.1177/0003702818791926.

[23] S. Musazzi, U. Perini, LIBS instrumental techniques, in: S. Musazzi, U. Perini (Eds.), Laser-Induc. Breakdown Spectrosc. Theory Appl., Springer, Berlin, Heidelberg, 2014, pp. 59–89, https://doi.org/10.1007/978-3-642-45085-3_3.

[24] R. Noll, Laser-induced breakdown spectroscopy, in: R. Noll (Ed.), Laser-Induc. Breakdown Spectrosc. Fundam. Appl., Springer, Berlin, Heidelberg, 2012, pp. 7–15, https://doi.org/10.1007/978-3-642-20668-9_2.

[25] J.P. Singh, S.N. Thakur, Laser-Induced Breakdown Spectroscopy, Elsevier, 2007.

[26] W. Shi, Q. Fang, X. Zhu, R.A. Norwood, N. Peyghambarian, Fiber lasers and their applications [Invited], Appl. Optic. 53 (2014) 6554–6568, https://doi.org/10.1364/AO.53.006554.

[27] T.A. Labutin, V.N. Lednev, A.A. Ilyin, A.M. Popov, Femtosecond laser-induced breakdown spectroscopy, J. Anal. At. Spectrom. 31 (2016) 90–118, https://doi.org/10.1039/C5JA00301F.

[28] Y. Li, D. Tian, Y. Ding, G. Yang, K. Liu, C. Wang, X. Han, A review of laser-induced breakdown spectroscopy signal enhancement, Appl. Spectrosc. Rev. 53 (2018) 1–35, https://doi.org/10.1080/05704928.2017.1352509.

[29] G. Galbács, V. Budavári, Z. Geretovszky, Multi-pulse laser-induced plasma spectroscopy using a single laser source and a compact spectrometer, J. Anal. At. Spectrom. 20 (2005) 974–980, https://doi.org/10.1039/B504373E.

[30] N. Jedlinszki, G. Galbács, An evaluation of the analytical performance of collinear multi-pulse laser induced breakdown spectroscopy, Microchem. J. 97 (2011) 255–263, https://doi.org/10.1016/j.microc.2010.09.009.

[31] G. Galbács, N. Jedlinszki, K. Herrera, N. Omenetto, B.W. Smith, J.D. Winefordner, A study of ablation, spatial, and temporal characteristics of laser-induced plasmas generated by multiple collinear pulses, Appl. Spectrosc. 64 (2010) 161–172, https://doi.org/10.1366/000370210790619609.

[32] V.I. Babushok, F.C. DeLucia, J.L. Gottfried, C.A. Munson, A.W. Miziolek, Double pulse laser ablation and plasma: laser induced breakdown spectroscopy signal enhancement, Spectrochim. Acta Part B At. Spectrosc. 61 (2006) 999–1014, https://doi.org/10.1016/j.sab.2006.09.003.

[33] J. Scaffidi, S.M. Angel, D.A. Cremers, Emission Enhancement Mechanisms in Dual-Pulse LIBS, ACS Publications, 2006.

[34] C. Schiavo, L. Menichetti, E. Grifoni, S. Legnaioli, G. Lorenzetti, F. Poggialini, S. Pagnotta, V. Palleschi, High-resolution three-dimensional compositional imaging by double-pulse laser-induced breakdown spectroscopy, J. Instrum. 11 (2016), https://doi.org/10.1088/1748-0221/11/08/C08002. C08002–C08002.

[35] D. Prochazka, T. Zikmund, P. Pořízka, A. Břínek, J. Klus, J. Šalplachta, J. Kynický, J. Novotný, J. Kaiser, Joint utilization of double-pulse laser-induced breakdown spectroscopy and X-ray computed tomography for volumetric information of geological samples, J. Anal. At. Spectrom. 33 (2018) 1993–1999, https://doi.org/10.1039/C8JA00232K.

[36] R. Grassi, E. Grifoni, S. Gufoni, S. Legnaioli, G. Lorenzetti, N. Macro, L. Menichetti, S. Pagnotta, F. Poggialini, C. Schiavo, V. Palleschi, Three-dimensional compositional mapping using double-pulse micro-laser-induced breakdown spectroscopy technique, Spectrochim. Acta Part B At. Spectrosc. 127 (2017) 1–6, https://doi.org/10.1016/j.sab.2016.11.004.

[37] J. Klus, P. Mikysek, D. Prochazka, P. Pořízka, P. Prochazková, J. Novotný, T. Trojek, K. Novotný, M. Slobodník, J. Kaiser, Multivariate approach to the chemical mapping of uranium in sandstone-hosted uranium ores analyzed using double pulse Laser-Induced Breakdown Spectroscopy, Spectrochim. Acta Part B At. Spectrosc. 123 (2016) 143–149, https://doi.org/10.1016/j.sab.2016.08.014.

[38] V. Zorba, X. Mao, R.E. Russo, Ultrafast laser induced breakdown spectroscopy for high spatial resolution chemical analysis, Spectrochim. Acta Part B At. Spectrosc. 66 (2011) 189–192, https://doi.org/10.1016/j.sab.2010.12.008.

[39] A.S. Eppler, D.A. Cremers, D.D. Hickmott, M.J. Ferris, A.C. Koskelo, Matrix effects in the detection of Pb and Ba in soils using laser-induced breakdown spectroscopy, Appl. Spectrosc. 50 (1996) 1175–1181, https://doi.org/10.1366/0003702963905123.

[40] K.T. Rodolfa, D.A. Cremers, Capabilities of surface composition analysis using a long laser-induced breakdown spectroscopy spark, Appl. Spectrosc. 58 (2004) 367–375, https://doi.org/10.1366/000370204773580185.

[41] V. Sturm, Optical micro-lens array for laser plasma generation in spectrochemical analysis, J. Anal. At. Spectrom. 22 (2007) 1495–1500, https://doi.org/10.1039/B708564H.

[42] A.J. Effenberger, J.R. Scott, Effect of atmospheric conditions on LIBS spectra, Sensors 10 (2010) 4907–4925, https://doi.org/10.3390/s100504907.

[43] C.C. García, M. Corral, J.M. Vadillo, J.J. Laserna, Angle-resolved laser-induced breakdown spectrometry for depth profiling of coated materials, Appl. Spectrosc. 54 (2000) 1027–1031, https://doi.org/10.1366/0003702001950526.

[44] P. Modlitbová, P. Pořízka, J. Kaiser, Laser-induced breakdown spectroscopy as a promising tool in the elemental bioimaging of plant tissues, TrAC Trends Anal. Chem. (Reference Ed.) 122 (2020), 115729, https://doi.org/10.1016/j.trac.2019.115729.

[45] B. Busser, S. Moncayo, J.-L. Coll, L. Sancey, V. Motto-Ros, Elemental imaging using laser-induced breakdown spectroscopy: a new and promising approach for biological and medical applications, Coord. Chem. Rev. 358 (2018) 70–79, https://doi.org/10.1016/j.ccr.2017.12.006.

[46] J.S. Becker, A. Matusch, B. Wu, Bioimaging mass spectrometry of trace elements – recent advance and applications of LA-ICP-MS: a review, Anal. Chim. Acta 835 (2014) 1–18, https://doi.org/10.1016/j.aca.2014.04.048.

[47] W. Li, X. Li, X. Li, Z. Hao, Y. Lu, X. Zeng, A review of remote laser-induced breakdown spectroscopy, Appl. Spectrosc. Rev. 55 (2020) 1–25, https://doi.org/10.1080/05704928.2018.1472102.

[48] P.D. Barnett, N. Lamsal, S.M. Angel, Standoff laser-induced breakdown spectroscopy (LIBS) using a miniature wide field of view spatial heterodyne spectrometer with sub-microsteradian collection optics, Appl. Spectrosc. 71 (2017) 583–590, https://doi.org/10.1177/0003702816687569.

[49] I.B. Gornushkin, B.W. Smith, U. Panne, N. Omenetto, Laser-induced breakdown spectroscopy combined with spatial heterodyne spectroscopy, Appl. Spectrosc. 68 (2014) 1076–1084, https://doi.org/10.1366/14-07544.

[50] A.B. Gojani, D.J. Palásti, A. Paul, G. Galbács, I.B. Gornushkin, Analysis and

classification of liquid samples using spatial heterodyne Raman spectroscopy, Appl. Spectrosc. 73 (2019) 1409–1419, https://doi.org/10.1177/0003702819863847.

[51] T. Zhang, H. Tang, H. Li, Chemometrics in laser-induced breakdown spectroscopy, J. Chemom. 32 (2018), e2983, https://doi.org/10.1002/cem.2983.

[52] S. Moncayo, L. Duponchel, N. Mousavipak, G. Panczer, F. Trichard, B. Bousquet, F. Pelascini, V. Motto-Ros, Exploration of megapixel hyperspectral LIBS images using principal component analysis, J. Anal. At. Spectrom. 33 (2018) 210–220, https://doi.org/10.1039/C7JA00398F.

[53] D.L. Blaney, R.C. Wiens, S. Maurice, S.M. Clegg, R.B. Anderson, L.C. Kah, S.L. Mouélic, A. Ollila, N. Bridges, R. Tokar, G. Berger, J.C. Bridges, A. Cousin, B. Clark, M.D. Dyar, P.L. King, N. Lanza, N. Mangold, P.-Y. Meslin, H. Newsom, S. Schröder, S. Rowland, J. Johnson, L. Edgar, O. Gasnault, O. Forni, M. Schmidt, W. Goetz, K. Stack, D. Sumner, M. Fisk, M.B. Madsen, Chemistry and texture of the rocks at Rocknest, Gale Crater: evidence for sedimentary origin and diagenetic alteration, J. Geophys. Res. Planets. 119 (2014) 2109–2131, https://doi.org/10.1002/2013JE004590.

[54] J. Yan, S. Li, K. Liu, R. Zhou, W. Zhang, Z. Hao, X. Li, D. Wang, Q. Li, X. Zeng, An image features assisted line selection method in laser-induced breakdown spectroscopy, Anal. Chim. Acta 1111 (2020) 139–146, https://doi.org/10.1016/j.aca.2020.03.030.

[55] C. Harris, M. Stephens, A combined corner and edge detector, in: Proc Fourth Alvey Vis. Conf, 1988, pp. 147–152.

[56] P. Pořízka, J. Klus, A. Hrdlička, J. Vrábel, P. Škarková, D. Prochazka, J. Novotný, K. Novotný, J. Kaiser, Impact of Laser-Induced Breakdown Spectroscopy data normalization on multivariate classification accuracy, J. Anal. At. Spectrom. 32 (2017) 277–288, https://doi.org/10.1039/C6JA00322B.

[57] E. Képeš, P. Pořízka, J. Klus, P. Modlitbová, J. Kaiser, Influence of baseline subtraction on laser-induced breakdown spectroscopic data, J. Anal. At. Spectrom. 33 (2018) 2107–2115, https://doi.org/10.1039/C8JA00209F.

[58] M. Bonta, H. Lohninger, M. Marchetti-Deschmann, A. Limbeck, Application of gold thin-films for internal standardization in LA-ICP-MS imaging experiments, Analyst 139 (2014) 1521–1531, https://doi.org/10.1039/c3an01511d.

[59] A.A. Green, M. Berman, P. Switzer, M.D. Craig, A transformation for ordering multispectral data in terms of image quality with implications for noise removal, IEEE Trans. Geosci. Rem. Sens. 26 (1988) 65–74, https://doi.org/10.1109/36.3001.

[60] P. Pořízka, J. Klus, E. Képeš, D. Prochazka, D.W. Hahn, J. Kaiser, On the utilization of principal component analysis in laser-induced breakdown spectroscopy data analysis, a review, Spectrochim. Acta Part B At. Spectrosc. 148 (2018) 65–82, https://doi.org/10.1016/j.sab.2018.05.030.

[61] S. Romppanen, H. Häkkänen, S. Kaski, Singular value decomposition approach to the yttrium occurrence in mineral maps of rare earth element ores using laser-induced breakdown spectroscopy, Spectrochim. Acta Part B At. Spectrosc. 134 (2017) 69–74, https://doi.org/10.1016/j.sab.2017.06.002.

[62] I.T. Jolliffe, Principal component analysis, Technometrics 45 (2003) 276.

[63] A. Limbeck, DS013 concrete, n.d. http://www.imagelab.at/en_data_repository.html. (Accessed 30 June 2020).

[64] K. Fukunaga, Introduction to Statistical Pattern Classification, academic press, San Diego Calif. USA, 1990.

[65] D.L. Massart, B.G. Vandeginste, L.M. Buydens, P.J. Lewi, J. Smeyers-Verbeke, S.D. Jong, Handbook of Chemometrics and Qualimetrics, Elsevier Science Inc., 1998.

[66] G.N. Lance, W.T. Williams, A general theory of classificatory sorting Strategies1. Hierarchical systems, Comput. J. 9 (1967) 373–380, https://doi.org/10.1093/comjnl/9.4.373.

[67] J.H. Ward, Hierarchical grouping to optimize an objective function, J. Am. Stat. Assoc. 58 (1963) 236–244, https://doi.org/10.1080/01621459.1963.10500845.

[68] H. Lohninger, Similarity map, help page of epina ImageLab, Release 3.20, (n.d.), http://www.imagelab.at/help/similarity_map.htm. (Accessed 30 June 2020).

[69] M. Zürcher, J.T. Clerc, M. Farkas, E. Pretsch, General theory of similarity measures for library search systems, Anal. Chim. Acta 206 (1988) 161–172, https://doi.org/10.1016/S0003-2670(00)80839-9.

[70] P.C. Mahalanobis, On the generalized distance in statistics, in: National Institute of Science of India, 1936.

[71] F.A. Kruse, A.B. Lefkoff, J.W. Boardman, K.B. Heidebrecht, A.T. Shapiro, P.J. Barloon, A.F.H. Goetz, The spectral image processing system (SIPS)-interactive visualization and analysis of imaging spectrometer data, AIP Conf. Proc. 283 (1993) 192–201, https://doi.org/10.1063/1.44433.

[72] Y. Du, C.-I. Chang, H. Ren, C.-C. Chang, J.O. Jensen, F.M. D'Amico, New hyperspectral discrimination measure for spectral characterization, Opt. Eng. 43 (2004) 1777–1786, https://doi.org/10.1117/1.1766301.

[73] J.M.P. Nascimento, J.M.B. Dias, Vertex component analysis: a fast algorithm to unmix hyperspectral data, IEEE Trans. Geosci. Rem. Sens. 43 (2005) 898–910, https://doi.org/10.1109/TGRS.2005.844293.

[74] T. Kohonen, Self-organized formation of topologically correct feature maps, Biol. Cybern. 43 (1982) 59–69, https://doi.org/10.1007/BF00337288.

[75] S. Pagnotta, M. Lezzerini, B. Campanella, G. Gallello, E. Grifoni, S. Legnaioli, G. Lorenzetti, F. Poggialini, S. Raneri, A. Safi, V. Palleschi, Fast quantitative elemental mapping of highly inhomogeneous materials by micro-Laser-Induced Breakdown Spectroscopy, Spectrochim. Acta Part B At. Spectrosc. 146 (2018) 9–15, https://doi.org/10.1016/j.sab.2018.04.018.

[76] Y. Tang, Y. Guo, Q. Sun, S. Tang, J. Li, L. Guo, J. Duan, Industrial polymers

[77] classification using laser-induced breakdown spectroscopy combined with self-organizing maps and K-means algorithm, Optik 165 (2018) 179–185.

[77] J. Klus, P. Pořízka, D. Prochazka, P. Mikysek, J. Novotný, K. Novotný, M. Slobodník, J. Kaiser, Application of self-organizing maps to the study of U-Zr-Ti-Nb distribution in sandstone-hosted uranium ores, Spectrochim. Acta Part B at, Spectroscopy (Glos.) 131 (2017) 66–73, https://doi.org/10.1016/j.sab.2017.03.008.

[78] G.J. McLachlan, Discriminant Analysis and Statistical Pattern Recognition, Wiley, N. Y., 1992.

[79] L. Chuen Lee, C.-Y. Liong, A. Aziz Jemain, Partial least squares-discriminant analysis (PLS-DA) for classification of high-dimensional (HD) data: a review of contemporary practice strategies and knowledge gaps, Analyst 143 (2018) 3526–3539, https://doi.org/10.1039/C8AN00599K.

[80] S. Wold, M. Sjöström, L. Eriksson, PLS-regression: a basic tool of chemometrics, Chemometr. Intell. Lab. Syst. 58 (2001) 109–130, https://doi.org/10.1016/S0169-7439(01)00155-1.

[81] L. Breiman, Random forests, Mach. Learn. 45 (2001) 5–32.

[82] L. Breiman, A. Cutler, Random forest. https://www.stat.berkeley.edu/~breiman/RandomForests/cc_home.htm, 2020. (Accessed 29 June 2020).

[83] L. Pagnin, L. Brunnbauer, R. Wiesinger, A. Limbeck, M. Schreiner, Multivariate analysis and laser-induced breakdown spectroscopy (LIBS): a new approach for the spatially resolved classification of modern art materials, Anal. Bioanal. Chem. (2020), https://doi.org/10.1007/s00216-020-02574-z.

[84] L. Brunnbauer, S. Larisegger, H. Lohninger, M. Nelhiebel, A. Limbeck, Spatially resolved polymer classification using laser induced breakdown spectroscopy (LIBS) and multivariate statistics, Talanta (2019), 120572, https://doi.org/10.1016/j.talanta.2019.120572.

[85] D. Livingstone, A Practical Guide to Scientific Data Analysis, Wiley Online Library, 2009.

[86] R.E. Bellman, Adaptive Control Processes: A Guided Tour, Princeton University Press, 2015.

[87] V. Vapnik, Pattern recognition using generalized portrait method, Autom. Remote Control 24 (1963) 774–780.

[88] A.J. Smola, B. Schölkopf, A tutorial on support vector regression, Stat. Comput. 14 (2004) 199–222, https://doi.org/10.1023/B:STCO.0000035301.49549.88.

[89] X. Li, S. Yang, R. Fan, X. Yu, D. Chen, Discrimination of soft tissues using laser-induced breakdown spectroscopy in combination with k nearest neighbors (kNN) and support vector machine (SVM) classifiers, Optic Laser. Technol. 102 (2018) 233–239, https://doi.org/10.1016/j.optlastec.2018.01.028.

[90] K.-L. Du, M.N. Swamy, Neural Networks and Statistical Learning, Springer Science & Business Media, 2013.

[91] J. El Haddad, M. Villot-Kadri, A. Ismaël, G. Gallou, K. Michel, D. Bruyère, V. Laperche, L. Canioni, B. Bousquet, Artificial neural network for on-site quantitative analysis of soils using laser induced breakdown spectroscopy, Spectrochim. Acta Part B At. Spectrosc. 79–80 (2013) 51–57, https://doi.org/10.1016/j.sab.2012.11.007.

[92] A. Koujelev, S.-L. Lui, Artificial neural networks for material identification, mineralogy and analytical geochemistry based on laser-induced breakdown spectroscopy, Artif. NEURAL Netw. Ind. Ctrl. Eng. Appl. (2011) 91.

[93] S. Pagnotta, M. Lezzerini, B. Campanella, S. Legnaioli, F. Poggialini, V. Palleschi, A new approach to non-linear multivariate calibration in laser-induced breakdown spectroscopy analysis of silicate rocks, Spectrochim. Acta Part B At. Spectrosc. 166 (2020), 105804, https://doi.org/10.1016/j.sab.2020.105804.

[94] H.K. Sanghapi, J. Jain, A. Bol'shakov, C. Lopano, D. McIntyre, R. Russo, Determination of elemental composition of shale rocks by laser induced breakdown spectroscopy, Spectrochim. Acta Part B At. Spectrosc. 122 (2016) 9–14, https://doi.org/10.1016/j.sab.2016.05.011.

[95] T. Hastie, R. Tibshirani, J. Friedman, The Elements of Statistical Learnin, Springer, New York, 2009.

[96] T. Wang, L. Jiao, C. Yan, Y. He, M. Li, T. Zhang, H. Li, Simultaneous quantitative analysis of four metal elements in oily sludge by laser induced breakdown spectroscopy coupled with wavelet transform-random forest (WT-RF), Chemometr. Intell. Lab. Syst. 194 (2019), 103854, https://doi.org/10.1016/j.chemolab.2019.103854.

[97] W.A.C. Hallada, Image sharpening for mixed spatial and spectral resolution satellite systems, May 09, 1983 - May 13, 1983, https://ntrs.nasa.gov/search.jsp?R=19850028100, 1983. (Accessed 29 June 2020).

[98] M.G.-A.C. author, X. Otazu, O. Fors, A. Seco, Comparison between Mallat's and the 'à trous' discrete wavelet transform based algorithms for the fusion of multispectral and panchromatic images, Int. J. Rem. Sens. 26 (2005) 595–614, https://doi.org/10.1080/01431160512331314056.

[99] A. Sussulini, J.S. Becker, J.S. Becker, Laser ablation ICP-MS: application in biomedical research, Mass Spectrom. Rev. 36 (2017) 47–57, https://doi.org/10.1002/mas.21481.

[100] J. Sabine Becker, Imaging of metals in biological tissue by laser ablation inductively coupled plasma mass spectrometry (LA–ICP–MS): state of the art and future developments, J. Mass Spectrom. 48 (2013) 255–268.

[101] B. Wu, J.S. Becker, Imaging techniques for elements and element species in plant science, Metallomics 4 (2012) 403–416.

[102] J. Kaiser, K. Novotný, M.Z. Martin, A. Hrdlička, R. Malina, M. Hartl, V. Adam, R. Kizek, Trace elemental analysis by laser-induced breakdown spectroscopy—biological applications, Surf. Sci. Rep. 67 (2012) 233–243.

[103] D. Santos, L.C. Nunes, G.G.A. De Carvalho, M.d.S. Gomes, P.F. De Souza,

F.d.O. Leme, L.G.C. Dos Santos, F.J. Krug, Laser-induced breakdown spectroscopy for analysis of plant materials: a review, Spectrochim. Acta, Part B 71 (2012) 3–13.

[104] G.S. Senesi, J. Cabral, C.R. Menegatti, B. Marangoni, G. Nicolodelli, Recent advances and future trends in LIBS applications to agricultural materials and their food derivatives: an overview of developments in the last decade (2010–2019). Part II. Crop plants and their food derivatives, TrAC Trends Anal. Chem. (Reference Ed.) 118 (2019) 453–469.

[105] B. Sezer, G. Bilge, I.H. Boyaci, Capabilities and limitations of LIBS in food analysis, TrAC Trends Anal. Chem. (Reference Ed.) 97 (2017) 345–353.

[106] R. Gaudiuso, N. Melikechi, Z.A. Abdel-Salam, M.A. Harith, V. Palleschi, V. Motto-Ros, B. Busser, Laser-induced breakdown spectroscopy for human and animal health: a review, Spectrochim. Acta Part B At. Spectrosc. 152 (2019) 123–148.

[107] P. Pořízka, P. Prochazková, D. Prochazka, L. Sládková, J. Novotný, M. Petrilak, M. Brada, O. Samek, Z. Pilát, P. Zemánek, Algal biomass analysis by laser-based analytical techniques—a review, Sensors 14 (2014) 17725–17752.

[108] S.J. Rehse, A review of the use of laser-induced breakdown spectroscopy for bacterial classification, quantification, and identification, Spectrochim. Acta Part B At. Spectrosc. 154 (2019) 50–69.

[109] M. Martinez, M. Baudelet, Calibration strategies for elemental analysis of biological samples by LA-ICP-MS and LIBS—A review, Anal. Bioanal. Chem. (2020) 1–10.

[110] S.C. Jantzi, V. Motto-Ros, F. Trichard, Y. Markushin, N. Melikechi, A. De Giacomo, Sample treatment and preparation for laser-induced breakdown spectroscopy, Spectrochim. Acta Part B At. Spectrosc. 115 (2016) 52–63.

[111] G.G.A. de Carvalho, M.B.B. Guerra, A. Adame, C.S. Nomura, P.V. Oliveira, H.W.P. de Carvalho, D. Santos, L.C. Nunes, F.J. Krug, Recent advances in LIBS and XRF for the analysis of plants, J. Anal. At. Spectrom. 33 (2018) 919–944.

[112] M. Bonta, S. Török, B. Hegedus, B. Döme, A. Limbeck, A comparison of sample preparation strategies for biological tissues and subsequent trace element analysis using LA-ICP-MS, Anal. Bioanal. Chem. 409 (2017) 1805–1814.

[113] M. Bonta, J.J. Gonzalez, C. Derrick Quarles, R.E. Russo, B. Hegedus, A. Limbeck, Elemental mapping of biological samples by the combined use of LIBS and LA-ICP-MS, J. Anal. At. Spectrom. 31 (2016) 252–258, https://doi.org/10.1039/C5JA00287G.

[114] L. Sancey, V. Motto-Ros, B. Busser, S. Kotb, J.M. Benoit, A. Piednoir, F. Lux, O. Tillement, G. Panczer, J. Yu, Laser spectrometry for multi-elemental imaging of biological tissues, Sci. Rep. 4 (2014) 6065.

[115] M. Martinez, C. Bayne, D. Aiello, M. Julian, R. Gaume, M. Baudelet, Multi-elemental matrix-matched calcium hydroxyapatite reference materials for laser ablation: evaluation on teeth by laser-induced breakdown spectroscopy, Spectrochim. Acta Part B At. Spectrosc. 159 (2019), 105650.

[116] V.K. Singh, A.K. Rai, P.K. Rai, P.K. Jindal, Cross-sectional study of kidney stones by laser-induced breakdown spectroscopy, Laser Med. Sci. 24 (2009) 749–759.

[117] E. Grifoni, S. Legnaioli, G. Lorenzetti, S. Pagnotta, F. Poggialini, V. Palleschi, From Calibration-Free to Fundamental Parameters Analysis: a comparison of three recently proposed approaches, Spectrochim. Acta Part B At. Spectrosc. 124 (2016) 40–46.

[118] P. Modlitbová, P. Pořízka, S. Střítežská, Š. Zezulka, M. Kummerová, K. Novotný, J. Kaiser, Detail investigation of toxicity, bioaccumulation, and translocation of Cd-based quantum dots and Cd salt in white mustard, Chemosphere 251 (2020), 126174.

[119] P.D. Ilhardt, J.R. Nuñez, E.H. Denis, J.J. Rosnow, E.J. Krogstad, R.S. Renslow, J.J. Moran, High-resolution elemental mapping of the root-rhizosphere-soil continuum using laser-induced breakdown spectroscopy (LIBS), Soil Biol. Biochem. 131 (2019) 119–132, https://doi.org/10.1016/j.soilbio.2018.12.029.

[120] P. Modlitbová, K. Novotný, P. Pořízka, J. Klus, P. Lubal, H. Zlámalová-Gargošová, J. Kaiser, Comparative investigation of toxicity and bioaccumulation of Cd-based quantum dots and Cd salt in freshwater plant Lemna minor L, Ecotoxicol. Environ. Saf. 147 (2018) 334–341.

[121] V.K. Singh, D.K. Tripathi, X. Mao, R.E. Russo, V. Zorba, Elemental mapping of lithium diffusion in doped plant leaves using laser-induced breakdown spectroscopy (LIBS), Appl. Spectrosc. 73 (2019) 387–394.

[122] Z. Xiande, C. Zhao, D. Xiaofan, D. Daming, Detecting and mapping harmful chemicals in fruit and vegetables using nanoparticle-enhanced laser-induced breakdown spectroscopy, Sci. Rep. Nat. Publ. Group. 9 (2019).

[123] C. Zhao, D. Dong, X. Du, W. Zheng, In-field, in situ, and in vivo 3-dimensional elemental mapping for plant tissue and soil analysis using laser-induced breakdown spectroscopy, Sensors 16 (2016) 1764.

[124] P. Modlitbová, A. Hlaváček, T. Švestková, P. Pořízka, L. Šimoníková, K. Novotný, J. Kaiser, The effects of photon-upconversion nanoparticles on the growth of radish and duckweed: bioaccumulation, imaging, and spectroscopic studies, Chemosphere 225 (2019) 723–734.

[125] J. Peng, Y. He, Z. Zhao, J. Jiang, F. Zhou, F. Liu, T. Shen, Fast visualization of distribution of chromium in rice leaves by re-heating dual-pulse laser-induced breakdown spectroscopy and chemometric methods, Environ. Pollut. 252 (2019) 1125–1132.

[126] J. Peng, Y. Sun, Q. Liu, Y. Yang, J. Zhou, W. Feng, X. Zhang, F. Li, Upconversion nanoparticles dramatically promote plant growth without toxicity, Nano Res 5 (2012) 770–782.

[127] Y. Gimenez, B. Busser, F. Trichard, A. Kulesza, J.M. Laurent, V. Zaun, F. Lux, J.M. Benoit, G. Panczer, P. Dugourd, O. Tillement, F. Pelascini, L. Sancey, V. Motto-Ros, 3D imaging of nanoparticle distribution in biological tissue by laser-induced breakdown spectroscopy, Sci. Rep. 6 (2016) 29936, https://doi.org/10.1038/srep29936.

[128] V. Motto-Ros, L. Sancey, Q.L. Ma, F. Lux, X.S. Bai, X.C. Wang, J. Yu, G. Panczer, O. Tillement, Mapping of native inorganic elements and injected nanoparticles in a biological organ with laser-induced plasma, Appl. Phys. Lett. 101 (2012), 223702.

[129] V. Motto-Ros, L. Sancey, X.C. Wang, Q.L. Ma, F. Lux, X.S. Bai, G. Panczer, O. Tillement, J. Yu, Mapping nanoparticles injected into a biological tissue using laser-induced breakdown spectroscopy, Spectrochim. Acta Part B At. Spectrosc. 87 (2013) 168–174.

[130] L. Sancey, S. Kotb, C. Truillet, F. Appaix, A. Marais, E. Thomas, Long-term in vivo clearance of gadolinium-based AGuIX (Activation and Guiding of Irradiation by X-Ray) nanoparticles and their biocompatibility after systemic injection, ACS Nano 9 (2015) 2477–2488.

[131] A. Moussaron, S. Vibhute, A. Bianchi, S. Gündüz, S. Kotb, L. Sancey, V. Motto-Ros, S. Rizzitelli, Y. Crémillieux, F. Lux, Ultrasmall nanoplatforms as calcium-responsive contrast agents for magnetic resonance imaging, Small 11 (2015) 4900–4909.

[132] S. Kunjachan, A. Detappe, R. Kumar, T. Ireland, L. Cameron, D.E. Biancur, V. Motto-Ros, L. Sancey, S. Sridhar, G.M. Makrigiorgos, Nanoparticle mediated tumor vascular disruption: a novel strategy in radiation therapy, Nano Lett. 15 (2015) 7488–7496.

[133] A. Detappe, S. Kunjachan, L. Sancey, V. Motto-Ros, D. Biancur, P. Drane, R. Guieze, G.M. Makrigiorgos, O. Tillement, R. Langer, Advanced multimodal nanoparticles delay tumor progression with clinical radiation therapy, J. Contr. Release 238 (2016) 103–113.

[134] S. Moncayo, F. Trichard, B. Busser, M. Sabatier-Vincent, F. Pelascini, N. Pinel, I. Templier, J. Charles, L. Sancey, V. Motto-Ros, Multi-elemental imaging of paraffin-embedded human samples by laser-induced breakdown spectroscopy, Spectrochim. Acta Part B At. Spectrosc. 133 (2017) 40–44.

[135] A. Vogel, V. Venugopalan, Mechanisms of pulsed laser ablation of biological tissues, Chem. Rev. 103 (2003) 577–644.

[136] V.K. Singh, Y. Kumar, J. Sharma, Importance of laser-induced breakdown spectroscopy for hard tissues (bone, teeth) and other calcified tissue materials, Laser Med. Sci. 30 (2015) 1763–1778, https://doi.org/10.1007/s10103-014-1549-9.

[137] M. Galiová, J. Kaiser, F.J. Fortes, K. Novotný, R. Malina, L. Prokeš, A. Hrdlička, T. Vaculovič, M.N. Fišáková, J. Svoboda, V. Kanický, J.J. Laserna, Multi-elemental analysis of prehistoric animal teeth by laser-induced breakdown spectroscopy and laser ablation inductively coupled plasma mass spectrometry, Appl. Optic. 49 (2010) C191–C199, https://doi.org/10.1364/AO.49.00C191.

[138] M. Galiová, J. Kaiser, K. Novotný, M. Ivanov, M. Nývltová Fišáková, L. Mancini, G. Tromba, T. Vaculovič, M. Liška, V. Kanický, Investigation of the osteitis deformans phases in snake vertebrae by double-pulse laser-induced breakdown spectroscopy, Anal. Bioanal. Chem. 398 (2010) 1095–1107, https://doi.org/10.1007/s00216-010-3976-1.

[139] Y. Markushin, N. Melikechi, Sensitive Detection of Epithelial Ovarian Cancer Biomarkers Using Tag-Laser Induced Breakdown Spectroscopy, Ovarian Cancer—Basic Sci. Perspect. Intech., 2012, pp. 153–170.

[140] N. Melikechi, Y. Markushin, Mono-and Multi-Element Coded Libs Assays and Methods, Google Patents, 2011.

[141] J.P. Robinson, B.P. Rajwa, V.P. Patsekin, E. Bae, Metal-antibody Tagging and Plasma-Based Detection, Google Patents, 2019.

[142] Z. Farka, T. Jurik, D. Kovář, L. Trnková, P. Skládal, Nanoparticle-based immunochemical biosensors and assays: recent advances and challenges, Chem. Rev. 117 (2017) 9973–10042.

[143] M. Konecna, K. Novotny, S. Krizkova, I. Blazkova, P. Kopel, J. Kaiser, P. Hodek, R. Kizek, V. Adam, Identification of quantum dots labeled metallothionein by fast scanning laser-induced breakdown spectroscopy, Spectrochim. Acta Part B At. Spectrosc. 101 (2014) 220–225.

[144] P. Modlitbová, Z. Farka, M. Pastucha, P. Pořízka, K. Novotný, P. Skládal, J. Kaiser, Laser-induced breakdown spectroscopy as a novel readout method for nanoparticle-based immunoassays, Microchim. Acta. 186 (2019) 629.

[145] C. Gondhalekar, E. Biela, B. Rajwa, E. Bae, V. Patsekin, J. Sturgis, C. Reynolds, I.-J. Doh, P. Diwakar, L. Stanker, Detection of E. coli labeled with metal-conjugated antibodies using lateral-flow assay and laser-induced breakdown spectroscopy, Anal. Bioanal. Chem. 412 (2020) 1291–1301.

[146] K. Rifai, F. Doucet, L. Özcan, F. Vidal, LIBS core imaging at kHz speed: Paving the way for real-time geochemical applications, Spectrochim. Acta Part B At. Spectrosc. 150 (2018) 43–48, https://doi.org/10.1016/j.sab.2018.10.007.

[147] J.O. Cáceres, F. Pelascini, V. Motto-Ros, S. Moncayo, F. Trichard, G. Panczer, A. Marín-Roldán, J.A. Cruz, I. Coronado, J. Martín-Chivelet, Megapixel multi-elemental imaging by Laser-Induced Breakdown Spectroscopy, a technology with considerable potential for paleoclimate studies, Sci. Rep. 7 (2017) 5080, https://doi.org/10.1038/s41598-017-05437-3.

[148] Q.L. Ma, V. Motto-Ros, W.Q. Lei, M. Boueri, L.J. Zheng, H.P. Zeng, M. Bar-Matthews, A. Ayalon, G. Panczer, J. Yu, Multi-elemental mapping of a speleothem using laser-induced breakdown spectroscopy, Spectrochim. Acta Part B At. Spectrosc. 65 (2010) 707–714, https://doi.org/10.1016/j.sab.2010.03.004.

[149] N. Hausmann, P. Siozos, A. Lemonis, A.C. Colonese, H.K. Robson, D. Anglos, Elemental mapping of Mg/Ca intensity ratios in marine mollusc shells using laser-induced breakdown spectroscopy, J. Anal. At. Spectrom. 32 (2017) 1467–1472, https://doi.org/10.1039/C7JA00131B.

[150] C. Fabre, D. Devismes, S. Moncayo, F. Pelascini, F. Trichard, A. Lecomte, B. Bousquet, J. Cauzid, V. Motto-Ros, Elemental imaging by laser-induced breakdown spectroscopy for the geological characterization of minerals, J. Anal. At. Spectrom. 33 (2018) 1345—1353, https://doi.org/10.1039/C8JA00048D.

[151] M. Gaft, Y. Raichlin, F. Pelascini, G. Panzer, V. Motto Ros, Imaging rare-earth elements in minerals by laser-induced plasma spectroscopy: molecular emission and plasma-induced luminescence, Spectrochim. Acta Part B At. Spectrosc. 151 (2019) 12—19, https://doi.org/10.1016/j.sab.2018.11.003.

[152] F. Trichard, S. Moncayo, D. Devismes, F. Pelascini, J. Maurelli, A. Feugier, C. Sasseville, F. Surma, V. Motto-Ros, Evaluation of a compact VUV spectrometer for elemental imaging by laser-induced breakdown spectroscopy: application to mine core characterization, J. Anal. At. Spectrom. 32 (2017) 1527—1534, https://doi.org/10.1039/C7JA00185A.

[153] C. Derrick Quarles, J.J. Gonzalez, L.J. East, J.H. Yoo, M. Morey, R.E. Russo, Fluorine analysis using laser induced breakdown spectroscopy (LIBS), J. Anal. At. Spectrom. 29 (2014) 1238—1242, https://doi.org/10.1039/C4JA00061G.

[154] J.R. Chirinos, D.D. Oropeza, J.J. Gonzalez, H. Hou, M. Morey, V. Zorba, R.E. Russo, Simultaneous 3-dimensional elemental imaging with LIBS and LA-ICP-MS, J. Anal. At. Spectrom. 29 (2014) 1292—1298, https://doi.org/10.1039/C4JA00066H.

[155] T. Xu, J. Liu, Q. Shi, Y. He, G. Niu, Y. Duan, Multi-elemental surface mapping and analysis of carbonaceous shale by laser-induced breakdown spectroscopy, Spectrochim. Acta Part B At. Spectrosc. 115 (2016) 31—39, https://doi.org/10.1016/j.sab.2015.10.008.

[156] J. Jain, C.D. Quarles, J. Moore, D.A. Hartzler, D. McIntyre, D. Crandall, Elemental mapping and geochemical characterization of gas producing shales by laser induced breakdown spectroscopy, Spectrochim. Acta Part B At. Spectrosc. 150 (2018) 1—8, https://doi.org/10.1016/j.sab.2018.09.010.

[157] J.A. Meima, D. Rammlmair, Investigation of compositional variations in chromitite ore with imaging laser induced breakdown spectroscopy and spectral angle mapper classification algorithm, Chem. Geol. 532 (2020) 119376, https://doi.org/10.1016/j.chemgeo.2019.119376.

[158] K. Rifai, L.-Ç. Özcan, F.R. Doucet, K. Rhoderick, F. Vidal, Ultrafast elemental mapping of platinum group elements and mineral identification in platinum-palladium ore using laser induced breakdown spectroscopy, Minerals 10 (2020) 207, https://doi.org/10.3390/min10030207.

[159] J. El Haddad, E.S. de Lima Filho, F. Vanier, A. Harhira, C. Padioleau, M. Sabsabi, G. Wilkie, A. Blouin, Multiphase mineral identification and quantification by laser-induced breakdown spectroscopy, Miner. Eng. 134 (2019) 281—290, https://doi.org/10.1016/j.mineng.2019.02.025.

[160] EU publications, Raw materials scoreboard 2018. https://op.europa.eu/en/publication-detail/-/publication/117c8d9b-e3d3-11e8-b690-01aa75ed71a1, 2018. (Accessed 29 June 2020).

[161] K. Jancsek, P. Janovszky, Gábor Galbács, M.-T. Tivadar, Quantitative determination of lithium in granite rock-forming minerals by laser-induced breakdown spectroscopy (LIBS), in: Book Abstr. Brno, 2019, p. 211. http://libs.ceitec.cz/files/281/213.pdf.

[162] M. Corsi, G. Cristoforetti, V. Palleschi, V. Salvetti, E. Tognoni, Surface compositional mapping of pigments on a roman fresco by CF-LIBS, in: Proc. First Int. Conf. Laser-Induc. Breakdown Appl, 2000, p. 74. Tirrenia, Italy.

[163] R. Grönlund, M. Lundqvist, S. Svanberg, Remote imaging laser-induced breakdown spectroscopy and remote cultural heritage ablative cleaning, Opt. Lett. 30 (2005) 2882—2884, https://doi.org/10.1364/OL.30.002882.

[164] R. Grönlund, M. Lundqvist, S. Svanberg, Remote imaging laser-induced breakdown spectroscopy and laser-induced fluorescence spectroscopy using nanosecond pulses from a mobile lidar system, Appl. Spectrosc. 60 (2006) 853—859, https://doi.org/10.1366/000370206778062138.

[165] F.J. Fortes, J. Cuñat, L.M. Cabalín, J.J. Laserna, In situ analytical assessment and chemical imaging of historical buildings using a man-portable laser system, Appl. Spectrosc. 61 (2007) 558—564, https://doi.org/10.1366/000370207780807722.

[166] L. Bassel, V. Motto-Ros, F. Trichard, F. Pelascini, F. Ammari, R. Chapoulie, C. Ferrier, D. Lacanette, B. Bousquet, Laser-induced breakdown spectroscopy for elemental characterization of calcitic alterations on cave walls, Environ. Sci. Pollut. Res. 24 (2017) 2197—2204, https://doi.org/10.1007/s11356-016-7468-5.

[167] O. Syta, B. Wagner, E. Bulska, D. Zielińska, G.Z. Żukowska, J. Gonzalez, R. Russo, Elemental imaging of heterogeneous inorganic archaeological samples by means of simultaneous laser induced breakdown spectroscopy and laser ablation inductively coupled plasma mass spectrometry measurements, Talanta 179 (2018) 784—791, https://doi.org/10.1016/j.talanta.2017.12.011.

[168] G.S. Senesi, B. Campanella, E. Grifoni, S. Legnaioli, G. Lorenzetti, S. Pagnotta, F. Poggialini, V. Palleschi, O. De Pascale, Elemental and mineralogical imaging of a weathered limestone rock by double-pulse micro-Laser-Induced Breakdown Spectroscopy, Spectrochim. Acta Part B At. Spectrosc. 143 (2018) 91—97, https://doi.org/10.1016/j.sab.2018.02.018.

[169] M. Hoehse, A. Paul, I. Gornushkin, U. Panne, Multivariate classification of pigments and inks using combined Raman spectroscopy and LIBS, Anal. Bioanal. Chem. 402 (2012) 1443—1450, https://doi.org/10.1007/s00216-011-5287-6.

[170] A. Giakoumaki, K. Melessanaki, D. Anglos, Laser-induced breakdown spectroscopy (LIBS) in archaeological science—applications and prospects, Anal. Bioanal. Chem. 387 (2007) 749—760, https://doi.org/10.1007/s00216-006-0908-1.

[171] H. Bette, R. Noll, G. Müller, H.-W. Jansen, Ç. Nazikkol, H. Mittelstädt, High-speed scanning laser-induced breakdown spectroscopy at 1000 Hz with single pulse evaluation for the detection of inclusions in steel, J. Laser Appl. 17 (2005) 183—190, https://doi.org/10.2351/1.1961738.

[172] R.R.V. Carvalho, J.A.O. Coelho, J.M. Santos, F.W.B. Aquino, R.L. Carneiro, E.R. Pereira-Filho, Laser-induced breakdown spectroscopy (LIBS) combined with hyperspectral imaging for the evaluation of printed circuit board composition, Talanta 134 (2015) 278—283, https://doi.org/10.1016/j.talanta.2014.11.019.

[173] C.M. Ahamer, K.M. Riepl, N. Huber, J.D. Pedarnig, Femtosecond laser-induced breakdown spectroscopy: elemental imaging of thin films with high spatial resolution, Spectrochim. Acta Part B At. Spectrosc. 136 (2017) 56—65, https://doi.org/10.1016/j.sab.2017.08.005.

[174] V.N. Lednev, P.A. Sdvizhenskii, M.Y. Grishin, V.V. Cheverikin, A.Y. Stavertiy, R.S. Tretyakov, M.V. Taksanc, S.M. Pershin, Laser-induced breakdown spectroscopy for three-dimensional elemental mapping of composite materials synthesized by additive technologies, Appl. Optic. 56 (2017) 9698—9705, https://doi.org/10.1364/AO.56.009698.

[175] P. Lucena, J.M. Vadillo, J.J. Laserna, Mapping of platinum group metals in automotive exhaust three-way catalysts using laser-induced breakdown spectrometry, Anal. Chem. 71 (1999) 4385—4391, https://doi.org/10.1021/ac9902998.

[176] F. Trichard, L. Sorbier, S. Moncayo, Y. Blouët, C.-P. Lienemann, V. Motto-Ros, Quantitative elemental imaging of heterogeneous catalysts using laser-induced breakdown spectroscopy, Spectrochim. Acta Part B At. Spectrosc. 133 (2017) 45—51, https://doi.org/10.1016/j.sab.2017.04.008.

[177] F. Trichard, F. Gaulier, J. Barbier, D. Espinat, B. Guichard, C.-P. Lienemann, L. Sorbier, P. Levitz, V. Motto-Ros, Imaging of alumina supports by laser-induced breakdown spectroscopy: a new tool to understand the diffusion of trace metal impurities, J. Catal. 363 (2018) 183—190, https://doi.org/10.1016/j.jcat.2018.04.013.

[178] H. Hou, L. Cheng, T. Richardson, G. Chen, M. Doeff, R. Zheng, R. Russo, V. Zorba, Three-dimensional elemental imaging of Li-ion solid-state electrolytes using fs-laser induced breakdown spectroscopy (LIBS), J. Anal. At. Spectrom. 30 (2015) 2295—2302, https://doi.org/10.1039/C5JA00250H.

[179] D. Rettenwander, R. Wagner, A. Reyer, M. Bonta, L. Cheng, M.M. Doeff, A. Limbeck, M. Wilkening, G. Amthauer, Interface instability of Fe-stabilized Li7La3Zr2O12 versus Li metal, J. Phys. Chem. C Nanomater. Interfaces. 122 (2018) 3780—3785, https://doi.org/10.1021/acs.jpcc.7b12387.

[180] S. Imashuku, H. Taguchi, T. Kawamata, S. Fujieda, S. Kashiwakura, S. Suzuki, K. Wagatsuma, Quantitative lithium mapping of lithium-ion battery cathode using laser-induced breakdown spectroscopy, J. Power Sources 399 (2018) 186—191, https://doi.org/10.1016/j.jpowsour.2018.07.088.

[181] C. Gottlieb, S. Millar, S. Grothe, G. Wilsch, 2D evaluation of spectral LIBS data derived from heterogeneous materials using cluster algorithm, Spectrochim. Acta Part B At. Spectrosc. 134 (2017) 58—68, https://doi.org/10.1016/j.sab.2017.06.005.

[182] C. Li, X. Wu, C. Zhang, H. Ding, J. Hu, G.-N. Luo, In situ chemical imaging of lithiated tungsten using laser-induced breakdown spectroscopy, J. Nucl. Mater. 452 (2014) 10—15, https://doi.org/10.1016/j.jnucmat.2014.04.041.

[183] R. Hai, C. Li, H. Wang, H. Ding, H. Zhuo, J. Wu, G.-N. Luo, Characterization of Li deposition on the first wall of EAST using laser-induced breakdown spectroscopy, J. Nucl. Mater. 438 (2013) S1168—S1171, https://doi.org/10.1016/j.jnucmat.2013.01.258.

[184] X. Wang, V. Motto-Ros, G. Panczer, D. De Ligny, J. Yu, J.M. Benoit, J.L. Dussossoy, S. Peuget, Mapping of rare earth elements in nuclear waste glass—ceramic using micro laser-induced breakdown spectroscopy, Spectrochim. Acta Part B At. Spectrosc. 87 (2013) 139—146, https://doi.org/10.1016/j.sab.2013.05.022.

[185] M. López-López, C. Alvarez-Llamas, J. Pisonero, C. García-Ruiz, N. Bordel, An exploratory study of the potential of LIBS for visualizing gunshot residue patterns, Forensic Sci. Int. 273 (2017) 124—131, https://doi.org/10.1016/j.forsciint.2017.02.012.

[186] L. Zou, B. Kassim, J.P. Smith, J.D. Ormes, Y. Liu, Q. Tu, X. Bu, In situ analytical characterization and chemical imaging of tablet coatings using laser induced breakdown spectroscopy (LIBS), Analyst 143 (2018) 5000—5007, https://doi.org/10.1039/C8AN01262H.

[187] J.P. Smith, L. Zou, Y. Liu, X. Bu, Investigation of minor elemental species within tablets using in situ depth profiling via laser-induced breakdown spectroscopy hyperspectral imaging, Spectrochim. Acta Part B At. Spectrosc. 165 (2020), 105769, https://doi.org/10.1016/j.sab.2020.105769.

[188] S.-H. Lee, J.-H. Choi, J.-H. In, S. Jeong, Fast compositional mapping of solar cell by laser spectroscopy technique for process monitoring, Int. J. Precis. Eng. Manuf.-Green Technol. 6 (2019) 189—196, https://doi.org/10.1007/s40684-019-00083-8.

[189] P. Veber, K. Bartosiewicz, J. Debray, G. Alombert-Goget, O. Benamara, V. Motto-Ros, M.P. Thi, A. Borta-Boyon, H. Cabane, K. Lebbou, F. Levassort, K. Kamada, A. Yoshikawa, M. Maglione, Lead-free piezoelectric crystals grown by the micro-pulling down technique in the BaTiO3—CaTiO3—BaZrO3 system, CrystEngComm 21 (2019) 3844—3853, https://doi.org/10.1039/C9CE00405J.

[190] D. Prochazka, P. Pořízka, J. Novotný, A. Hrdlička, K. Novotný, P. Šperka, J. Kaiser, Triple-pulse LIBS: laser-induced breakdown spectroscopy signal enhancement by combination of pre-ablation and re-heating laser pulses,

J. Anal. At. Spectrom. 35 (2020) 293–300, https://doi.org/10.1039/C9JA00323A.

[191] D.V. S, S.D. George, V.B. Kartha, S. Chidangil, U.V. K, Hybrid LIBS-Raman-LIF systems for multi-modal spectroscopic applications: a topical review, Appl. Spectrosc. Rev. (2020) 1–29, https://doi.org/10.1080/05704928.2020.1800486, 0.

[192] K.M.M. Shameem, K.S. Choudhari, A. Bankapur, S.D. Kulkarni, V.K. Unnikrishnan, S.D. George, V.B. Kartha, C. Santhosh, A hybrid LIBS–Raman system combined with chemometrics: an efficient tool for plastic identification and sorting, Anal. Bioanal. Chem. 409 (2017) 3299–3308, https://doi.org/10.1007/s00216-017-0268-z.

[193] M. Hoehse, A. Paul, I. Gornushkin, U. Panne, Multivariate classification of pigments and inks using combined Raman spectroscopy and LIBS, Anal. Bioanal. Chem. 402 (2012) 1443–1450, https://doi.org/10.1007/s00216-011-5287-6.

Pavlína Modlitbová is a postdoc in Laser spectroscopy laboratory at CEITEC BUT, who achieved her PhD degree in 2016 at Faculty of Chemistry BUT in the field of terrestrial nanoecotoxicology. As a PhD student she was a trainee at the Zoology department at University of Ljubljana for eight months. Since then, she personally focus on using laser spectroscopy in the analysis of biological samples especially in the detection of various trace elements, new xenobiotics as nanoparticles (Cd-based, gold, and photon upconversion NPs) or microplastics in plants. Her main research interest is in various bio-applications of LIBS.

Andreas Limbeck is an expert in the field of atomic spectroscopy with more than 15 years' experience in the development of advanced analytical procedures for the reliable determination of inorganic components in a wide range of technological, environmental as well as biological samples. In the last years, he developed advanced expertise in the application of the laser-based techniques LA-ICP-MS and LIBS for the spatially resolved chemical analysis of solid materials, in particular for the quantitative determination of elemental distributions in various materials. Since 2015 he is associate professor at the Faculty of Technical Chemistry at TU Wien.

Jozef Kaiser received his Ph.D. at the Faculty of Mechanical Engineering, Brno University of Technology (BUT) in 2001 and was promoted to a full professor in 2013. He has an extensive experience in laser spectroscopy and computed tomography when dealing more than 20 years with the state-of-the-art and cooperating with world-renowned laboratories, such as Synchrotron Elettra Trieste, IT, Oak Ridge National Laboratory in Oak Ridge, US-TN and the University of Tokushima in Tokushima, JP. In 2013, he established and leads a research group Materials Characterization and Advanced Coatings at CEITEC BUT. Since then, he founded four technological start-ups.

Lukas Brunnbauer, MSc received his BSc and MSc in Technical Chemistry from the TU Wien. Currently he is doing his PhD at TU Wien in the research group "Surface Analytics, Trace Analytics and Chemometry" headed by Assoc. Prof. Dr. Andreas Limbeck in cooperation with Infineon Austria AG. His research is mainly focused on polymer analysis using a tandem LA-ICP-MS/LIBS setup.

Patrick Janovszky received his B.Sc. and later M.Sc. degrees in Chemistry from the University of Szeged, Hungary. He is currently working on his PhD thesis at the same university under the supervision of Prof. G. Galbács on LIBS and LA-ICP-MS method development for the multielemental analysis of environmental samples. His professional experience includes the trace elemental and isotope ratio analysis of biological, geological and plant samples by various spectroscopy techniques.

Hans Lohninger is working at the Institute of Chemical Technologies and Analytics at Technische Universität Wien. He holds an MSc from the University of Vienna and a PhD from the TU Wien. His interests currently focus on hyperspectral imaging (HSI) and the combination of chemometrics with HSI. He has developed many applications of HSI in a wide range of fields, covering spectroscopic techniques such as MS, SIMS, infrared, Raman, UVVIS, LIBS, EDX and THz. Besides his academic obligations he is running a small software development company which provides both custom-specific solutions to chemometric problems and general-purpose software for hyperspectral imaging.

Albert Kéri received his B.Sc. in Environmental Engineering (2014) and his M.Sc. in Chemistry (2016) from the University of Szeged, Hungary. The topic of his PhD thesis — that he defended in 2020 at the University of Szeged — was ICP-MS based analytical method development for the investigation of multi-component nanoparticles. He participated in several national and European founded research and R + D projects where he developed ICP-MS and LIBS based analytical methods. Currently he is a postdoctoral researcher at the Inorganic and Analytical Chemistry Department at University of Szeged.

Pavel Porizka studied physics and nanotechnology at the Brno University of Technology (BUT) in Brno, Czech Republic where he received a Ph.D. degree in 2014. Considering scientific internships, he joined Federal Institute for Materials Research and Testing in Berlin, DE and later he was a Fulbright postdoc fellow at the University of Florida in Gainesville, US-FL. Currently, he is a postdoc and the leader of Laser spectroscopy laboratory at CEITEC BUT and an associate professor at the Faculty of Mechanical Engineering BUT. His main research interest ranges from machine learning through industrial to bio-applications of laser spectroscopic techniques.

Gábor Galbács is holding MSc diplomas in chemistry and physics, as well as in environmental sciences (University of Szeged, Hungary). He obtained a PhD/CSc degree from the same university in 1998 and a DSc title from the Hungarian Academy of Sciences in 2013, both in the field of analytical chemistry. His research is diverse, but focuses on fundamental studies and instrumentation/method development for laser and plasma analytical spectroscopy, mostly LIBS, ICP-MS and ICP-AES. He is a full professor and the head of the Department of Inorganic and Analytical Chemistry at the University of Szeged since 2014.

4.4 Article 4

The fourth publication is entitled "Combined LA-ICP-MS/LIBS: powerful analytical tools for the investigation of polymer alteration after treatment under corrosive conditions". As LIBS provides polymer specific signals which can be used to differentiate between different polymer types, in this article the possibility of using LIBS signals to assess polymer degradation is evaluated. When it comes to polymer degradation often not only the alteration of the polymer itself is of interest but also the uptake of inorganic species. To provide adequate sensitivity to analyze the uptake of inorganic species, a combined LA-ICP-MS/LIBS system was employed enabling the detection of polymer specific signals using LIBS and using LA-ICP-MS for the measurement of inorganic species. Three different polymeric sample types were investigated within this work: high-performance polyimides (PI) used in the semiconductor industry, mixtures of inorganic pigments and polymeric binders from the field of cultural heritage science and polystyrene (PS) often used for characterizations in the field of microplastics. In a first step, pigment/binder combinations were exposed to UV-radiation for different amounts of time (1-6 weeks) causing degradation of the sample. Time-dependant degradation of the sample surface was confirmed using FTIR-spectroscopy. In a next step the sample surface was analyzed using LIBS and polymer specific emission signals were evaluated. As the signal intensity of the C_2-swan band at 515 nm correlated with the signal changes of the FTIR-measurements during the ageing of the samples, it was confirmed that LIBS can be used to assess polymer degradation. With LIBS not only allowing analysis of the sample surface, but also enabling depth profiling, the degradation of the samples can also be investigated related to the sample depth. Samples were also exposed to corrosive conditions (O_3 and SO_2) in a weathering chamber. Depth profiling measurements of these samples confirmed the degradation not only on the sample surface but until a depth of approximately 15 µm. High-performance PIs from the semiconductor industry were also exposed to various corrosive conditions such as SO_2 and H_2S for 192 h in a weathering chamber. In this case, LA-ICP-MS was used to evaluate the uptake of different sulfur species. Again, uptake of sulfur was not only confirmed on the sample surface but sulfur was detected until a depth of 6 µm. Additionally, a substantial difference between the uptake of SO_2 and H_2S was observed. The third investigated sample was a PS-film which was exposed to a combination of UV-radiation and HNO_3 with a subsequent exposure to cadmium in artificial seawater. Using a tandem LA-ICP-MS/LIBS system, a simultaneous analysis of the oxidation of the PS film using LIBS and the cadmium uptake using LA-ICP-MS was possible. Depth profiling again revealed oxidation of the sample not only on the surface but until a depth of 10 µm and an increased uptake of cadmium on the aged sample side compared to an unaged sample.

References

1. *Plastics Europe. Plastics - the facts 2019*. https ://www.plast icseu rope.org/appli catio n/files /9715/7129/9584/FINAL web_versi on_Plast ics_the_facts 2019_14102 019.pdf (2019).
2. Akovali, G. *Polymers in Construction* (Rapra Technology Limited, Column House, 2005).
3. Hayakawa, A., Murata, Y., Nakanishi, Y. & Tohriiwa, N. Epoxy resin composition for semiconductor encapsulation. (1998).
4. Kinjo, N., Ogata, M., Nishi, K., Kaneda, A. & Dušek, K. Epoxy Molding Compounds as Encapsulation Materials for Microelectronic Devices. in *Speciality Polymers/Polymer Physics* (eds. Godovsky, Yu. K. et al.) 1–48 (Springer Berlin Heidelberg, 1989).
5. Institute, G. C. *Modern Paints Uncovered: Proceedings from the Modern Paints Uncovered Symposium* (Getty Publications, Los Angeles, 2007).
6. Lodge, R. G. A history of synthetic painting media with special reference to commercial materials. *Preprints of Papers Presented at the Sixteenth Annual Meeting of the AIC. New Orleans,* 118–127 (1988).
7. Göpferich, A. Mechanisms of polymer degradation and erosion. *Biomaterials* **17**, 103–114 (1996).
8. Grassie, N. & Scott, G. *Polymer Degradation and Stabilisation* (CUP Archive, Cambridge, 1988).
9. Hamid, S. H. *Handbook of Polymer Degradation* (CRC Press, Boca Raton, 2000).
10. Jacobsen, J. B., Krog, J. P., Rimestad, L., Riis, A. & Holm, A. H. Climate-protective packaging: using basic physics to solve climatic challenges for electronics in demanding applications. *IEEE Ind. Electron. Mag.* **8**, 51–59 (2014).
11. Ambat, R., Jensen, S. G. & Møller, P. H. Corrosion reliability of electronic systems. *ECS Trans.* https ://doi.org/10.1149/1.29006 50 (2008).
12. Valdez Salas, B. *et al.* Copper corrosion by atmospheric pollutants in the electronics industry. *ISRN Corros.* **2013**, 1–7 (2013).
13. Minzari, D., Jellesen, M. S., Møller, P. & Ambat, R. Morphological study of silver corrosion in highly aggressive sulfur environments. *Eng. Fail. Anal.* **18**, 2126–2136 (2011).
14. Schueller, R. Creep Corrosion on lead-free printed circuit boards in high sulfur environments. in *SMTA International Conference* 643–654 (2007).
15. Mass, J. *et al.* SR-FTIR imaging of the altered cadmium sulfide yellow paints in Henri Matisse's Le Bonheur de vivre (1905–6)—examination of visually distinct degradation regions. *Analyst* **138**, 6032–6043 (2013).
16. Manfredi, M., Barberis, E. & Marengo, E. Prediction and classification of the degradation state of plastic materials used in modern and contemporary art. *Appl. Phys. A* **123**, 35 (2016).
17. Izzo, F. C., van den Berg, K. J., van Keulen, H. & Ferrari, B. Zendri E (2014) Modern oil paints—formulations, organic additives and degradation: some case studies. In *Issues in Contemporary Oil Paint* (eds van den Berg, K. J. *et al.*) 75–104 (Springer, Berlin, 2014). https ://doi.org/10.1007/978-3-319-10100 -2_5.
18. Cole, M., Lindeque, P., Halsband, C. & Galloway, T. S. Microplastics as contaminants in the marine environment: a review. *Mar. Pollut. Bull.* **62**, 2588–2597 (2011).
19. Turner, A. & Holmes, L. A. Adsorption of trace metals by microplastic pellets in fresh water. *Environ. Chem.* **12**, 600–610 (2015).
20. Holmes, L. A., Turner, A. & Thompson, R. C. Adsorption of trace metals to plastic resin pellets in the marine environment. *Environ. Pollut.* **160**, 42–48 (2012).
21. Ashton, K., Holmes, L. & Turner, A. Association of metals with plastic production pellets in the marine environment. *Mar. Pollut. Bull.* **60**, 2050–2055 (2010).
22. Wilkie, C. A. TGA/FTIR: an extremely useful technique for studying polymer degradation. *Polym. Degrad. Stab.* **66**, 301–306 (1999).
23. Trchová, M., Šeděnková, I., Tobolková, E. & Stejskal, J. FTIR spectroscopic and conductivity study of the thermal degradation of polyaniline films. *Polym. Degrad. Stab.* **86**, 179–185 (2004).
24. Bhargava, R., Wang, S.-Q. & Koenig, J. L. FTIR Microspectroscopy of PolymericSystems. In *Liquid Chromatography/FTIR Microspectroscopy/ MicrowaveAssisted Synthesis 137–191* (ed. Kausch, H.) (Springer, Berlin, 2013). https ://doi.org/10.1007/b1105 2.
25. Lenz, R., Enders, K., Stedmon, C. A., Mackenzie, D. M. A. & Nielsen, T. G. A critical assessment of visual identification of marine microplastic using Raman spectroscopy for analysis improvement. *Mar. Pollut. Bull.* **100**, 82–91 (2015).
26. Li, L. *MALDI Mass Spectrometry for Synthetic Polymer Analysis* (Wiley, Hoboken, 2009).
27. Rial-Otero, R., Galesio, M., Capelo, J.-L. & Simal-Gándara, J. A Review of synthetic polymer characterization by Pyrolysis–GC–MS. *Chromatographia* **70**, 339–348 (2009).
28. Liu, X. & Yu, W. Evaluating the thermal stability of high performance fibers by TGA. *J. Appl. Polym. Sci.* **99**, 937–944 (2006).
29. Celina, M. C. Review of polymer oxidation and its relationship with materials performance and lifetime prediction. *Polym. Degrad. Stab.* **98**, 2419–2429 (2013).
30. Pereira, J. S. F. *et al.* Evaluation of sample preparation methods for polymer digestion and trace elements determination by ICPMS and ICPOES. *J. Anal. At. Spectrom.* **26**, 1849–1857 (2011).
31. Flores, E. M. M., Muller, E. I., Duarte, F. A., Grinberg, P. & Sturgeon, R. E. Determination of Trace Elements in Fluoropolymers after Microwave-Induced Combustion. *Anal. Chem.* **85**, 374–380 (2013).
32. Resano, M., Aramendía, M., Devos, W. & Vanhaecke, F. Direct multi-element analysis of a fluorocarbon polymer via solid samplingelectrothermal
vaporization-inductively coupled plasma mass spectrometry. *J. Anal. At. Spectrom.* **21**, 891–898 (2006).
33. Börno, F., Richter, S., Deiting, D., Jakubowski, N. & Panne, U. Direct multi-element analysis of plastic materials via solid sampling electrothermal vaporization inductively coupled plasma optical emission spectroscopy. *J. Anal. At. Spectrom.* **30**, 1064–1071 (2015).
34. Villaseñor, Á, Boccongelli, M. & Luis Todolí, J. Quantitative elemental analysis of polymers through laser ablation—inductively coupled plasma by using a dried droplet calibration approach. *DDCA. J. Anal. At. Spectrom.* **33**, 1173–1183 (2018).
35. Voss, M. *et al.* A new approach to calibration and determination of selected trace elements in food contact polymers by LA-ICPMS. *Talanta* **170**, 488–495 (2017).
36. Liu, K. *et al.* A review of laser-induced breakdown spectroscopy for plastic analysis. *TrAC Trends Anal. Chem.* **110**, 327–334 (2019).
37. Banaee, M. & Tavassoli, S. H. Discrimination of polymers by laser induced breakdown spectroscopy together with the DFA method. *Polym. Test.* **31**, 759–764 (2012).
38. Unnikrishnan, K. *et al.* Analytical predictive capabilities of Laser Induced breakdown spectroscopy (LIBS) with principal component analysis (PCA) for plastic classification. *RSC Adv.* **3**, 25872–25880 (2013).
39. Bonta, M. & Limbeck, A. Metal analysis in polymers using tandem LA-ICP-MS/LIBS: eliminating matrix effects using multivariate calibration. *J. Anal. At. Spectrom.* **33**, 1631–1637 (2018).
40. Koch, J. & Günther, D. Review of the state-of-the-art of laser ablation inductively coupled plasma mass spectrometry. *Appl. Spectrosc.* **65**, 155–162 (2011).
41. Limbeck, A. *et al.* Recent advances in quantitative LA-ICP-MS analysis: challenges and solutions in the life sciences and environmental chemistry. *Anal. Bioanal. Chem.* **407**, 6593–6617 (2015).
42. Wiesinger, R., Schreiner, M. & Kleber, Ch. Investigations of the interactions of CO2, O3 and UV light with silver surfaces by in situ IRRAS/QCM and ex situ TOF-SIMS. *Appl. Surf. Sci.* **256**, 2735–2741 (2010).
43. Kester, D. R., Duedall, I. W., Connors, D. N. & Pytkowicz, R. M. Preparation of Artificial Seawater1. *Limnol. Oceanogr.* **12**, 176–179 (1967).
44. Farhadian, A. H. *et al.* A novel approach for investigation of chemical aging in composite propellants through laser-induced breakdown spectroscopy (LIBS). *J. Therm. Anal. Calorim.* **124**, 279–286 (2016).
45. Liang, D. *et al.* Degradation of polyacrylate in the outdoor agricultural soil measured by FTIR-PAS and LIBS. *Polymers* **10**, 1296

(2018).

46. Anzano, J. M., Bello-Gálvez, C. & Lasheras, R. J. Identification of Polymers by Means of LIBS. In *Laser-Induced Breakdown Spectroscopy: Theory and Applications 421–438* (eds Musazzi, S. & Perini, U.) (Springer, Berlin, 2014). https ://doi.org/10.1007/978-3-642-45085 -3_15.

47. Brunnbauer, L., Larisegger, S., Lohninger, H., Nelhiebel, M. & Limbeck, A. Spatially resolved polymer classification using laser induced breakdown spectroscopy (LIBS) and multivariate statistics. *Talanta* https ://doi.org/10.1016/j.talan ta.2019.12057 2 (2019).

48. Grégoire, S. *et al.* Laser-induced breakdown spectroscopy for polymer identification. *Anal. Bioanal. Chem.* **400**, 3331–3340 (2011).

49. López-Aparicio, S. *et al.* Measurement of organic and inorganic pollutants in microclimate frames for paintings. *E-Preserv. Sci.* **7**, 59–70 (2010).

50. Blades, N., Oreszczyn, T., Cassar, M. & Bordass, W. *Guidelines on pollution control in museum buildings* (Museums Association, London, 2000).

51. Pintus, V., Wei, S. & Schreiner, M. Accelerated UV ageing studies of acrylic, alkyd, and polyvinyl acetate paints: Influence of inorganic pigments. *Microchem. J.* **124**, 949–961 (2016).

52. Anghelone, M., Jembrih-Simbürger, D. & Schreiner, M. Influence of phthalocyanine pigments on the photo-degradation of alkyd artists' paints under different conditions of artificial solar radiation. *Polym. Degrad. Stab.* **134**, 157–168 (2016).

53. Wiesinger, R. *et al.* Pigment and binder concentrations in modern paint samples determined by ir and raman spectroscopy. *Angew. Chem. Int. Ed.* **57**, 7401–7407 (2018).

54. Panighello, S., Van Elteren, J. T., Orsega, E. F. & Moretto, L. M. Laser ablation-ICP-MS depth profiling to study ancient glass surface degradation. *Anal. Bioanal. Chem.* **407**, 3377–3391 (2015).

55. Fehrenbacher, J. S., Spero, H. J., Russell, A. D., Vetter, L. & Eggins, S. Optimizing LA-ICP-MS analytical procedures for elemental depth profiling of foraminifera shells. *Chem. Geol.* **407–408**, 2–9 (2015).

56. Lopez, G., Valdez, B. & Schorr, M. Chapter13: H2S Pollution and Its Effect on Corrosion of Electronic Components. In *Air Quality: New Perspective* (eds Badilla, G. L. *et al.*) (BOD—Books on Demand, Norderstedt, 2012).

57. SungSoon C. & ByungJin M. Corrosive tendency of Ag plated lead frame applied to white LED. in *18th IEEE International Symposium on the Physical and Failure Analysis of Integrated Circuits (IPFA)* 1–3 (2011). https ://doi.org/10.1109/IPFA.2011.59927 36.

58. Jellesen, M. S., Verdingovas, V., Conseil, H., Piotrowska, K. & Ambat, R. Corrosion in electronics: Overview of failures and countermeasures. In *Proceedings EuroCorr 2014* (2014).

59. Frick, A. & Günther, D. Fundamental studies on the ablation behaviour of carbon in LA-ICP-MS with respect to the suitability as internal standard. *J. Anal. At. Spectrom.* **27**, 1294–1303 (2012).

4.5 Article 5 (Submitted manuscript)

The fifth submitted manuscript is entitled "Strategies for Trace Metal Quantification in Polymers using LIBS". In this work, the challenge of providing quantitative measurements of trace metals in polymers is investigated. Quantification using direct-solid sampling techniques such as LIBS is a challenging task no matter what sample type is investigated. As described before, the absolute signal response during LIBS analysis is highly dependent on the samples' matrix meaning that matrix-matched standards are required for accurate quantitative results. Well-characterized matrix-matched standards are only available for widely used and standardized materials. Therefore, in many cases other approaches for quantification have to be applied. In this work, the unique capabilities of LIBS are used for quantification in unknown polymer types or polymer types with an unknown composition. LIBS provides not only adequate sensitivity for trace metal analysis but also polymer specific signals. Combining these capabilities with multivariate data evaluation strategies, this work demonstrates the advantages of using LIBS for the quantification of trace metals in of polymers. Therefore, a library of in-house prepared polymer standards of 8 different polymer types (Acrylic, PAN, PI, PMMA, PSU, PVA, PVC, and PVP) containing various levels of K is prepared and analyzed. Using this library of standards, the performance of the multivariate data evaluation strategies are evaluated by considering each polymer type as a test type which is treated as an unknown polymer. Two different multivariate data evaluation strategies are presented in this work: A RDF classification model which matches the unknown test polymer type to a known polymer type using its univariate calibration model for quantification. The second approach is based on a PLS model which is built from the data of the polymer library. For quantification, the PLS model is applied to the test polymer types' standards. The deviations from these two multivariate data evaluation strategies are compared to bench mark values of matrix-matched quantification (best-case) and non-matrix matched quantification (worst case). Obtained results demonstrate, that multivariate data evaluation approaches provide significantly more reliable quantitative results compared to non-matrix matched quantification.

Strategies for Trace Metal Quantification in Polymer Samples with an Unknown Matrix using LIBS

Lukas Brunnbauer[1*], Jhanis Gonzalez[2,3], Hans Lohninger[1], Julia Bode[4], Carla Vogt[4], Michael Nelhiebel[5], Silvia Larisegger[5] and Andreas Limbeck[1*]

[1]TU Wien, Institute of Chemical Technologies and Analytics, Getreidemarkt 9/164-I[2]AC, 1060 Vienna, Austria

[2]Applied Spectra, Inc., West Sacramento, CA, USA

[3]Lawrence Berkeley National Lab, Berkeley, CA, USA

[4]TU Bergakademie Freiberg, Institute of Analytical Chemistry, Leipziger Str. 29, 09599 Freiberg, Germany

[5]KAI Kompetenzzentrum Automobil- und Industrieelektronik GmbH, Technologiepark Villach Europastraße 8, 9524 Villach, Austria

*Corresponding author:

lukas.brunnbauer@tuwien.ac.at

andreas.limbeck@tuwien.ac.at

Abstract

Providing unique advantages, laser-based analytical techniques such as LIBS have gained more and more popularity for quantitative elemental analysis in the last few years. However, to obtain reliable quantitative results, matrix-matched standards are required. A particular material of interest for quantitative trace metal analysis is synthetic polymers, which is among the most widely used materials in our modern world. As the exact composition of a polymer under investigation (polymer type and applied additives) is often not known, the selection of an appropriate matrix-matched standard is difficult. In this work, we investigate and assess different approaches for quantifying potassium in unknown polymer types or polymers with an unknown composition where matrix-matched standards cannot be employed. This is of great interest in the semiconductor industry where monitoring of mobile ions in applied polymers is crucial, and the composition of the polymer is often not known due to confidentiality. We use the unique capabilities of LIBS, providing adequate sensitivity for potassium, and additionally delivering polymer-specific emission signals. Two different multivariate approaches (Random Decision Forest classification combined with conventional univariate calibration and a Partial Least Squares model) are developed and applied. Therefore, an in-house prepared library of standards of 8 different polymer types (Acrylic, PAN, PI, PMMA, PSU, PVA, and PVC) is prepared. The errors obtained from the multivariate approaches are compared with conventional matrix-matched as well as non-matrix-matched quantification. With our developed approaches, for some samples quantitative determination of potassium in the low µg/g range in unknown polymer types is achieved with a relative error less than 20% which is comparable to conventional matrix-matched quantification. For all other samples, relative errors in the range of 30%-90% are obtained. Thus, the deviation from the nominal concentration is less than a factor of 2 for all investigated polymer types, which is sufficient for the determination of trace metals in many applications. The presented results pose a significant improvement compared to non-matrix-matched quantification which often leads to deviations up to a factor 10 from the nominal concentration.

1. Introduction

Besides different physical properties such as hardness, strength, durability, and resilience, trace metal content is one of the most critical polymers' characteristics influencing their applications [1]. In the semiconductor industry, the employment of high purity materials, such as polymers, is crucial, as contaminants of mobile ions can affect electronic devices' performance and lifetime [2,3]. In sectors such as the food packaging industry, the content of trace metals in the polymers used is monitored because of the possible migration of toxic species into the food [4,5]. Investigating trace metals in microplastics is also of significant interest as these contaminants may cause an additional ecological impact on exposed environments [6,7]. Therefore, the determination of trace metal contents in wide ranges of different polymer applications is of great interest and poses a challenge for analytical chemistry.

Conventional analytical approaches for the determination of the trace metal content in polymers include microwave-assisted digestion [8], dry ashing [9] or microwave-induced combustion [10] of the sample for conversion into solutions with subsequent liquid Inductively Coupled Plasma-Mass Spectrometry (ICP-MS) or Inductively Coupled Plasma-Optical Emission Spectroscopy (ICP-OES) measurement [11]. All these approaches have in common an easier path to quantification based on the availability of certified liquid standards. Nevertheless, certain drawbacks must be considered: harsh and hazardous chemicals must be employed to ensure complete digestion of the sample, including manual sample handling which is laborious, time-consuming, and susceptible to contamination. When using digestion protocols to determine trace metal content in polymers, incomplete digestion or volatilization of analytes may underestimate the actual trace metal content. At the same time, contamination by manual sample handling may cause an overestimation. Additionally, the samples are usually diluted, limiting the analysis's sensitivity, and only bulk information is available.

For these reasons, direct solid sampling approaches such as X-ray fluorescence spectroscopy (XRF) to detect metal traces in polymers have recently been reported in the literature [12,13]. Laser-based techniques such as Laser-Induced Breakdown Spectroscopy (LIBS) [14,15] and Laser Ablation-Inductively Coupled Plasma-Mass Spectrometry LA-ICP-MS [16–18] have also been applied successfully for metal analysis in polymers. These direct-solid sampling techniques all benefit from eliminating the sample preparation steps, thus reducing the chemicals and time required for the analysis. Additionally, the risk of contaminants is reduced significantly as less manual sample handling is required. Besides advantages regarding the lack of sample preparation, direct solid-sampling techniques can provide information about the spatial distribution in the form of images or depth profiles [19–21], which is not accessible with conventional liquid analysis.

Nevertheless, direct-solid sampling techniques come with one significant drawback: quantification is a challenging task. Due to matrix effects occurring during the measurement, matrix-matched standards are necessary to obtain reliable quantitative results [22–24]. Besides the availability of matrix-matched standards being limited for some materials, also information about the exact matrix of the sample under investigation is necessary for proper selection and application. The matrix-matched requirement is especially problematic for polymers. This type of material usually exhibits a wide variety of chemical structures and properties, such as optical absorption behavior, and hardness influencing the ablation process. Different additives, which are often used in the polymer industry to adjust material properties [25], can also lead to varying matrix-effects. When analysing polymer samples used in industrial applications, due to confidentiality, often the exact sample composition (polymer type and applied additives) is not known. Additionally, in the field of microplastics analysis, information on the polymer type of individual particles is also not known a priori. Therefore, the selection of suitable matrix-matched standards is difficult, hampering quantification with conventional calibration approaches without prior comprehensive sample characterization.

In contrast to XRF and LA-ICP-MS, LIBS provides not only elemental information but additional characteristic molecular features for each type of polymer, which we will use to overcome the aforementioned quantification issues of polymeric samples with an unknown composition. In the field of LIBS, various approaches have recently been published reporting on multivariate data evaluation for different forms of polymer analysis, with most focusing on their classification [26,27]. Besides classification, the use of multivariate calibration models for quantification from LIBS data for different materials was reported [28–30].

The presented work focuses on demonstrating the advantages of LIBS concerning quantifying the potassium content in unknown polymer types or polymers with an unknown composition using multivariate statistics. Therefore, a library consisting of in-house prepared standards of 8 different polymer types was prepared, and broadband LIBS spectra were recorded. We applied and evaluated two different multivariate data evaluation strategies based on a Random Decision Forest (RDF) classification model and a Partial Least Squares (PLS) model. To assess the performance of the applied procedures, benchmarks are required. Therefore, conventional matrix-matched and non-matrix-matched quantification is evaluated.

2. Experimental

2.1 Chemicals

High-purity silicon wafers (n-doped) used as substrate materials were provided by Infineon Austria AG (Villach, Austria). Polyimide (PI) P84 in powder form (>98% purity) was obtained by HP Polymer GmbH (Lenzing, Austria). Polyacrylonitrile (PAN), Poly (methyl methacrylate) (PMMA), Polysulfone (PSU), Polyvinyl acetate (PVA), Polyvinyl chloride (PVC), and Polyvinyl pyrrolidone (PVP) in powder form were obtained from Arcos Organics, Geel, Belgium. Acrylic

varnishes (TerraGloss UV) were obtained from ACTEGA Terra GmbH, Lehrte, Germany. Surface additives used for the preparation of acrylic standards were obtained from BYK-Gardner GmbH, Geretsried, Germany. Conostan, SPS Science, Quebec, Canada, provided oil-based standards for spiking acrylic varnish. A polyester film used as a substrate material for acrylic standards was obtained from BYK-Gardner GmbH, Geretsried, Germany. N-Methyl-2-pyrrolidon (NMP) with p.a. grade quality was obtained from Merck (Darmstadt, Germany). Potassium trifluoromethane sulfonate (98%) soluble in NMP used to prepare spike solutions were acquired from Sigma-Aldrich, Buchs, Switzerland.

2.2 Preparation of polymer standards

For the preparation of PAN, PI, PMMA, PSU, PVA, PVC, and PVP standards, polymer powders were dissolved in NMP, obtaining solutions with concentrations ranging from 10 to 20 wt% depending on the polymer type. A stock solution for spiking was prepared by dissolving Potassium trifluoromethane sulfonate in NMP. Different concentration levels of K were prepared by diluting the prepared stock solutions using NMP. NMP standards were used to spike the prepared polymer solutions, and the obtained mixtures were thoroughly homogenized using a vortex mixer. Thin films of spiked polymer were prepared by applying 50 µl of the mixtures to cut high purity Si wafer with 10 mm x 10 mm using a pipette and cured at 80°C for 12 hours. The thickness of produced polymer thin films was 10 µm, determined by a Dektak XT Profilometer (Bruker Corporation, USA). A more detailed description of these standards' preparation is given by Bonta et al. [14].

For acrylic standards, a 1:1 mixture of two different acrylic varnishes, varying in viscosity, was used. An anti-foaming agent and a surface additive were added. Potassium was added in the form of a certified oil-based standard. The mixture was dispersed thoroughly using an Ultra Turrax® by IKA Werke GmbH & CO. KG, Staufen, Germany. Thin films of varnish were applied onto a 100 µm thick polyester substrate with uniform layer thickness with the help of wire-wound rods and an automatic film applicator (Automatic Film Applicator S by BYK-Gardner GmbH, Geretsried, Germany). A layer thickness of 25 µm was chosen. The varnish was put into a UV-chamber (Dinies Technologies GmbH, Villingendorf, Germany) and hardened under UV-light for a few minutes. To prevent inhibition of the radical polymerization by oxygen, the UV-chamber was flushed with nitrogen.

Potassium concentrations of the prepared standards were in the range of 0-70 µg/g. For each polymer type, between 4 and 8 standards were prepared. A Table containing the concentration of each standard is provided in the supplementary material.

2.3 LIBS Instrumentation and data evaluation

A LIBS system (Model J200) equipped with a 266 nm Nd: YAG laser by Applied Spectra, Inc. (West Sacramento, California) was used for LIBS measurements. The light emitted by the laser-induced plasma was collected and was transferred to a Czerny-Turner spectrometer covering a wavelength range from 186-1048 nm and detected using a CCD chip. Samples

were placed in a sealed chamber mounted on an XY stage continuously flushed with Ar. Each polymer standard was analyzed using a pattern consisting of 10 parallel line scans with a total length of 1.8 mm. With a distance of 0.15 mm between each laser-shot, a total number of 120 spectra were recorded per standard. To improve signal-to-noise ratios and reduce the amount of data, sets of 6 shots were accumulated, resulting in 20 spectra per standard. The accumulated spectra were normalized to the Euclidean norm to reduce shot-to-shot variations which is commonly used in LIBS analysis [31]. This normalization approach reduced the Relative Standard Deviation (RSD) of the 20 LIBS spectra per standard on average from 11% to 7%. The RSD of the potassium signal of the standard with the highest nominal concentration for each polymer type was in a range of 7% (PVA) to 12% (PVC), confirming the homogeneity of the standards.

Each laser-shot was performed with a separation distance of 0.15 mm to the previous measurement, avoiding previous measurements' influences (cross-contamination). LIBS parameters were optimized in preliminary experiments to assure sufficient sensitivity for potassium while avoiding full penetration of the prepared polymer standards to exclude LIBS signals from the substrate and provide polymer-specific molecular information. The data acquisition starting time, or gate delay, was set to a compromised value between using a short gate delay (<1 μs), where atomic emission signals (e.g., K, C, H, O) usually show a higher signal-to-noise ratio and a longer gate delay (>1 μs) where molecular emission signals (e.g., CN violet band, C_2 swan band) show a higher signal-to-noise ratio. Used LIBS parameters are summarized in Table 2. Crater depths after LIBS measurements were measured using a Dektak XT Profilometer (Bruker Corporation, USA) and were used to determine ablation rates.

Table 1: LIBS parameters used for the analysis of polymer standards.

LIBS parameters	
Laser wavelength (nm)	266
Laser energy (mJ)	3.12
Spot size (μm)	100
Repetition rate (Hz)	10
Gate delay (μs)	1
Gate width (ms)	1.05
Atmosphere	Ar

LIBS data were collected using Axiom 2.0 software provided by the manufacturer. Univariate and multivariate data evaluation was carried out using Epina ImageLab 3.34 (Retz, Austria).

3. Results and Discussion

In this work, different approaches for quantifying the potassium content in unknown polymer types or polymers with an unknown composition are investigated and evaluated.

Potassium was selected as the analyte of interest because the contamination of mobile ions in polymers is of great interest in the semiconductor industry [32,33].

LIBS spectra were obtained from in-house prepared standards of 8 different investigated polymer types (Acrylic, PAN, PI, PMMA, PSU, PVA, PVC, and PVP) containing potassium levels in the range of 0-70 µg/g. Figure 1 shows an overview of the different data evaluation approaches followed in this work. In a first step, univariate calibration curves are calculated for all investigated polymer types. Errors obtained from matrix-matched quantification are calculated and used as a best-case benchmark. In a second step, quantification of unknown polymer types is considered where matrix-matched quantification is not feasible. Therefore, non-matrix-matched quantification is investigated where each of the investigated polymer types is evaluated using the univariate calibration functions of all remaining polymer types. Next, two multivariate data evaluation strategies are presented based on a Random Decision Forest (RDF) classification model and a Partial Least Squares (PLS) model where each investigated polymer type is considered as unknown one after the other. The idea behind the RDF approach is a matching of the unknown polymer type to the closest-matching polymer from the dataset to minimize the error from non-matrix-matched quantification. The PLS approach is based on building a statistical model estimating the potassium concentration using the LIBS data from the different polymer types.
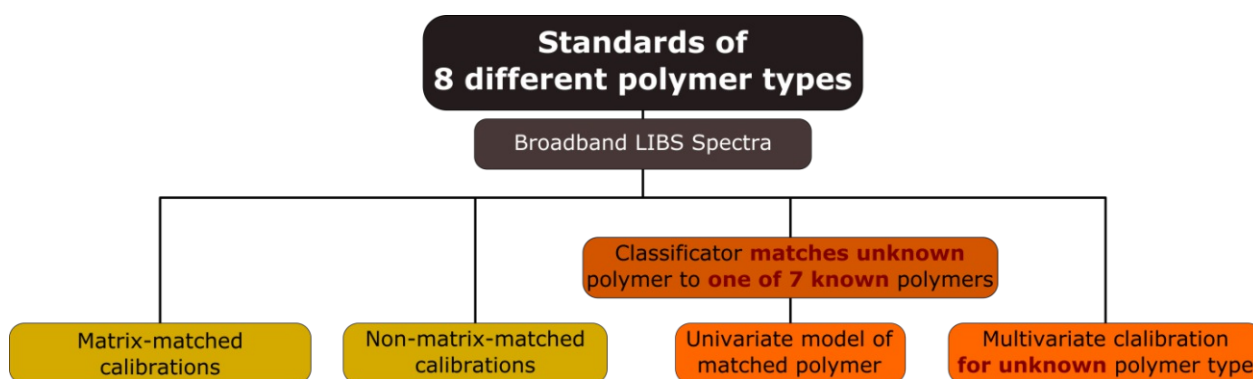
Figure 1: Overview of all different data evaluation approaches presented in this work.

3.1 Matrix-matched univariate calibrations

The first step in this study involved the performance evaluation of the classical univariate calibration approach for each polymer type. Therefore, the emission signal of potassium (766.14 nm - 766.90 nm) is integrated after normalization of the spectra to the Euclidean norm. A background correction was performed by averaging and subtracting the background signal at 765.60 nm - 766.04 nm and 767.01 nm - 767.55 nm next to the potassium emission line.

Univariate calibration models with correlation coefficients (R^2) ranging from 0.971 (PAN) to 0.998 (PSU) are obtained for all polymer types confirming the applicability of the in-house prepared standards. Limits of quantification (LOQ) are determined for each polymer type

according to DIN 32645 and are in a range of 0.3 µg/g (PSU) to 1.4 µg/g (PMMA). The standard with the lowest potassium concentration of each polymer type is at least 4.3 times higher than the LOQ, also confirming the standards' applicability.

Different slopes of different polymer types' calibration curves are observed, ranging from 0.0018 a.u./µg·g^{-1} (PI) to 0.0440 a.u./µg·g^{-1} (PVA). The slopes of the remaining 6 polymer types lie in-between forming two groups of similar slopes (Group 1: Acrylic, PMMA, PVC; Group 2: PAN, PSU, PVP). Table 2 gives an overview of the figures of merit of the obtained univariate calibration functions as well as the ablation rate and carbon content for each polymer type.

The variability in the observed slopes of the univariate calibration curves can be explained by matrix-effects that occur when analyzing different polymer types with LIBS. Different polymer types show different absorption behavior resulting in different ablation rates and different fluctuating plasma energies, leading to different atomization and excitation efficiency of the analyte within the laser-induced plasma.

We investigate two different normalization strategies to reduce the variability of observed slopes: normalization to the ablation rate, which is already reported in the literature [34,35], and normalization to the carbon content of the polymer. Comparing the ablation rate and the carbon content of each polymer type with the slope of the univariate calibration curve (Table 2), no correlation is observed. For example, PAN and PI exhibit identical ablation rates and comparable carbon contents but the slopes of the calibration are significantly different. Acrylic and PVC show similar slopes although the carbon content and the ablation rate are significantly different. Therefore, slope variations cannot be explained by different ablation rates or carbon content. Thus for potential reduction of matrix effects additional material properties must be considered, or other more sophisticated approaches for data evaluation are needed.

Table 2: Figures of merit of observed univariate calibration functions and properties of the investigated polymer types.

	R^2	LOQ (µg/g)	wt% C (%)	Ablation rate (µm/shot)	Slope (a.u./µg·g^{-1})
Acrylic	0.992	0.7	68	0.7	0.0221
PAN	0.971	1.2	68	0.6	0.0052
PI	0.990	0.6	72	0.6	0.0018
PMMA	0.956	1.4	60	1.1	0.0223
PSU	0.998	0.3	73	1.3	0.0056
PVA	0.976	1.1	53	5.7	0.0400
PVC	0.992	0.5	38	1.8	0.0197
PVP	0.974	1.0	65	0.5	0.0060

In the next step errors for matrix-matched quantification are estimated. These errors will be used as best-case benchmark values to assess the performance of the proposed multivariate models for the quantification in unknown polymer types. Therefore, the potassium

concentration of the standards in the concentration range of 8 – 25 µg/g of all polymer types are evaluated by the corresponding univariate calibration of the same polymer type using a leave-one-out (LOO) cross-validation. Relative errors are calculated according to

$$Relative\ Error = \left|\frac{c_{estimated}-c_{nominal}}{c_{nominal}}\right| \cdot 100 \qquad\qquad (1)$$

where $c_{estimated}$ is the estimated potassium concentration of the evaluated standard and $c_{nominal}$ is the nominal concentration of the evaluated standard. The obtained relative errors are averaged for each polymer type. Relative errors shown in the diagonal line of Figure 2 (marked green) correspond to matrix-matched quantification. Derived values range from 7% (Acrylic) to 17% (PI and PMMA), resulting in an averaged relative error of 11% (n=8) for all polymers. The order of magnitude of the observed error is in good agreement with relative errors reported in the field of LIBS and other direct-solid sampling techniques such as LA-ICP-MS using matrix-matched standards for quantification [36–39]. All other cells in Figure 2Table 1 correspond to non-matrix-matched quantification when a polymer type is evaluated by the univariate calibration of a different polymer type and will be discussed in the next chapter.

Relative error (%)

Applied univariate calibration

Evaluated polymer type

	Acrylic	PAN	PI	PMMA	PSU	PVA	PVC	PVP
Acrylic	7	538	1815	22	523	23	28	425
PAN	118	11	278	94	19	75	140	28
PI	157	105	17	125	76	83	190	129
PMMA	38	466	1602	17	454	16	52	365
PSU	155	37	216	116	9	71	194	76
PVA	19	479	1634	11	464	9	31	377
PVC	18	643	2105	47	619	10	9	517
PVP	121	79	528	86	98	59	154	12

Figure 2: Relative errors obtained when evaluating the potassium content in standards with a concentration range of 8-25 µg/g of all polymer types by the different univariate calibration curves of all polymer types. The case of matrix-matched quantification is marked in green whereas all the other cells represent non-matrix-matched quantification. The best-case for non-matrix-matched quantification is marked in orange and the worst-case for non-matrix-matched quantification is marked in blue.

3.2 Quantification strategies for unknown polymer types

3.2.1 Non-matrix-matched quantification

When performing quantitative analysis of unknown polymer types or polymers with an unknown composition, non-matrix-matched quantification is the only conventional approach available. In this case, the potassium content of an unknown polymer type is assessed using the univariate calibration functions of a different polymer type. In this chapter, the expected errors from non-matrix-matched quantification are evaluated. Therefore, the standards in

the concentration range of 8 – 25 µg/g of each polymer type are evaluated by the univariate calibration functions of the other polymer types within our dataset and relative errors are calculated. The results are shown in Figure 2.

In this case, a high variability of the relative errors is observed. In some cases, low relative errors are obtained for non-matrix-matched quantification (e.g. evaluating PVA using the univariate calibration of PMMA results in a relative error of 11%), in other cases huge errors are obtained (e.g. evaluating PVC using the univariate calibration of PI results in a relative error of 2105%). For each polymer type evaluated with the calibration curves of the remaining polymer types, the best-case with the lowest relative error is marked in orange and the worst-case with the highest relative error is marked in blue in Figure 2. Interpreting the results presented in Figure 2 with the perspective of quantification of the potassium content in unknown polymer types it can be concluded that non-matrix-matched calibration can provide reliable quantification in some cases. Nevertheless, choosing a random calibration curve for the quantification of an unknown polymer type is not a feasible approach as expected errors cannot be estimated and may result in deviations more than a factor of 10 from the nominal content. For example, only 3 out of the 56 possible standard and unknown polymer combinations results in errors comparable to matrix-matched calibrations whereas 31 combinations show a relative error >100% and 10 combinations show a relative error >500%. To improve the performance of quantification of unknown polymer types, multivariate data evaluation strategies are investigated in the next part of this work.

3.2.2 Multivariate evaluation strategies

To evaluate the performance of multivariate data evaluation models for the quantitative determination of the potassium content in unknown polymer types, each of the 8 investigated polymer types will be considered an unknown polymer type and is evaluated by a multivariate model based on the remaining 7 known polymer types. For the multivariate models we use not only the emission signal of potassium for quantification but also polymer-specific signals from the LIBS spectrum, including atomic emission signals of the main components of the investigated polymers (C, H, and O) and molecular signals (CN violet band and C_2 swan band) A representative LIBS spectrum with marked emission signals used for multivariate models is shown in Figure 3.
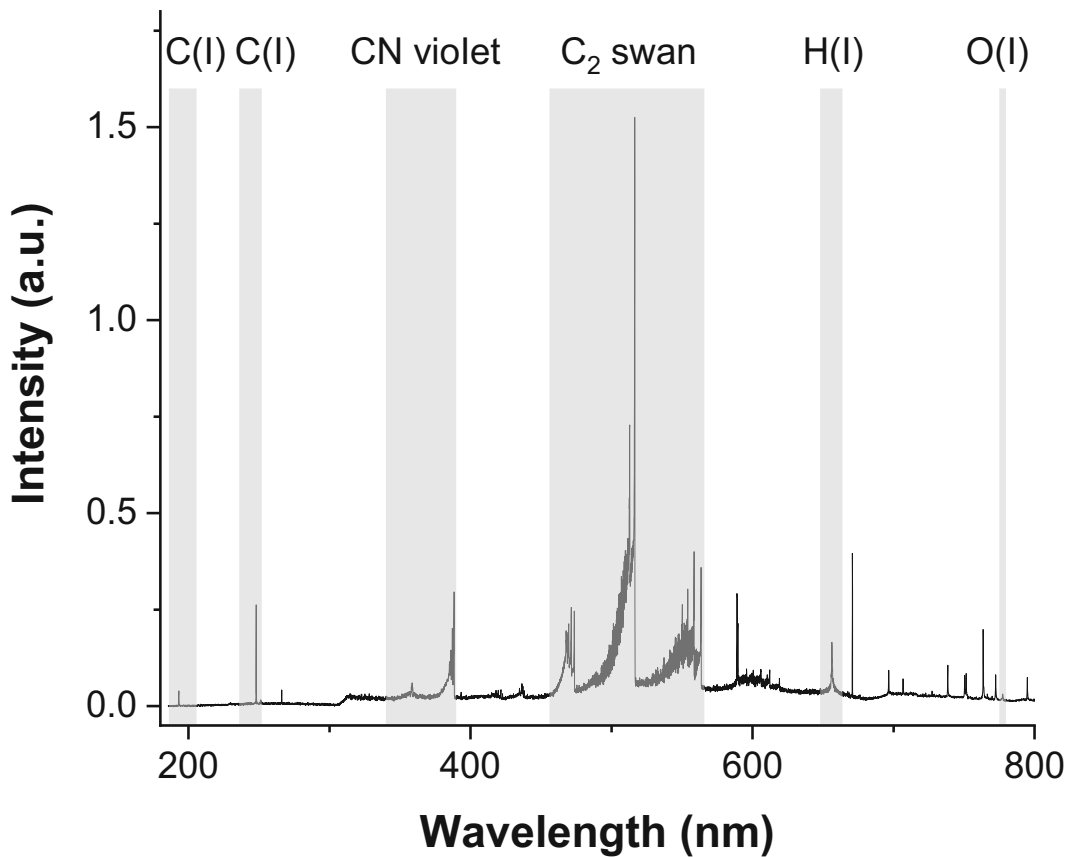
Figure 3: Exemplary broadband LIBS spectrum of PI with marked polymer-specific emission signals used for multivariate data processing.

3.2.2.1 Multivariate classification (RDF) combined with univariate calibration

The first multivariate approach for the quantification of the potassium content in unknown polymer types is based on a Random Decision Forest (RDF) classification model, commonly used in LIBS data analysis [40,41]. In this study, we use the RDF analysis to select the appropriate calibration model for a particular unknown polymer type. For example, we use the RDF analysis to find the closest match to the unknown polymer type among the 7 known polymer types. Then, we apply the univariate calibration model corresponding to the matched standard material to evaluate the unknown polymer type. Assuming that the similarity in the broadband LIBS spectra is indicative for the matrix-effects observed in univariate calibration models, in the best-case scenario the polymer type yielding the lowest non-matrix-matched error (marked orange in Figure 2) is selected by the RDF for the corresponding unknown polymer type.

The RDF uses all intensities of the marked regions of the obtained LIBS spectra (Figure 3) as input variables. The model is built with 75 trees and a resampling factor of 0.5. 8 different RDFs were calculated, each excluding one of the polymer types. Therefore, e.g., PI will not

be classified as PI because PI was not part of the training set for this respective RDF. Instead, the built RDF will find the polymer type out of the remaining 7 types with the closest matching LIBS spectrum to PI. A majority vote on the classification is used to determine the matched polymer type.

To evaluate the described approach, each polymer type from our sample set is considered an unknown polymer type, and relative errors for the standards within the concentration range 8-25 µg/g are calculated and shown in Table 3. Evaluating the polymer types PI, PMMA, and PVA, the best-case result with the lowest possible relative error is obtained by this approach. PAN and PVP are matched to the second-best-case. The other polymer types are not matched to the best-case scenario by the RDF resulting in non-optimal results. Nevertheless, the worst-case scenario is only selected for PSU. These results indicate the benefit of the application of a classification model for subsequent non-matrix-matched quantification of unknown polymer types. Compared to the random selection of non-matrix-matched standards, which delivers useful results only in a limited number of cases, the RDF approach provides significant advances. Nevertheless, for some polymer types the results are still not satisfying, thus further improvements are necessary.

3.2.2.2 Multivariate calibration (PLS)

The second multivariate approach for quantifying the potassium content in unknown polymer types is based on a PLS regression model, which is also commonly used in the field of LIBS [42,43]. In this study, PLS models are built using data of 7 of the 8 polymer types. The obtained PLS model is used to quantify the omitted polymer type. The same regions of the broadband LIBS spectra (Figure 3) used for the RDF are used as input variables for the PLS model. Moreover, the corresponding element-specific signals for potassium (766.10 nm - 766.91 nm and 769.44 nm - 770.41 nm) were added to the polymer specific emission signals as input variables. Similar to the RDF approach, 8 different PLS models are calculated, each excluding one of the 8 polymer types treated as an unknown polymer type for this model. The number of factors for each PLS model was optimized by calculating a cross-validation and choosing the number of factors with the lowest Root Mean Square Error of Prediction (RMSEP).

Relative errors for the standards within a concentration range 8-25 µg/g obtained from this approach are shown in Table 3. The PLS approach employed for the quantification of unknown polymer types shows promising results with adequate relative errors in the two-digit range for all polymer types. PI, PMMA, and PVP yield even lower relative errors compared to the best-case non-matrix-matched quantification within our dataset. PVC shows the highest relative error. One reason for this may be that PVC is the only polymer type within our dataset containing a halogen. This might have an influence on polymer-specific signals observed in the LIBS spectrum due to different reactions within the laser-induced plasma resulting in a significant influence on the performance of the PLS approach. Nevertheless, the PLS approach applied for the quantification of unknown polymers enables

a reliable estimation of the potassium concentration in all investigated polymer types. Compared to the RDF approach, the PLS approach provides a more universal application.

Table 3: Results of the multivariate approaches for the quantification of unknown polymer types where each of the 8 investigated polymer type was considered unknown.

| Polymer type considered unknown | RDF Approach | | PLS Approach |
	Matched polymer type	Relative error (%)	Relative error (%)
Acrylic	PVP	425	38
PAN	PVP	28	30
PI	PSU	76	54
PMMA	PVA	16	16
PSU	PI	216	74
PVA	PMMA	11	19
PVC	PVP	517	90
PVP	PAN	79	45

4. Conclusion

In this work we investigate the possibility of using LIBS for the quantitative analysis of potassium in unknown polymer types where matrix-matched standards cannot be used. In a first step we evaluated univariate calibration curves of 8 different polymer types where significant matrix-effects were observed. Relative errors of matrix-matched quantification and non-matrix-matched quantification were calculated and used as benchmark values to assess the performance of multivariate approaches for the quantification in unknown polymer types. Figure 4 shows the errors obtained from presented data evaluation approaches. The selected standards for the evaluation of relative errors are in a concentration range of 8-25 µg/g which is only one order of magnitude higher compared to obtained LOQs.
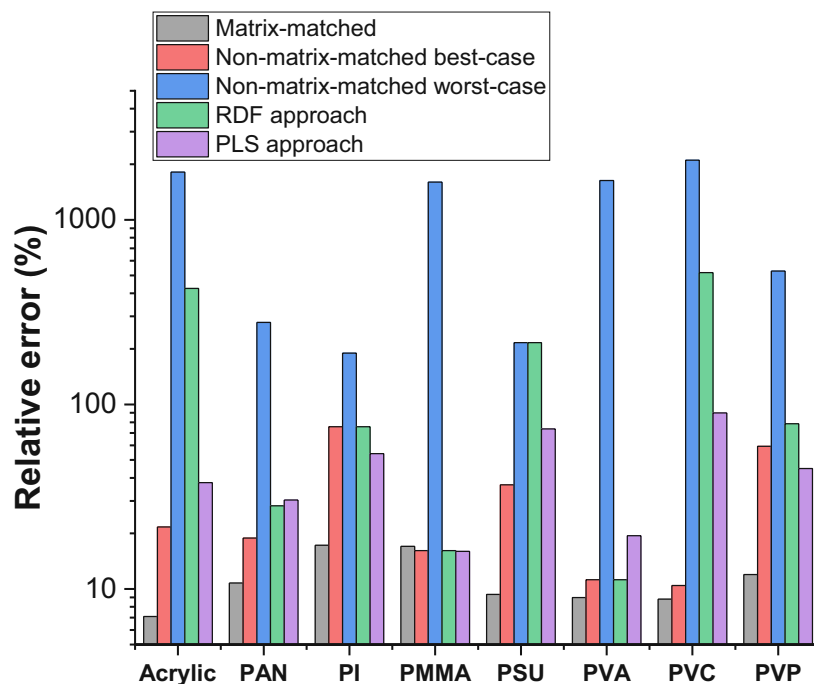
Figure 4: Overview of the relative errors obtained for the different data evaluation strategies for the quantification of unknown polymers presented in this work.

Naturally, matrix-matched quantification yields the lowest relative errors ranging from 7% to 17%. As for the quantification of polymer samples where the exact composition is not known, matrix-matched quantification cannot be employed, conventionally only non-matrix matched quantification can be used. Since different polymer types come with a wide range of physical and chemical properties, the relative errors obtained from non-matrix-matched quantification heavily depend on the polymer type selected for quantification. The presented results show that conventional non-matrix-matched quantification using a random polymer type as a reference material for an unknown polymer type is not feasible, as the expected error cannot be estimated. By chance, an appropriate polymer type can be selected for non-matrix-matched quantification resulting in relative errors of 20% or less. However, in most of the cases relative errors resulting from non-matrix-matched quantification can result in deviations more than a factor 10 from the nominal concentration which is not suitable for research tasks or industrial/environmental routine analysis. Considering polymer-specific signals provided by LIBS broadband spectra significantly improved the quality of the analysis. The two developed multivariate approaches based on a RDF- and a PLS-model for the quantitative analysis of the potassium content in unknown polymer types yield relative errors ranging from 11% to 517%% and 16% to 90% respectively. Comparing the findings for these two multivariate approaches, the RDF approach delivers inadequate results for some polymers (e.g. Acrylic or PVC), whereas the PLS-model allows a universal application for all polymer types. Considering that the quantification of the multivariate models is carried out without the use of matrix-matched standards, precise

quantification cannot be expected but the presented approaches enable a reliable estimate of the potassium content in the low µg/g range which is sufficient for many applications.

In further works, more elements will be added to the standards for a broader range of applications. Additionally, the influence of an increase in the number of polymer types available in the library on the obtained errors will be investigated.

Acknowledgements

Competing interests

There are no competing interests to declare.

Supplementary Material

Marked standards were used for the calculation of relative errors.

Polymer type	Nominal K concentration (µg/g)
Acrylic	0
	10
	25
	50
PAN	0
	8
	16
	21
	27
	46
PI	0
	6
	11
	17
	23
	31
	63
PMMA	0
	6
	11
	17
	23
	32

	56
PSU	0
	6
	10
	15
	51
	65
PVA	0
	6
	11
	19
	24
	32
	47
PVC	0
	5
	11
	16
	20
	33
	54
	65
PVP	0
	5
	9
	17
	21
	31
	53
	66

References

(1) Characteristics, Applications and Properties of Polymers. In *Polymer Engineering Science and Viscoelasticity: An Introduction*; Brinson, H. F., Brinson, L. C., Eds.; Springer US: Boston, MA, 2008; pp 55–97. https://doi.org/10.1007/978-0-387-73861-1_3.

(2) Slusser, G. J.; MacDowell, L. Sources of Surface Contamination Affecting Electrical Characteristics of Semiconductors. *J. Vac. Sci. Technol. A* **1987**, *5* (4), 1649–1651. https://doi.org/10.1116/1.574539.

(3) Atkinson, S. Essential High-Purity Sealing Materials for Semiconductor Manufacturing. *Seal. Technol.* **2018**, *2018* (7), 5–7. https://doi.org/10.1016/S1350-4789(18)30284-8.

(4) Song, H.; Li, B.; Lin, Q.-B.; Wu, H.-J.; Chen, Y. Migration of Silver from Nanosilver–Polyethylene Composite Packaging into Food Simulants. *Food Addit. Contam. Part A* **2011**, *28* (12), 1758–1762. https://doi.org/10.1080/19440049.2011.603705.

(5) Whitt, M.; Vorst, K.; Brown, W.; Baker, S.; Gorman, L. Survey of Heavy Metal Contamination in Recycled Polyethylene Terephthalate Used for Food Packaging. *J. Plast. Film Sheeting* **2013**, *29* (2), 163–173. https://doi.org/10.1177/8756087912467028.

(6) Cole, M.; Lindeque, P.; Halsband, C.; Galloway, T. S. Microplastics as Contaminants in the Marine Environment: A Review. *Mar. Pollut. Bull.* **2011**, *62* (12), 2588–2597. https://doi.org/10.1016/j.marpolbul.2011.09.025.

(7) Turner, A.; Holmes, L. A. Adsorption of Trace Metals by Microplastic Pellets in Fresh Water. *Environ. Chem.* **2015**, *12* (5), 600–610. https://doi.org/10.1071/EN14143.

(8) D. Iop, G.; R. Krzyzaniak, S.; S. Silva, J.; M. Flores, E. M.; B. Costa, A.; A. Mello, P. Feasibility of Microwave-Assisted Ultraviolet Digestion of Polymeric Waste Electrical and Electronic Equipment for the Determination of Bromine and Metals (Cd, Cr, Hg, Pb and Sb) by ICP-MS. *J. Anal. At. Spectrom.* **2017**, *32* (9), 1789–1797. https://doi.org/10.1039/C7JA00123A.

(9) Arnquist, I. J.; Thomas, M.-L. P.; Grate, J. W.; Bliss, M.; Hoppe, E. W. A Dry Ashing Assay Method for the Trace Determination of Th and U in Polymers Using Inductively Coupled Plasma Mass Spectrometry. *J. Radioanal. Nucl. Chem.* **2016**, *3* (307), 1883–1890. https://doi.org/10.1007/s10967-015-4343-7.

(10) Flores, E. M. M.; Muller, E. I.; Duarte, F. A.; Grinberg, P.; Sturgeon, R. E. Determination of Trace Elements in Fluoropolymers after Microwave-Induced Combustion. *Anal. Chem.* **2013**, *85* (1), 374–380. https://doi.org/10.1021/ac3029213.

(11) Pereira, J. S. F.; Knorr, C. L.; Pereira, L. S. F.; Moraes, D. P.; Paniz, J. N. G.; Flores, E. M. M.; Knapp, G. Evaluation of Sample Preparation Methods for Polymer Digestion and Trace Elements Determination by ICPMS and ICPOES. *J. Anal. At. Spectrom.* **2011**, *26* (9), 1849–1857. https://doi.org/10.1039/C1JA10050E.

(12) Węgrzynek, D. Quantitative Elemental Mapping and Characterization of the Homogeneity of Element Distribution in Polymer Foils by Microbeam X-Ray Fluorescence Spectrometry. *X-Ray Spectrom.* **2001**, *30* (1), 56–61. https://doi.org/10.1002/xrs.460.

(13) Bichinho, K. M.; Pires, G. P.; Stedile, F. C.; dos Santos, J. H. Z.; Wolf, C. R. Determination of Catalyst Metal Residues in Polymers by X-Ray Fluorescence. *Spectrochim. Acta Part B At. Spectrosc.* **2005**, *60* (5), 599–604. https://doi.org/10.1016/j.sab.2004.11.012.

(14) Bonta, M.; Limbeck, A. Metal Analysis in Polymers Using Tandem LA-ICP-MS/LIBS: Eliminating Matrix Effects Using Multivariate Calibration. *J. Anal. At. Spectrom.* **2018**, *33* (10), 1631–1637. https://doi.org/10.1039/C8JA00161H.

(15) Aquino, F. W. B.; Paranhos, C. M.; Pereira-Filho, E. R. Method for the Production of Acrylonitrile–Butadiene–Styrene (ABS) and Polycarbonate (PC)/ABS Standards for Direct Sb Determination in Plastics from e-Waste Using Laser-Induced Breakdown Spectroscopy. *J. Anal. At. Spectrom.* **2016**, *31* (6), 1228–1233. https://doi.org/10.1039/C6JA00038J.

(16) Voss, M.; Nunes, M. A. G.; Corazza, G.; Flores, E. M. M.; Müller, E. I.; Dressler, V. L. A New Approach to Calibration and Determination of Selected Trace Elements in Food Contact Polymers by LA-ICP-MS. *Talanta* **2017**, *170*, 488–495. https://doi.org/10.1016/j.talanta.2017.04.048.

(17) Villaseñor, Á.; Boccongelli, M.; Luis Todolí, J. Quantitative Elemental Analysis of Polymers through Laser Ablation – Inductively Coupled Plasma by Using a Dried Droplet Calibration Approach, DDCA. *J. Anal. At. Spectrom.* **2018**, *33* (7), 1173–1183. https://doi.org/10.1039/C8JA00055G.

(18) P. Thieleke, J.; Vogt, C. A Calibration Strategy for LA-ICP-MS Using Isotope Dilution for Solid Reference Materials. *J. Anal. At. Spectrom.* **2016**, *31* (6), 1198–1205. https://doi.org/10.1039/C6JA00042H.

(19) Galbács, G. A Critical Review of Recent Progress in Analytical Laser-Induced Breakdown Spectroscopy. *Anal. Bioanal. Chem.* **2015**, *407* (25), 7537–7562. https://doi.org/10.1007/s00216-015-8855-3.

(20) Becker, J. S.; Matusch, A.; Wu, B. Bioimaging Mass Spectrometry of Trace Elements – Recent Advance and Applications of LA-ICP-MS: A Review. *Anal. Chim. Acta* **2014**, *835*, 1–18. https://doi.org/10.1016/j.aca.2014.04.048.

(21) Vanhoof, C.; R. Bacon, J.; T. Ellis, A.; Vincze, L.; Wobrauschek, P. 2018 Atomic Spectrometry Update – a Review of Advances in X-Ray Fluorescence Spectrometry and Its Special Applications. *J. Anal. At. Spectrom.* **2018**, *33* (9), 1413–1431. https://doi.org/10.1039/C8JA90030B.

(22) Limbeck, A.; Bonta, M.; Nischkauer, W. Improvements in the Direct Analysis of Advanced Materials Using ICP-Based Measurement Techniques. *J. Anal. At. Spectrom.* **2017**, *32* (2), 212–232. https://doi.org/10.1039/C6JA00335D.

(23) Günther, D.; Hattendorf, B. Solid Sample Analysis Using Laser Ablation Inductively Coupled Plasma Mass Spectrometry. *TrAC Trends Anal. Chem.* **2005**, *24* (3), 255–265. https://doi.org/10.1016/j.trac.2004.11.017.

(24) Mans, C.; Simons, C.; Hanning, S.; Janßen, A.; Alber, D.; Radtke, M.; Reinholz, U.; Bühler, A.; Kreyenschmidt, M. New Polymeric Candidate Reference Materials for XRF and LA-ICP-MS— Development and Preliminary Characterization. *X-Ray Spectrom.* **2009**, *38* (1), 52–57. https://doi.org/10.1002/xrs.1120.

(25) Bart, J. C. J. *Additives in Polymers: Industrial Analysis and Applications*; John Wiley & Sons, 2005.

(26) K. Unnikrishnan, V.; S. Choudhari, K.; D. Kulkarni, S.; Nayak, R.; B. Kartha, V.; Santhosh, C. Analytical Predictive Capabilities of Laser Induced Breakdown Spectroscopy (LIBS) with Principal Component Analysis (PCA) for Plastic Classification. *RSC Adv.* **2013**, *3* (48), 25872–25880. https://doi.org/10.1039/C3RA44946G.

(27) Banaee, M.; Tavassoli, S. H. Discrimination of Polymers by Laser Induced Breakdown Spectroscopy Together with the DFA Method. *Polym. Test.* **2012**, *31* (6), 759–764. https://doi.org/10.1016/j.polymertesting.2012.04.010.

(28) Hernández-García, R.; Villanueva-Tagle, M. E.; Calderón-Piñar, F.; Durruthy-Rodríguez, M. D.; Aquino, F. W. B.; Pereira-Filho, E. R.; Pomares-Alfonso, M. S. Quantitative Analysis of Lead Zirconate Titanate (PZT) Ceramics by Laser-Induced Breakdown Spectroscopy (LIBS) in Combination with Multivariate Calibration. *Microchem. J.* **2017**, *130*, 21–26. https://doi.org/10.1016/j.microc.2016.07.024.

(29) Braga, J. W. B.; Trevizan, L. C.; Nunes, L. C.; Rufini, I. A.; Santos, D.; Krug, F. J. Comparison of Univariate and Multivariate Calibration for the Determination of Micronutrients in Pellets of Plant Materials by Laser Induced Breakdown Spectrometry. *Spectrochim. Acta Part B At. Spectrosc.* **2010**, *65* (1), 66–74. https://doi.org/10.1016/j.sab.2009.11.007.

(30) Stipe, C. B.; Hensley, B. D.; Boersema, J. L.; Buckley, S. G. Laser-Induced Breakdown Spectroscopy of Steel: A Comparison of Univariate and Multivariate Calibration Methods. *Appl. Spectrosc.* **2010**, *64* (2), 154–160. https://doi.org/10.1366/000370210790619500.

(31) Guezenoc, J.; Gallet-Budynek, A.; Bousquet, B. Critical Review and Advices on Spectral-Based Normalization Methods for LIBS Quantitative Analysis. *Spectrochim. Acta Part B At. Spectrosc.* **2019**, *160*, 105688. https://doi.org/10.1016/j.sab.2019.105688.

(32) Nishi, Y.; Doering, R. *Handbook of Semiconductor Manufacturing Technology*; CRC Press, 2000.

(33)   Bentarzi, H. *Transport in Metal-Oxide-Semiconductor Structures: Mobile Ions Effects on the Oxide Properties*; Springer Science & Business Media, 2011.

(34)   C. Windom, B.; W. Hahn, D. Laser Ablation —Laser Induced Breakdown Spectroscopy (LA-LIBS): A Means for Overcoming Matrix Effects Leading to Improved Analyte Response. *J. Anal. At. Spectrom.* **2009**, *24* (12), 1665–1675. https://doi.org/10.1039/B913495F.

(35)   Lazic, V.; Fantoni, R.; Colao, F.; Santagata, A.; Morone, A.; Spizzichino, V. Quantitative Laser Induced Breakdown Spectroscopy Analysis of Ancient Marbles and Corrections for the Variability of Plasma Parameters and of Ablation Rate. *J. Anal. At. Spectrom.* **2004**, *19* (4), 429–436. https://doi.org/10.1039/B315606K.

(36)   Günther, D.; Horn, I.; Hattendorf, B. Recent Trends and Developments in Laser Ablation-ICP-Mass Spectrometry. *Fresenius J. Anal. Chem.* **2000**, *368* (1), 4–14. https://doi.org/10.1007/s002160000495.

(37)   Koch, J.; Günther, D. Review of the State-of-the-Art of Laser Ablation Inductively Coupled Plasma Mass Spectrometry. *Appl. Spectrosc.* **2011**, *65* (5), 155A-162A. https://doi.org/10.1366/11-06255.

(38)   Sezer, B.; Velioglu, H. M.; Bilge, G.; Berkkan, A.; Ozdinc, N.; Tamer, U.; Boyaci, I. H. Detection and Quantification of a Toxic Salt Substitute (LiCl) by Using Laser Induced Breakdown Spectroscopy (LIBS). *Meat Sci.* **2018**, *135*, 123–128. https://doi.org/10.1016/j.meatsci.2017.09.010.

(39)   Liu, Y.; Chu, Y.; Hu, Z.; Zhang, S.; Ma, S.; Khan, M. S.; Chen, F.; Zhang, D.; Guo, L.; Lau, C. High-Sensitivity Determination of Trace Lead and Cadmium in Cosmetics Using Laser-Induced Breakdown Spectroscopy with Ultrasound-Assisted Extraction. *Microchem. J.* **2020**, *158*, 105322. https://doi.org/10.1016/j.microc.2020.105322.

(40)   Tang, H.; Zhang, T.; Yang, X.; Li, H. Classification of Different Types of Slag Samples by Laser-Induced Breakdown Spectroscopy (LIBS) Coupled with Random Forest Based on Variable Importance (VIRF). *Anal. Methods* **2015**, *7* (21), 9171–9176. https://doi.org/10.1039/C5AY02208H.

(41)   Brunnbauer, L.; Larisegger, S.; Lohninger, H.; Nelhiebel, M.; Limbeck, A. Spatially Resolved Polymer Classification Using Laser Induced Breakdown Spectroscopy (LIBS) and Multivariate Statistics. *Talanta* **2019**, 120572. https://doi.org/10.1016/j.talanta.2019.120572.

(42)   Kuhn, K.; Meima, J. A.; Rammlmair, D.; Ohlendorf, C. Chemical Mapping of Mine Waste Drill Cores with Laser-Induced Breakdown Spectroscopy (LIBS) and Energy Dispersive X-Ray Fluorescence (EDXRF) for Mineral Resource Exploration. *J. Geochem. Explor.* **2016**, *161*, 72–84. https://doi.org/10.1016/j.gexplo.2015.11.005.

(43)   Yaroshchyk, P.; L. Death, D.; J. Spencer, S. Comparison of Principal Components Regression, Partial Least Squares Regression, Multi-Block Partial Least Squares Regression, and Serial Partial Least Squares Regression Algorithms for the Analysis of Fe in Iron Ore Using LIBS. *J. Anal. At. Spectrom.* **2012**, *27* (1), 92–98. https://doi.org/10.1039/C1JA10164A.

5. Conclusion

In this work, the potential of LIBS and LA-ICP-MS for advanced characterization of polymeric samples was investigated. Using the techniques' unique characteristics, novel material characterization methods were developed allowing a more comprehensive characterization of polymeric samples which is not accessible with conventional techniques used for polymer analysis. The unique ability of LIBS enabling the detection of polymers main elemental constituents such as C, H, N, and O and also providing molecular information combined with the possibility to record images and depth profiles offers a wide range of applications in many different fields. LA-ICP-MS offers an excellent sensitivity for trace element analysis and provides complementary information for polymer characterization. As both techniques are based on the same principle of laser ablation, they can be employed in a so-called tandem setup where LIBS and LA-ICP-MS data is recorded simultaneously from the same measurement. Three different applications for polymer characterization using the aforementioned techniques are presented and discussed.

In the first part, LIBS combined with multivariate statistics is used to perform spatially resolved classification of polymers. Discrimination of polymers using LIBS data usually requires a high SNR of the polymer specific signals. Conventionally, multiple measurements can be accumulated to achieve satisfying results. In the case of imaging experiments or depth profiling, only single-shot LIBS spectra are available which increases the demand on data evaluation strategies. With optimized LIBS parameters and sophisticated data evaluation strategies such as RDF and k-means clustering, it was not only possible to resolve the lateral distribution of two different polymer types within a 2D structured sample but also a depth profile of a polymer multi-layer system was recorded and the distribution of the different polymer types present were correctly classified. The developed approach was also applied to samples from the field of cultural heritage science where a simultaneous classification of organic binder materials and inorganic pigments was achieved. Therefore, LIBS proofed to be a suitable method for studying and investigating the distribution of different polymer types within structured samples.

In the second part LIBS and LA-ICP-MS depth profiling is used to investigate polymer degradation and uptake of inorganic species in accelerated stress tests of a wide range of different polymeric materials. Weathering conditions of the accelerated stress tests included UV-radiation and exposure to corrosive gases (H_2S, SO_2 and O_3) as well as exposure to artificial seawater spiked with heavy

metals. A polymer specific LIBS signal (C_2 swan band) was identified which can be used to assess the degradation of the polymer under investigation. These findings were confirmed using FT-IR spectroscopy. Additionally, oxidation of the polymer is observed using the oxygen emission signal. In the conducted weathering experiments, alteration of the samples was not limited to the sample surface but also propagation to the bulk was observed. Combining LIBS data with LA-ICP-MS measurements allowed to monitor the uptake of sulfur containing species as well as heavy metals which was correlated with the ageing of the sample. The combination of LA-ICP-MS and LIBS enabled a comprehensive study of alteration of polymeric samples by analyzing depth profiles

The third part of this work investigates strategies for the quantification of trace metals in unknown polymer types using LIBS. Therefore, a library of in-house prepared polymer standards was prepared and analyzed with LIBS. Two different multivariate data evaluation strategies based on a RDF and a PLS model are evaluated when used for the quantification of unknown polymers. Obtained results were compared to matrix-matched quantification and non-matrix-matched quantification. Matrix-matched quantification is the gold standard for LIBS and usually provides the most reliable result but is not applicable for unknown polymer types. When analyzing unknown polymer types, non-matrix-matched quantification is the only conventional approach available. However, with this approach obtained errors can hardly be estimated and therefore it does not provide reasonable results for the quantification of unknown polymer types. The two investigated multivariate data evaluation strategies proofed to provide reliable quantitative results outperforming non-matrix-matched quantification. Therefore, they are a promising approach for the quantification in unknown polymer types or polymers with no matrix-matched standards available.

The presented work shows the application of LA-ICP-MS and LIBS for the field of polymer characterization and provides information not accessible with standard techniques for polymer analysis. Nevertheless, some improvements are still required for certain applications. With improved instrumentation, better lateral resolution as well as depth resolution can be obtained. Additionally, investigation of uptake of inorganic species can benefit from a higher sensitivity. Using a tandem LA-ICP-MS/LIBS approach can help to overcome some of the above mentioned limitations. Even though for this approach further instrumental developments are necessary. Especially improvements in the washout performance are essential to establish the tandem approach for routine investigations.

6. Curriculum Vitae

⌂ Meiselstraße 14/1/6, 1150 Wien   ✆ +43 677 61678409   ✉ lubrunnbauer@gmail.com

CURRICULUM VITAE

Personal Information

Date of birth	14.03.1992
Place of birth	Salzburg
Citizenship	Austria

Professional Experience

01/2018 - recent

PhD student at TU Wien in cooperation with Infineon AG and KAI GmbH
- Research in the field of material characterization with a focus on polymers and trace metal analysis
- Contribution to 6 peer-reviewed publications
- Attendance of 10 international scientific conferences with multiple oral and poster presentations
- Supervision of Bachelor- and Master theses
- Experience with several analytical techniques (LA-ICP-MS, LIBS, ICP-MS/OES, SEM, TEM)

01/2020 - 04/2020

Applied Spectra, Inc. Sacramento, USA
- Guest researcher working on polymer analysis using ns/fs LIBS systems

07/2016 - 09/2016

Infineon Villach
- Internship at Infineon Villach in the department of wet chemical etching working in a clean room environment
- Participation in the set-up of a new tool for single wafer cleaning

10/2013 - 06/2016

TU Wien
- Tutor in several lab courses in the field of analytical chemistry

07/2015 - 09/2015

Infineon Villach
- Internship at Infineon Villach in the department of wet chemical etching working in a clean room environment
- Investigating etch rates of different semiconductor materials

10/2010 - 06/2011

Red Cross Salzburg
- Alternative civilian service performing ambulance transports

Dipl.-Ing. Lukas Brunnbauer

🏠 Meiselstraße 14/1/6, 1150 Wien   📞 +43 677 61678409   ✉ lubrunnbauer@gmail.com

Education

01/2018 - recent

PhD program TU Wien
- PhD thesis: Advanced Polymer Characterization using LA-ICP-MS and LIBS

01/2020 - 04/2020

Master Program "Technical Chemistry", TU Wien
- Focus on applied physical and analytical chemistry
- Master thesis: "Corrosion investigations with the system copper/polyimide for microelectronics"
- Passed with distinction
- Degree: Dipl.-Ing. (equivalent M.Sc.)

08/2016 - 01/2017

ERASMUS Uppsala University
- Research project on the synthesis and characterization of quasicrystals in the REAuSi-system

10/2011 – 04/2015

Bachelor Program "Technical Chemistry", TU Wien
- Degree: B.Sc

Additional Skills

IT-Skills

- **Data analysis:** MS Excel (proficient), OriginLab Origin (proficient)
- **Presentations:** MS Powerpoint (expert)
- **Word processing:** MS Word (expert), LaTeX (proficient)
- **Design:** Inkscape (proficient)
- **Programming:** Python 3 (novice)

Languages

- German (mother tongue)
- English (C1)
- French (A2)

Academic Achievements

- JAAS Poster Prize (2020 Conference on Plasma Spectrochemistry, Tuscon, Arizona)
- Travelling grant of the TU Wien for a stay in Sacramento, USA
- Performance scholarship of the TU Wien 2017

TU Bibliothek Your knowledge hub

TU WIEN

7. List of Publications

7.1 Peer-Reviewed Articles

L. Brunnbauer, J. Gonzalez, H. Lohninger, J. Bode, C. Vogt, M. Nelhiebel, S. Larisegger and A. Limbeck, *"Strategies for Trace Metal Quantification in Polymer Samples with an Unknown Matrix using LIBS "*, submitted to Spectrochimica Acta Part B: Atomic Spectroscopy

A. Limbeck, L. Brunnbauer, H. Lohninger, P. Porizka, P. Modlitbova, J. Kaiser, P. Janovszky, A. Keri and G. Galbacs, *"Methodology and applications of elemental mapping by laser induced breakdown spectroscopy"*, Analytica Chimica Acta 1147 (2021) https://doi.org/10.1016/j.aca.2020.12.054

L. Brunnbauer, M. Mayr, S. Larisegger, M. Nelhiebel, L. Pagnin, R. Wiesinger, M. Schreiner and A. Limbeck, *"Combined LA-ICP-MS/LIBS: powerful analytical tools for the investigation of polymer alteration after treatment under corrosive conditions"*, Scientific Reports 12513 (2020) doi:10.1038/ s41598-020-69210-9

L. Brunnbauer, S. Larisegger, H. Lohninger, M. Nelhiebel and A. Limbeck, *"Spatially resolved polymer classification using Laser Induced Breakdown Spectroscopy (LIBS) and multivariate statistics"*, Talanta 120572 (2019) doi:10.1016/ j.talanta.2019.120572L.

L. Pagnin, L. Brunnbauer, R. Wiesinger, A. Limbeck and M. Schreiner, *"Multivariate analysis and laser-induced breakdown spectroscopy (LIBS): a new approach for the spatially resolved classification of modern art materials"*, Anal. Bioanal. Chem. (2020) doi:10.1007/s00216-020-02574-z

W. Knierzinger, R. Drescher-Schneider, K-H. Knorr, S. Drollinger, A. Limbeck, L. Brunnbauer, F. Horak, D. Festi and M. Wagreich, *"Anthropogenic and climate signals in late-Holocene peat layers of an ombrotrophic bog in the Styrian Enns valley (Austrian Alps)"*, E&G Quaternary Sci. J., 69, 121–137, https://doi.org/10.5194/egqsj-69-121-2020, 2020

W. Knierzinger, D. Festi, A. Limbeck, F. Horak, L. Brunnbauer, S. Drollinger, M. Wagreich, J.-J.S. Huang, M. Strasser, K.-H. Knorr, H. Reschreiter, S. Gier, W. Kofler, C. Herzig, K. Kowarik, *"Multi-proxy analyses of a minerotrophic fen to reconstruct prehistoric periods of human activity associated with salt mining in the Hallstatt region (Austria)"*,

J. Archaeol. Sci. Rep. 36 (2021) 102813. https://doi.org/10.1016/j.jasrep.2021.102813.

7.2 Oral Presentations at Conferences

Presenting author is underlined.

A. Limbeck, L. Pagnin, R. Wiesinger, M. Schreiner and L. Brunnbauer, *"Assessment of Polymer Degradation by the Combined Use of LIBS and LA-ICP-MS"*, International Workshop on LIBS 2020, Szeged, Hungary

L. Brunnbauer, L. Pagnin, R. Wiesinger, M. Schreiner and A. Limbeck, *"Analysis of Contemporary Art Materials using Laser Induced Breakdown Spectroscopy (LIBS)"*, Winter Conference on Plasma Spectrochemistry 2020, Tucson, USA

A. Limbeck, L. Brunnbauer, M. Bonta, L. Pagnin, R. Wiesinger, and M. Schreiner, *"Tandem LA-ICP-MS/LIBS For Improved Polymer Characterization"*, Winter Conference on Plasma Spectrochemistry 2020, Tucson, USA

A. Limbeck, L. Brunnbauer, M. Bonta, L. Pagnin, R. Wiesinger and M. Schreiner, *"Advanced Polymer Analysis using Tandem LA-ICP-MS/LIBS"*, Workshop on tandem LIBS/LA-ICP-MS 2019, Berlin, Germany

L. Brunnbauer, S. Larisegger, M. Nelhiebel and A. Limbeck, *"Spatially Resolved Polymer Classification using Laser Induced Breakdown Spectroscopy (LIBS)"*: Colloquium Analytische Atomspektroskopie (CANAS) 2019, Freiberg, Germany

A. Limbeck, L. Brunnbauer, M. Mayr, L. Pagnin, R. Wiesinger and Manfred Schreiner, *"Degradation of Modern Art Materials: comprehensive examination by the combined use of LIBS and LA-ICP-MS"*, 15th International Conference on Laser Ablation 2019, Maui, USA

L. Brunnbauer, M. Mayr, M. Bonta, W. Mack, H. Preu, C. Schäffer, S. Larisegger, M. Nelhiebel and A. Limbeck, *"LA-ICP-MS and LIBS: Analytical Techniques for Lateral Resolved Elemental Analysis applied to Corrosion Studies in Semiconductor Devices"*: Eurocorr 2019, Sevilla, Spain

L. Brunnbauer, L. Pagnin, M, Schreiner and A. Limbeck, *"Investigation of Polymer Degradation of Modern Art Materials Using LIBS and Multivariate Statistics"*: ANAKON 2019, Münster, Germany

M. Mayr, L. Brunnbauer, S. Larisegger, M. Nelhiebel, J. Lohninger and A. Limbeck, *"Investigation of Polymer Degradation under Corrosive Conditions Using Tandem LA-ICP-MS/LIBS"*, 30th MassSpec-Forum 2019, Vienna, Austria

L. Brunnbauer, S. Larisegger, M. Nelhiebel, J, Lohninger and A. Limbeck, *"Spatial distinction of different polymers for the accurate determination of their trace metal content using LIBS"*, ASAC-JunganalytikerInnen-Forum (JAF) 2018, Vienna, Austria

7.3 Poster Presentations at Conferences

Presenting author is underlined.

L. Brunnbauer, J. Gonzalez, and A. Limbeck, *"Matrix Effects in Quantitative Polymer Analysis: A Comparison of ns and fs Laser Systems"*, International Workshop on LIBS 2020, Szeged, Hungary

L. Brunnbauer, S. Larisegger, M. Nelhiebel and A. Limbeck, *"Matrix Independent Quantification of Trace Metals in Polymers using Laser Induced Breakdown Spectroscopy (LIBS)"*, Winter Conference on Plasma Spectrochemistry 2020, Tucson, USA

K. Kubíčkova, P. Pořízka, M. Kaška, A. Fibir, L. Krbal, L. Brunnbauer, A. Limbeck and J. Kaiser, *"Implementation of laser spectroscopy in skin tumor analysis"*, EMSLIBS 2019, Brno, Czech Republic

L. Brunnbauer, M. Mayr, S. Larisegger, M. Nelhiebel and A. Limbeck, *"Tandem LA-ICP-MS/LIBS Analysis of Polymer Coatings: Investigating Degradation under exposure to UV-radiation and SO_2"*, Eurocorr 2019, Sevilla, Spain

L. Brunnbauer and A. Limbeck, *"Polymer classification in structured samples using laser induced breakdown spectroscopy (LIBS)"*, 20. Tagung Festkörperanalytik, Vienna, Austria

L. Pagnin, L. Brunnbauer, R. Wiesinger, A. Limbeck and M. Schreiner, *"Multispectral Investigations for Characterizing UV-light Degradation of Modern Art Materials"*, 20. Tagung Festkörperanalytik, Vienna, Austria

L. Pagnin, L. Brunnbauer, R. Wiesinger, A. Limbeck, and M. Schreiner, *"Multispectral Investigations for Characterizing UV-light Degradation of Modern Art Materials"*, YHIP 2019, Lisbon, Portugal

L. Brunnbauer, L. Pagnin, M. Schreiner and A. Limbeck, *"Depth Profiling of UV-light Degradation of Modern Art Materials Using LIBS"*, European Winter Conference on Plasma Spectrochemistry (EWCPS) 2019, Pau, France

P. Janovszky, A. Kéri, L. Brunnbauer, A. Limbeck and G. Galbács, *"Quantitative Multielemental Mapping Of Biological Samples By Laser Induced Breakdown Spectroscopy: A Case Study of Pig Tissues"*, European Winter Conference on Plasma Spectrochemistry (EWCPS) 2019, Pau, France

L. Brunnbauer, S. Larisegger, M. Nelhiebel, J. Lohninger and A. Limbeck, *"Investigation of Polymer Degradation under Corrosive Conditions Using Tandem LA-ICP-MS/LIBS"*, European Winter Conference on Plasma Spectrochemistry (EWCPS) 2019, Pau, France

L. Brunnbauer, S. Larisegger, M. Nelhiebel, J. Lohninger and A. Limbeck, *"Accurate analysis of trace metals in polymers with varying composition using LIBS and multivariate statistics"*, 14th European Workshop on Laser Ablation (EWLA) 2018, Pau, France